PERFORMANCE BASED DESIGN OF SHEAR WALL BUILDING

By

Prakash K. Siyani
(07MCL016)

DEPARTMENT OF CIVIL ENGINEERING
Ahmedabad 382481

May 2009

PERFORMANCE BASED DESIGN OF SHEAR WALL BUILDING

Major Project

Submitted in partial fulfillment of the requirements

For the degree of

Master of Technology in Civil Engineering
(Computer Aided Structural Analysis & Design)

By

Prakash K. Siyani
(07MCL016)

Guide

Dr. P. V. Patel

DEPARTMENT OF CIVIL ENGINEERING
Ahmedabad 382481
May 2009

CERTIFICATE

This is to certify that the Major Project entitled "Performance Based Design of Shear Wall Building" submitted by Mr. Prakash K. Siyani (07MCL016), towards the partial fulfillment of the requirements for the degree of Master of Technology in Civil Engineering (Computer Aided Structural Analysis and Design) of Nirma University of Science and Technology, Ahmedabad is the record of work carried out by him under my supervision and guidance. In my opinion, the submitted work has reached a level required for being accepted for examination. The results embodied in this major project, to the best of my knowledge, haven't been submitted to any other university or institution for award of any degree or diploma.

Dr. P.V. Patel
Guide,
Professor,
Department of Civil Engineering,
Institute of Technology,
Nirma University,
Ahmedabad

Dr. P. H. Shah
Professor and Head,
Department of Civil Engineering,
Institute of Technology,
Nirma University,
Ahmedabad

Dr. K Kotecha
Director,
Institute of Technology,
Nirma University,
Ahmedabad

Examiner

Examiner

Date of Examination

ACKNOWLEDGEMENT

I express my deep sense of gratitude and sincere thanks to my guide **Dr. P. V. Patel**, Professor, Department of Civil Engineering, Institute of Technology, Nirma University, Ahmedabad. I express my hearty thanks to him who, right from the conceptualization of the problem to the finishing stage of the Major Project part molding my work. From the very beginning of the thesis, his valuable discussions and continuous reviews and suggestions helped me a lot during this study.

My sincere thanks to **Prof. G. N. Patel**, Professor, Department of Civil Engineering, **Dr. P. H. Shah**, Head, Department of Civil Engineering, Institute of Technology, Nirma University, Ahmedabad and **Prof. C. H. Shah,** structural consultant for their valuable guidance, suggestion and critical discussions that not only helped in my Major Project but also in shaping my career. I am also thankful to **Dr. K Kotecha**, Director, Institute of Technology for his kind support in all respects during my study.

I am really thankful to my friends, who have been great supporters in my Major Project work.

And most importantly, I express my deep sense of gratitude to my parents, for their endless love and moral support that constantly encouraged me.

Many others helped me directly and indirectly, I also convey my thanks to them.

Prakash K. Siyani

(Roll No: 07MCL016)

ABSTRACT

Earthquakes are known to produce one of the most destructive forces on earth. It has been seen that during past earthquakes many of the buildings were collapsed. Therefore, realistic method for analysis and design are required. Performance Based Design is the modern approach for earthquake resistant design. It is an attempt to predict the performance of buildings under expected seismic event. A structure designed with Performance Based Design (PBD) concept does not developed undesirable failure mechanism during earthquake. The analysis can be performed on new as well as existing buildings and the performance of buildings in future earthquake can be evaluated.

The present study is an attempt to understand the fundamentals and procedure of Performance Based Design of R.C.C. shear wall building. A Nonlinear Static Analysis (Pushover Analysis) is widely used to obtain the inelastic deformation capability of building, which depends on localized damage (hinges formation) in various elements of building. The results of push analysis are compared using default hinge properties as per ATC 40 and user defined hinge properties as per stress strain relationship. In practice, ATC 40 based default hinge properties are used due to convenience and simplicity. But the observation clearly show that the user defined hinge model is better than the default hinge model in reflecting nonlinear behavior compatible with the element properties. The software used for performing performance based design is ETABS 9.07.

Pushover analysis is based on static nonlinear analysis performed by imposing an assumed distribution of lateral loads over the height of a structure. The lateral loads are incremented monotonically from zero to the ultimate level corresponding to the incipient collapse of the structure. The response behavior of structure is evaluated by measurement of strength of structure. There are several methods for estimating seismic demands for performance-based design of buildings. The accuracy of design is based on applied pattern of loads inducing deformation in the structure which should be similar to that induced by the earthquake ground motion. The result of pushover analysis in term of capacity, demand and performance point are compared as obtained from inverted triangular distribution of lateral load pattern based on codal formula, and lateral

load distribution generated from site specific response spectra and time history analysis.

Performance criteria are described in terms of performance levels and hazard levels. The design objectives in current building codes consider as life safety in minor and moderate earthquakes, and collapse prevention in major earthquake. However, the actual design in achieving the objectives is not known. Performance based design is iterative in nature compared to one step analysis and design as per IS: 1893(Part1)-2002. The process of analysis and design is repeated till expected performance objectives are meet. 20 story shear wall building is considered for performance based design.

Basic information related to Performance Based Design are discussed in Chapter 1. It also includes objective of study and scope of work. Chapter 2 presents the literature review on topic related to performance based design. Modeling techniques and software application of ETABS (Extended Three Dimensional Analysis of Building Structure) with theoretical derivation of performance point as per ATC 40 are covered in Chapter 3. Derivation of hinge properties and comparison of 3D frame result using different hinge properties are discussed in Chapter 4. Pushover analysis result in term of capacity, demand, performance point, hinge formation pattern at performance point for lateral load distribution over the height of structure considering time history and response spectrum is discussed in Chapter 5. In Chapter 6, site specified time history and site specific response spectra analyses are presented. Performance based design objective and criteria are discussed in Chapter 7. Also 20 story shear wall building design based on performance level is presented. Finally in Chapter 8, summary of study, conclusions and future scope of work are given.

CONTENTS

LIST OF FIGURES

LIST OF TABLES

ABBREVIATION NOTATION AND NOMENCLATURE

C_a	Coefficient of Acceleration
CP	Collapse Prevention
CSM	Capacity Spectrum Method
C_v	Coefficient of Velocity
E_D	Cyclic hysteretic energy dissipation at displacement S_d
E_{So}	Elastic energy store in system at displacement of S_d
DBE	Design Basis Earthquake
f_c	Cylindrical strength of concrete
f_{ck}	Flexural strength of concrete
F	Inertia force
IO	Immediate Occupancy
L_p	Plastic hinge length
LS	Life safety
M_y	Yielding Moment
M_u	Ultimate Moment
MCE	Maximum Considered Earthquake
P	Axial Force
Q_i	Design lateral force at each floor i
S_a	Spectral Acceleration
S_d	Spectral Displacement
T	Time period
$\ddot{u}_g$	Ground acceleration
V	Base Shear
V_y	Yield Shear
V_u	Ultimate Shear
W_i	Seismic weight of floor i
β_{eff}	Effective structural damping
β_0	Structural damping
ε_c	Compression fiber strain
ε_s	Tension steel strain
θ_y	Yield Rotation
θ_u	Ultimate Rotation
δ	Displacement

λ	Damping modification factor
ζ_n	Damping ratio
ω_n	Natural frequency

1. INTRODUCTION

1.1 GENERAL

Earthquakes are one of the most destructive forces. They are random in nature and unpredictable. The earthquake causes large-scale damages compared to other force. The present generation design code based on equivalent elastic force approaches is ineffective in preventing destructive consequences due to earthquake. Currently two analysis tools are offered with different levels of complexity and required computational effort; nonlinear static analysis (push over) and nonlinear dynamic analysis (time-history). Nonlinear analysis procedures become important in identifying the patterns and levels of damage for a structure's inelastic behavior and understanding the failure modes of the structure during severe seismic events [1].

Performance based design is modern approach to earthquake resistant design. The purpose of Performance-Base Design (PBD) is give to realistic assessment about performance of a structure when subjected to either particular or generalized earthquake ground motion. It is assumed that the structure components are able to resist earthquake ground motion by yielding in to inelastic range, absorbing energy and acting in a ductile manner. Nowadays pushover analysis is widely used for performance based design of new structures and retrofitting of existing structures. The purpose of pushover analysis is to evaluate the expected performance of a structural system by estimating its strength and deformation demand in design earthquake. Normally, this method depends on each country's condition in economy, technical level and regional seismic intensity. But recently performance based design method is considered as more effective one worldwide including Japan and China. In fact, some seismic codes have begun to include performance assessment of structural systems in their codes (e.g., Eurocode 8, Japanese Design Code). So, next generation codes will include additional performance indicator [1].

1.2 PERFORMANCE BASED DESIGN

In the performance-based design approach, acceptability criteria are established in term of performance level or damage levels for a specified earthquake ground motion. As per current performance-based design practice, the structures are considered capable to resist minor earthquake without significant damage, moderate earthquakes with repairable damage and major earthquakes without collapse [2].

1.2.1 Performance Level

A performance level is described in term of limiting damage condition which may be considered satisfactory for a given building. The target performance objective is divided into Structural Performance Level and Non-structural Performance Level. Based on the combination of these two performances the overall building performance is determined [2].

1.2.1.1 Structural Performance Level

- Immediate Occupancy (SP-1): Limited Structure damage with basic vertical and lateral force resisting system retaining most of their pre-earthquake characteristics and capacities.
- Damage Control (SP-2): This term is actually not a specified value but damage is considered somewhere between Immediate Occupancy and Life Safety.
- Life Safety (SP-3): Significant damage with some margin against total or partial collapse. Repair may not be economically feasible.
- Limited Safety (SP-4): This term is actually not a specific level. It is somewhere between Life Safety and structure stability.
- Structural Stability (SP-5): Substantial Structure damage in which the structure system is on the verge of experiencing partial or total collapse. Significant risk of injury exists. Repair may not be technically or economically feasible.
- Not Considered (SP-6): Placeholder for situation where only non-structural seismic evaluation or retrofit is performed.

1.2.1.2 Non-structural Performance Level

- Operational (NP-A): Non-structural elements are generally in place and in working condition. Backup system for failure of external utilities, communications and transportation has been provided.
- Immediate Occupancy (NP-B): Non-structure elements are generally in place but may not be working in condition.
- Life Safety (NP-C): Considerable damage to nonstructural component and system but no collapse of non-structural heavy items.
- Reduced Hazards (NP-D): Extensive damage to non-structural component but should not include collapse of large and heavy items that can cause significant injury to groups of people.
- Not Considered (NP-E): Non-structural element, other than that have an effect on structural response, are not evaluated.

The point of localized damage in structure is often called as hinge. As per above performance level, force versus deformation curve is divided as shown in Fig. 1.1. Five points labeled as A, B, C, D, and E are used to define the force deflection behavior of the hinge and three points labeled as IO, LS and CP are used to define the acceptance criteria for the hinge [2].

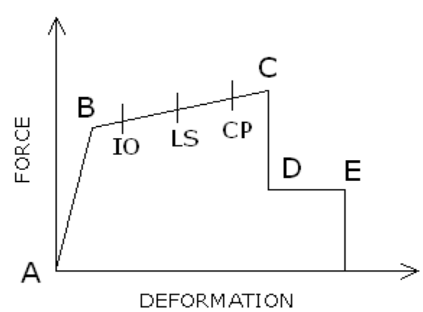

Fig.1.1 Force-deformation for pushover hinge

Where,

IO = Immediate Occupancy

LS = Life Safety

CP = Collapse Prevention

C = Strength Degradation

C-D = Initial failure of the component

D-E = Residual Resistance

Various performance levels are considered depending on type of damages in the structure. Negligible impact on building is considered at an operational level. Building is safe to occupancy but possibly not useful until the repaired is considered as an immediate occupancy level. Building is safe during event but possibly not afterward is considered as a life safety level and building is very near to collapse is considered as collapse prevention. These stages are shown in Fig. 1.2.

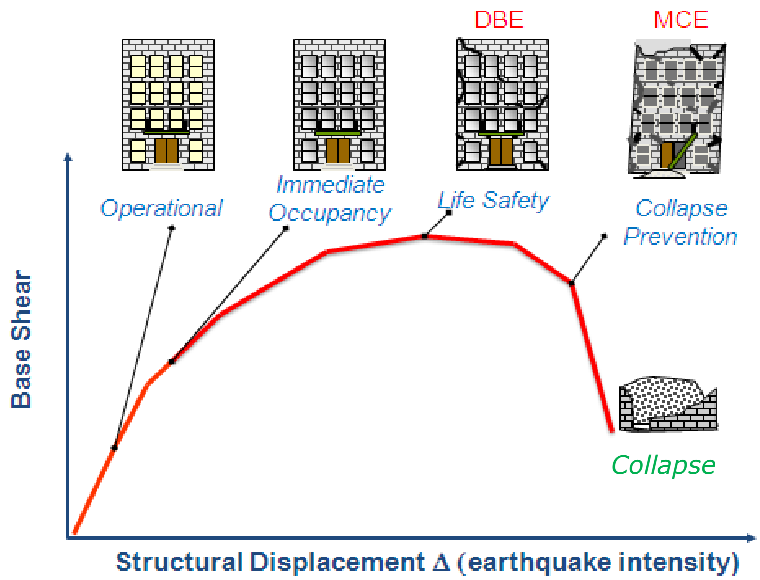

Fig.1.2 Standard performance level

1.3 STATIC NONLINEAR ANALYSIS

In performance based design response of structure is considered beyond elastic limit as opposed to code based approach. Static non-linear analysis is one of the analysis technique used for performance based design. Pushover or capacity based analysis is more popular as a static nonlinear analysis, which is described in this section.

Two types of pushover analysis are as:

- **Force controlled**

Used when load is known and structure is desired to support this load. For gravity load on structure force controlled, push over analysis is used.

- **Displacement controlled**

Used when load is unknown but displacement is known and structure is desired to lose their strength and become unstable. For lateral load on structure displacement controlled, pushover analysis is used.

Three main steps involved in this analysis procedure.

1. Evaluation of Capacity of building i.e. Representation of the structure's ability to resist a force
2. Evaluation of Demand curve i.e. Representation of earthquake ground motion
3. Determination of Performance point i.e. Intersection point of demand curve and capacity curve

1.3.1 Capacity

Fig. 1.3 is represents the increasing lateral displacement as a function of the force applied monotonically from zero to the ultimate level corresponding to the incipient collapse of the structure and response behavior is gauged by measurement of strength of structure. The simplified nonlinear procedure is followed for the generation of the capacity curve.

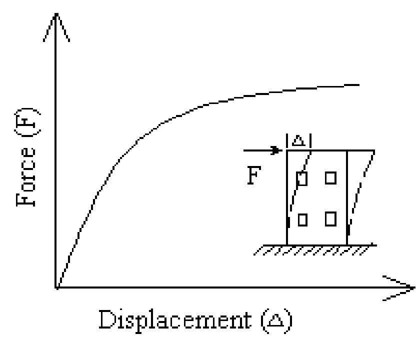

Fig. 1.3 Capacity curve

This capacity curve is in form of Base Shear versus Displacement curve which is converted in to Spectral Acceleration (S_a) versus Spectral Displacement (S_d) curve. An approximate effective damping is also calculated based on the shape of the capacity curve.

1.3.2 Demand

Spectral Acceleration (S_a) versus Time Period (T) curve is given in IS:1893(Part1)-2002 which is converted in to Spectral Acceleration (S_a) versus Spectral Displacement (S_d) curve.

Capacity curve and Demand curve are generated in spectral coordinates to find-out performance point a_p and d_p. The equal displacement a′ and d′ is good starting point for the iterative process as shown in Fig.1.4.

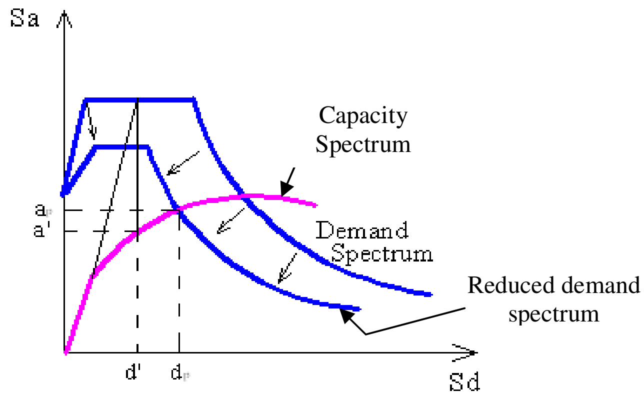

Fig. 1.4 Demand spectra curve

The location of performance point must satisfy two relationships: (1) the point must lie on the capacity spectrum curve in order to represent the structure at a given displacement, and (2) the point must lie on a demand spectrum curve or 5% damped design spectrum, that represent the nonlinear demand at the same structural displacement. For this methodology, spectral reduction factors are given in term of effective damping. An approximate effective damping is calculated based on the shape of capacity curve, different soil profile, and resulting hysteresis loop.

1.3.3 Performance

The intersection of the pushover capacity and demand spectrum curves defines as the "performance point" as shown in Fig. 1.5. Allowable tolerance is considered within 5% of the displacement of the trial performance point.

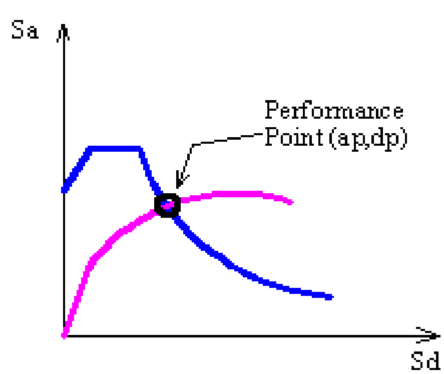

Fig. 1.5 performance point

Using the Performance Point or Target Displacement, the global response of the structure and individual component deformations are compared with specific performance goals for building as per ATC 40 [13] criteria.

1.4 PERFORMANCE BASED DESIGN PROCEDURE

The steps followed in performance based design are shown in Fig. 1.6.

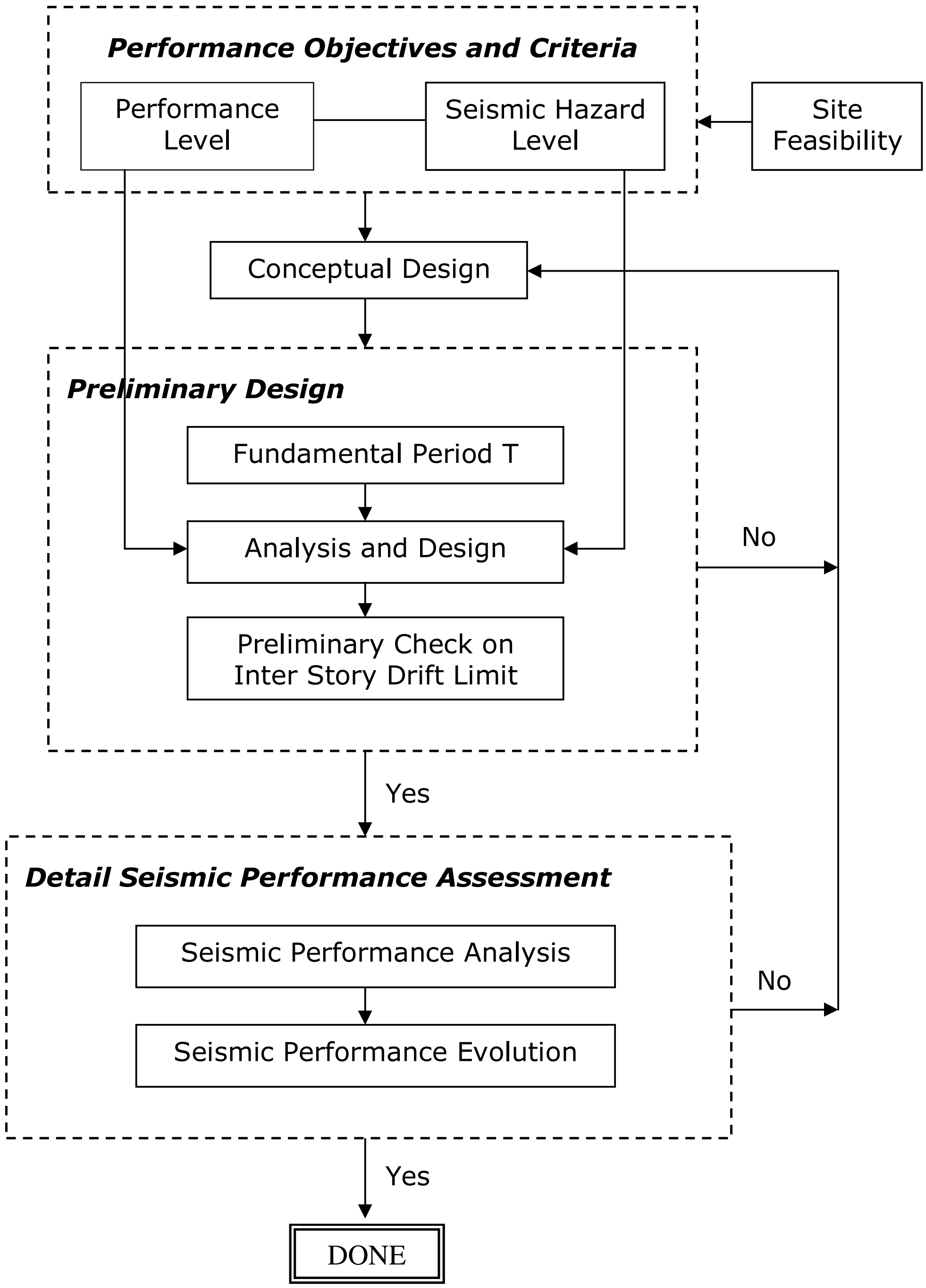

Fig. 1.6 Flow chart of performance based design

Performance based design is carried out in follow steps:

(1) Select the performance level of building in association with architect, structure engineer and client based on site condition are expected.

(2) Preliminary design is carried out as per Indian code. The story drift limit is checked as per IS:1893(Part1)-2002.

(3) If design is safe than performance based analysis is carried out to meet the performance objective which is interpreted by both quantified hazard level and quantified performance level.

(4) If performance point is not meet to objective revise the design by increasing or decreasing percentage of steel or size of member.

The process of analysis and design is repeated till expected performance objectives are met. Capacity and demand both change with structural design. Performance based design is iterative in nature compared to one step analysis and design as per IS:1893(Part1)-2002.

1.5 TIME HISTORY ANALYSIS

Time-history analysis is used to determine time-dependent response of the structure which can be obtained through direct numerical integration of its differential equations of motion given by:

$$Ku(t) + C\dot{u}(t) + M\ddot{u}(t) = r(t) \qquad \text{. . . . (1.1)}$$

Where *K* is the stiffness matrix; *C* is the damping matrix; M is the diagonal mass matrix of structure; $u, \dot{u},$ and $\ddot{u}$ are the displacement, velocity and accelerations of structure; and *r* is applied load.

1.6 OBJECTIVES OF STUDY

The objective of present work is to understand performance based design of RCC shear walled buildings. Various methods of analysis like static nonlinear Pushover analysis and Time history analysis of multistory building are to be studied. The main objectives of present work are as follows:

- Study of capacity spectrum, demand spectrum and performance point through Pushover analysis.

- To study the bilinear representation of capacity spectrum and derivation of damping for spectral reduction of building through hysteretic loops.
- Study of nonlinear hinge properties as per IS code and failure effect on structural element.
- Understand the effect of lateral force distribution pattern on structure during pushover analysis.
- To study the effect of site specific response spectra and time history analysis on nonlinear behavior of structure using Push over analysis.
- Parametric study to understand the Performance based design of shear walled building.

1.7 SCOPE OF WORK

To achieve above objectives the scope of work is decided as follow:

- Pushover analysis of 3D frames model and 3D shear wall building model using ETABS nonlinear version 9.5.
- Comparison of hinge properties per IS code and ATC 40.
- Development of Excel sheet for static non linear analysis - spectrum capacity curve, spectrum demand curve and performance point and its comparison with software results.
- Comparison the nonlinear static analysis result in term of structural capacity, demand and performance point of Frame structure using different lateral load pattern generated from site specific response spectrum, time history analysis and as per IS:1893(Part1)-2002.
- Parametric study of shear wall building using site specific response spectrum and time history analysis, considering parameters as a height of building using ETABS.
- Carryout the performance based design of shear wall building using ETABS software.

The plan of multistoried shear wall framed building considered for the modeling and nonlinear analysis are shown in Fig.1.7.

Data consider for performance based design are:

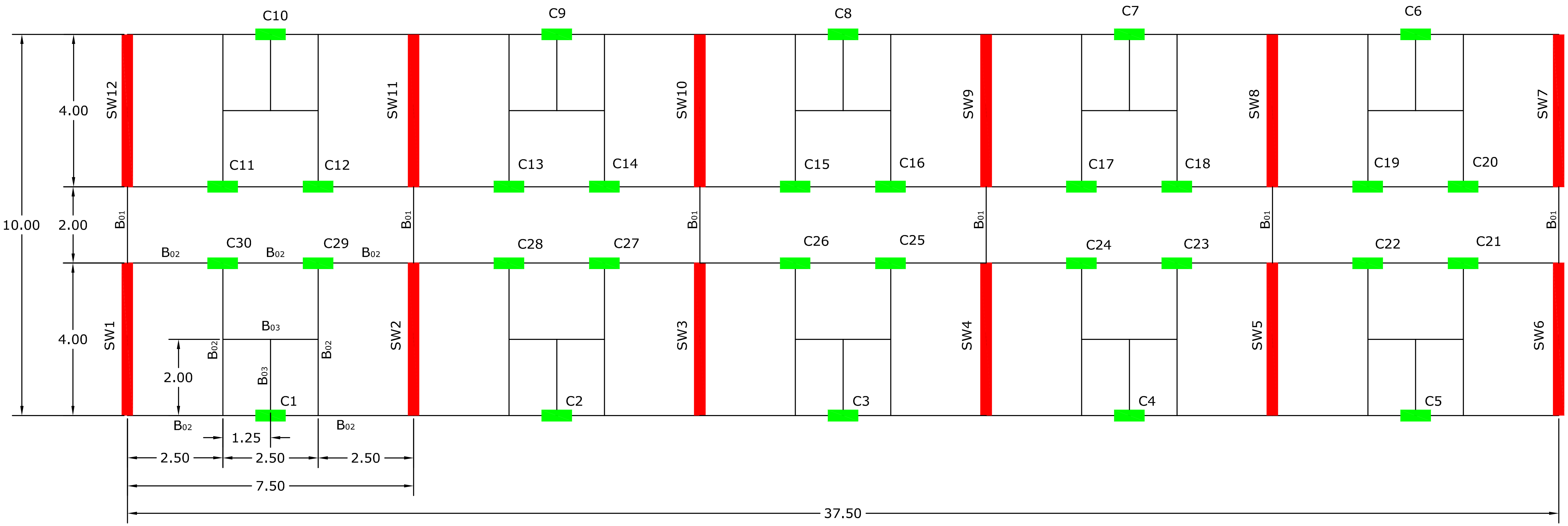

Table 1.1 Sizes of various members in shear wall building

No. of storey	Column Size in m	Shear wall Thickness in m	Beam Size in m
10-Storey	0.30 x 0.50	0.20 x 4.00	
15-Storey	0.30 x 0.60	0.20 x 4.00	B_{01} = 0.25 x 0.60
20-Storey	0.30 x 0.60	0.25 x 4.00	B_{02} = 0.25 x 0.55
25-Storey	0.30 x 0.90	0.25 x 4.00	B_{03} = 0.25 x 0.45
30-Storey	0.30 x 1.00	0.30 x 4.00	

Fig. 1.7 Plan View of Shear Wall Building

- Earthquake Zone – III
- Importance factor - 1.5
- Response reduction factor – 5
- L.L. on slab - 3 kN/ m^2
- Slab thickness - 150 mm
- Height of each story - 3m
- Wall thickness: W_1 - 115 mm

Table 1.1 shows the size of structured elements for multistory shear wall frame building.

Extended Three dimensional Analysis of Building Structures (ETABS) is used for the modeling and nonlinear analysis of the buildings.

10, 15, 20, 25, 30 story buildings are considered for performance based design and for parametric study. It includes comparison of Time period, base shear, story drift, story displacement, forces in shear wall using site specific response spectra and time history.

20 story building is considered for performance based design at various levels.

1.8 ORGANIZATION OF MAJOR PROJECT

The contents of major project are divided in to various chapters as follows;

An introduction of performance based design is covered in Chapter 1. It also includes the objectives of study and scope of work. Basic information about performance level, pushover analysis, and time-history analysis are discussed. It also includes the problem formulation for parametric study.

The literature review is presented in Chapter 2. It provides an overview of the available books, publications, and papers from various journals on the topic of nonlinear analysis. This chapter provides the understanding and importance of performance based design of structures.

Software implementation (modeling) for performance based design of shear wall building is described in Chapter 3. This chapter discusses use of ETABS for modeling for static nonlinear analysis. Three procedures for the performance based design are described and theoretical back ground for pushover analysis is covered.

Effects of hinge properties on nonlinear analysis are covered in Chapter 4. Theoretical procedure for finding moment rotation relationship is covered in this chapter. One 3D frame example is considered for understanding the role of plastic hinge properties in pushover analysis.

Time history and response spectra analysis for frame structure building is briefly discussed in Chapter 5. It mainly includes procedure of Time history analysis and Response spectra analysis using ETABS. Lateral load distribution over the height of structure considering time history and response spectrum is evaluated. Results are obtained in form of capacity, demand, performance point, Hinge formation pattern at performance point.

Time history and response spectra analysis for shear wall structure is discussed in Chapter 6. The parametric study is carried out to understand the behavior of shear wall buildings with the increase in height. Results are obtained in form of Time period, base shear, and story drift. The results are discussed in detail with graphical representation. Compared the Axial, shear and bending force results considering site response spectra, time history and IS: 1893-2002 specified response spectra.

Performance based design criteria for various performance levels is briefly discussed in Chapter 7. In this Chapter, 20 story shear wall building is considered for performance based design and results are represented in form of Time period, base shear, story drift, story displacement at performance point and percentage of steel in structure element.

The summary of the study, conclusion and future scope of work are presented in Chapter 8.

2. LITERATURE SURVEY

2.1 GENERAL

Literature in form of research papers, books and guideline regarding various aspects of performance based design are referred and review is presented in this chapter. The objective of literature review is to develop basic understanding about capacity curve, capacity spectrum, demand spectrum, performance level, pushover analysis, time history analysis etc.

2.2 LITERATURE REVIEW

The publication of **Applied Technology Council (ATC 40) [13]** provides guidelines for performance based design of building. It includes objectives, retrofit strategies, linear as well as nonlinear analysis procedure, modeling rules, foundation effect on performance design and descriptive limits of expected performance. It also includes example of inelastic analysis of building.

The publication of **FEMA 273 [16]** provides technical guidelines for the seismic rehabilitation of building. This document covers modeling and procedure of linear static analysis, linear dynamic analysis, nonlinear static analysis and nonlinear dynamic analysis. This document includes the performance based design for retrofit of an existing structure. This method can also be applicable for the new design. It also gives information regarding to foundations and geotechnical aspects.

2.2.1 Performance Based Design

Rui Pinho [1] provided information on inelastic analysis of concrete structure. Two case studies were considered, First was on multi-span continuous deck Motorway Bridge. Second concerned the dynamic analysis of a multi-story RC building with four story and three-bay with soft story at third floor. He considered artificial acceleration time history for 475 year and 975 year return period. Finally he compared the result of displacement and story drift of analytical and experimental work.

The handbook of **Farzad Naeim [2]** contains information about performance based seismic engineering. Information about ATC 40, FEMA 273 and FEMA 274 is included. Nonlinear Static (push over) Procedure, inelastic component behavior, force and corresponding inelastic displacement relationship, during the earthquake and actual hysteretic behavior are covered. One example of ATC 40 document is also included. It provides basic information on building performance level, pseudo lateral load, acceptance criteria to satisfy performance point requirement, target displacement etc.

Ahmed Ghobarah [4] provided basic introductions related to performance based design and displacement based design. Also the scope of recent studies investigated on PBD was presented. He discussed different topics like, various performance level based on damage state and drift limits, design evolution based on earthquake hazard level, challenges and future trends, design criteria based on different performance level, design methodology and deformation controlled design. Finally he concluded that developments in performance based design in seismic engineering would be directed toward a general design methodology that permit performance based design at multiple performance and hazard level.

After Kutch earthquake of January 26, 2001 in Gujarat, India, doubt arised about our professional practices, building by-laws, construction material, building codes and education for civil engineering. **Vipul Prakash [8]** provided information on seismic performance objective in India. He compared the result of base shear and horizontal seismic coefficient in IS 1893 during 1962 to 2002, effect of soil condition on spectral acceleration as per Indian code, ATC-40, FEMA 302 and FEMA 356. He presented the computed values of acceleration based site coefficient, F_a, and velocity-based site coefficient, F_v, by IS 1893-2002 and FEMA 302. He discussed about some questions like, "Are ductile design required by the new Indian seismic code?", "Why does India need to embrace performance-based engineering now?", "Why is civil engineering education flawed in India and how to remedy it to further the cause of performance-based engineering?".

The history of performance based design was introduced by **Singmund A. Freeman et al. [9].** Origin of the CSM (capacity spectrum method) was discussed. Capacity of structure could be determined on the basis of on-site observation, review of available drawing, calculations to approximate force-displacement relationships and engineering judgment. The Department of the army, the navy and the air force had published technical manuals of design guidelines for new construction in the early 1980s.

Andreas J. Kappos et al. [11] described design procedure for flexural plastic hinge zones based on serviceability criteria, selection of seismic action for PBD, set-up of the partial inelastic modal (PIM), verification of serviceability criteria, flexural design of non-dissipating zones on the basis of life safety criteria. They gave procedure for time history and push over analysis in SAP 2000. They analyzed a six story building using push-over and dynamic time history analysis and compared the result of inter story drift for different time history with various level of demand (serviceability, life safety, collapse prevent). They also compared the design in terms of economy with different serviceability condition.

Freeman [21] discussed performance based earthquake engineering (PBEE) during his 40 years of professional career. A case study for San Fernando earthquake was presented for buildings like hotel, veteran administrative hospital and Puget naval shipyard. A brief discussion about good features of PBEE over the current codes like UBC, ICBO, and SEAOC was presented. The origin of capacity spectrum method and the changes made in the building code after San Fernando earthquake were presented. He concluded that as two buildings are never similar no building code can provide essential safety against earthquake forces for a site specific and material specific problem. It is only through PBEE that one can approach a nearly exact seismic force resisting element through experimentation and judgment.

Ashraf Habibullah [15] described on push over analysis of a three-dimensional building in SAP2000. Step by step procedure for push over analysis was presented. Interpretation of analysis result was also presented.

2.2.2 Dynamic analysis

Based on the intensity of earthquake, performance level should be considered. In case of frequent earthquake consider minimum structural damage or repairable. Design Basis Earthquake (DBE) consider up to code level damage while Maximum Consider Earthquake (MCE) consider up to collapse prevention level. **Andrew, Hooper and Morgen [3]** studied core wall building which was designed for design basis earthquake and maximum considered earthquake. They used seven different site-specific ground motions for nonlinear time history analysis. When they had compared the result of story drift, they found it below the acceptable criteria line (2% inter story drift). NLTHA demand and DBE

(Amplification Factor 2) demand for wall shear force were nearly same in Y dir. But difference was more in X direction. Core wall moments in both the directions considering NLTHA demand were about 2 times DBE demand. So amplification factor can be considered as 2. The ratio of NLTHA and DBE demand was approximately 2 for all time period.

The book of **Anil K. Chopra [22]** contains information about theory and application of earthquake engineering. The applications of higher mode contribution to estimate the peak response of multi degree of freedom system directly from the earthquake response or design spectrum are presented. Procedure for response history analysis (RHA) and response spectrum analysis (RSA) are also discussed. It includes the details on construction of response and design spectra, effects of damping and yielding, distinction between response and design spectra.

2.2.3 Plastic Hinge Properties

Park and Paulay [17] discussed about structural mechanics and properties of structural element. Ultimate deformation, stress and strain relationship, ductility of member with flexure, moment curvature and rotation relationship, plastic hinge length are discussed in his book.

Mehmet Inel, Hayri Baytan Ozmen [18] had considered four storey and seven storey concrete building for study purpose. They observed that plastic hinge length and transverse reinforcement spacing had no influence on the base shear capacity; while these parameters had effects on the displacement capacity of the frames. The observations clearly showed that the user-defined hinge model was better than the default-hinge model in reflecting nonlinear behavior compatible with the element properties.

2.2.4 Force Pattern in Pushover Analysis

Sashi Kunnath and Erol Kalkan [12] investigated the correlation between demand estimates for various lateral load patterns used in non-linear static analysis and mean value of seven time history analysis. Results reported in this paper were based on a comprehensive set of pushover and non-linear time-history analyses carried out on eight and twelve story steel and concrete moment frames. They compared the result of inter-story story drift by pushover analysis and mean value of time-history analysis. They discussed about yield rotation, ductility demand, cyclic demand in typical beam and column of eight and twelve story building of steel and concrete.

Mark A. Aschheim et al. [20] provided information related to improvement of the accuracy of the target displacement estimates. For multi-degree of freedom system ATC 40 is not much effective. ATC 55, which is nearly completed, is highly focused on the development of improved inelastic analysis procedures. The example of 9 story steel frame building and 8 story reinforced concrete shear wall was discussed. They had compared the result of pushover analysis considering first mode, multimode, SRSS, Inverted triangular, rectangular lateral load pattern considering 11 recorded ground motion. Maximum drift 4% in steel frame and 2% in R.C.C. shear wall was considered. In this example coefficient of variation at 90% confidence level was observed. Finally they concluded that substantial errors could occur when estimating the response quantities such as inter story drift, story shear, and overturning moment using various load vectors.

Kalkan and Kunnath [23] proposed a new pushover analysis procedure through method of modal combination (MMC) for seismic performance in building. The MMC procedure accounted for higher mode effects by combining the response of individual modal pushover analysis and incorporated the effects of varying dynamic characteristics during the inelastic response. The inertia forces were generated for each mode and applied along the height of the building. MMC was based on invariant force distributions derived from the factored combination of independent modal contributions. They had studied four, six and thirteen story building with three different ground motions to predict expected seismic demand.

Evolution of lateral load pattern in pushover analysis was discussed by **Korkmaz and Sari [24].** They had considered lateral load pattern for pushover analysis as a triangular, as per IBC (international building code) (k=2) specification and rectangular. Four different framed structures were consider, which were typical reinforced concrete (R\C) frame systems and had four different natural periods. Pushover and nonlinear time history analyses results were compared to choose the best load distribution for specific natural period for this type of frame structure.

2.3 SUMMARY

In this chapter, review of relevant literature is carried out. The review of literature includes, modeling procedure for push over analysis, basic concept of performance based design, effect of hinge properties on nonlinear analysis.

3. MODELING FOR PERFORMANCE BASED DESIGN

3.1 GENERAL

After conceptual architectural planning of building, the structural engineers plans position of structure elements to make strong, stable and economical structure. Proper positioning and geometrical arrangement of column, beam and shear wall make a structure efficient and economical. In past modeling was carried out based on the mathematical parameter and some simplifying assumptions, which were based on the structural behavior depending on type of loading system and support condition. Today with increase in the growth of tall structures, accurate method and analysis tools are required. Nowadays modeling is carried out using software rather than manual method because of complexity of geometry, loading, limited time and economical design of structure.

Some of the software widely used for Nonlinear Analysis are Drain – 2DX, ETABS & SAP 2000. For present study, ETABS Version 9.5 [19] is used. The ETABS supports Indian Code of practices and nonlinear hinge properties can be defined as per FEMA – 273 [16] & ATC – 40 [13].

3.2 MODELING OF SHEAR WALL BUILDING IN ETABS

ETABS gives a facility for static nonlinear analysis of building. A typical example of modeling 20 story building is explained in this section. The plan of building is shown in Fig. 1.6. Column size and shear wall size of building are considered as per Table 1.1.

Steps for Modeling shear wall building in ETABS are as follows;

1. Grid lines are very important to create a model of building. In Fig. 3.1, a grid lines for 20 story building are generated.
2. Material properties are defined as per Indian code as shown in Fig. 3.2. Beams and columns are assigned as a rectangular element as shown in Fig. 3.3. Slab is defined as a membrane element and wall is defined as a shell element as shown in Fig. 3.4.

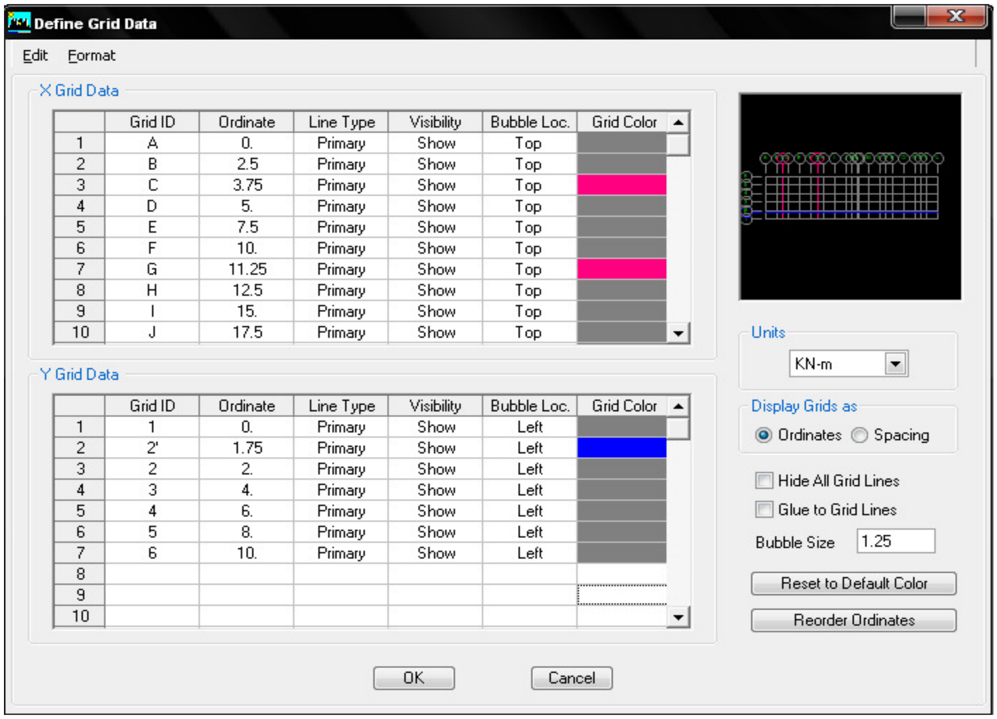

Fig. 3.1 Generation geometry

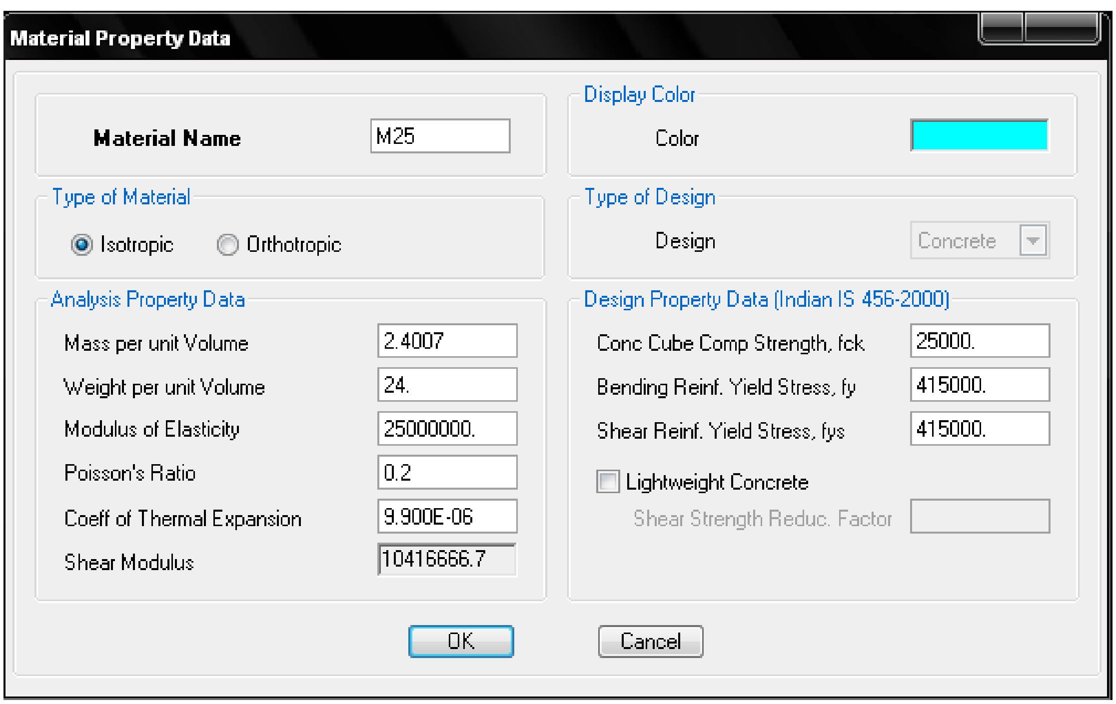

Fig. 3.2 Material property

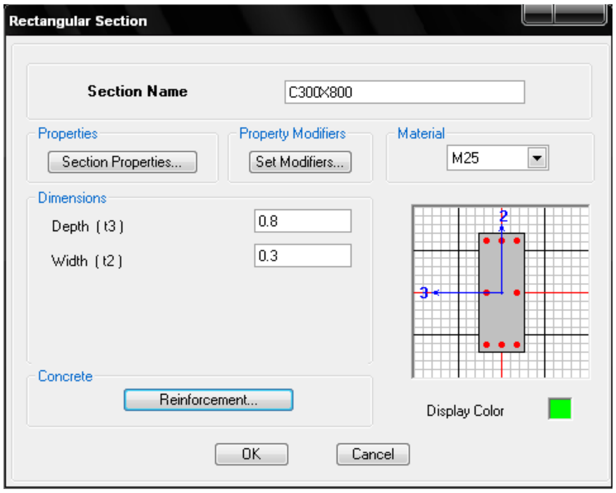

Fig. 3.3 Defining frame element

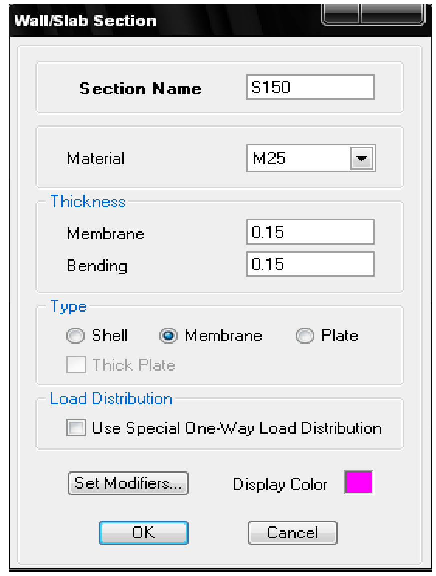

Fig. 3.4 Defining wall and slab

3. Prepare a model using draw line objects and draw area object.
4. Support condition is important parameter for any type of structure. It is based on foundation conditions. Fig. 3.5 shows definition of fixed support. Final 3D model with all structure elements is shown in Fig. 3.6.

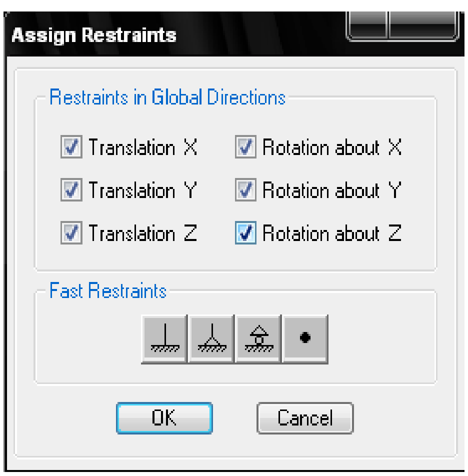

Fig. 3.5 Support condition

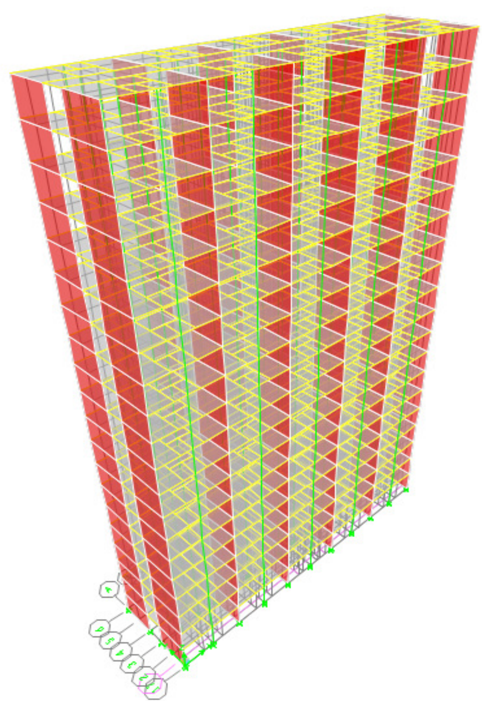

Fig. 3.6 3D model of 20 story building

5. Loading parameters are defined as per Indian Code as shown in Fig. 3.7 and 3.8. Consider dead load and super imposed load as a gravity load in vertical downward direction and earthquake load as lateral load in horizontal direction. Earthquake load is defined as per IS 1893-2002. Live load is considered as 3 kN/m^2 and wall load is considered as a super imposed dead load and is considered as 7.2 kN/m except at roof level on beam.

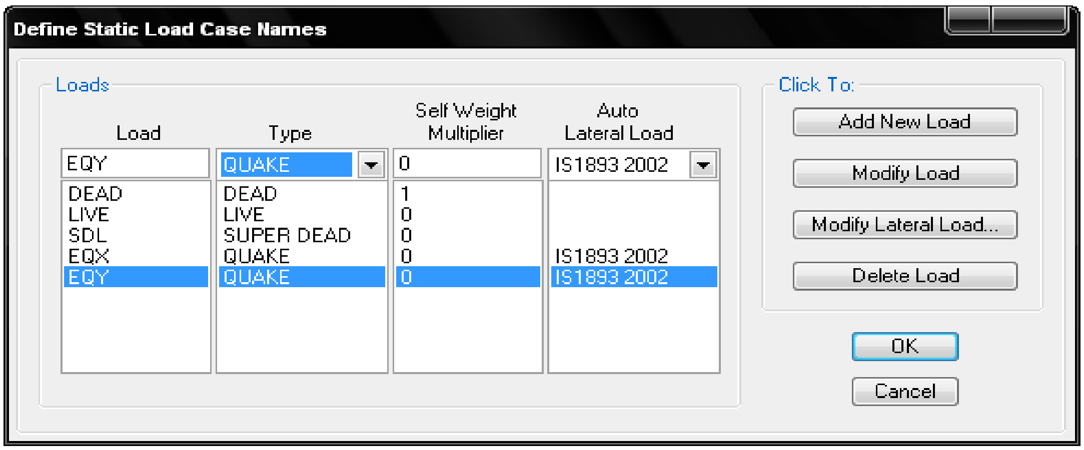

Fig. 3.7 Define a static load case

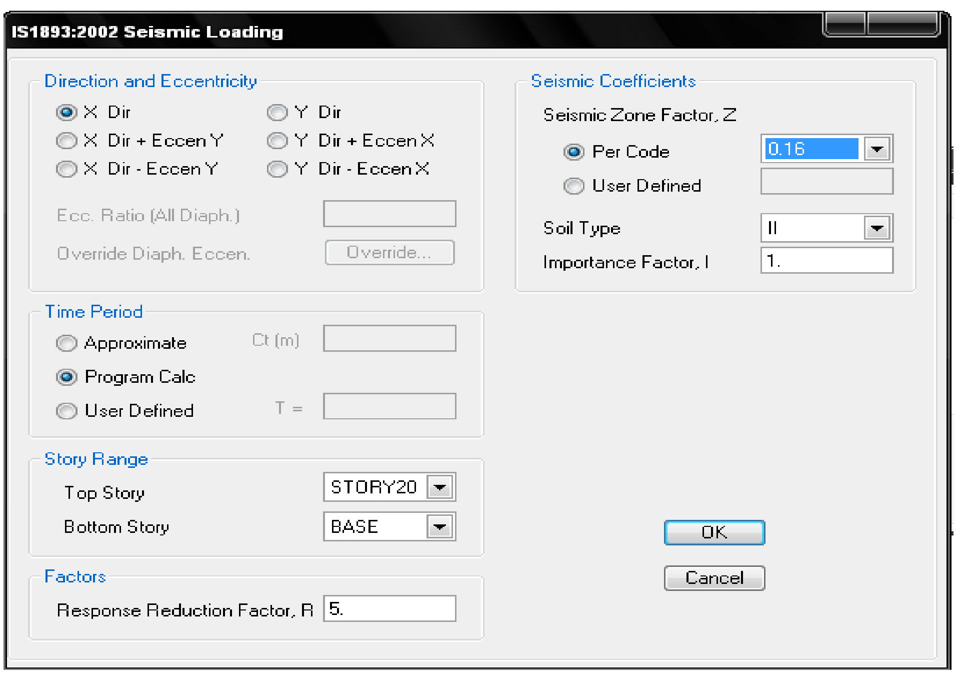

Fig. 3.8 Define a seismic loading as per IS: 1893-2002

6. Mass source is defined in modeling as shown in Fig. 3.9. As per IS: 1893-2002, 25% live load (of 3 kN/m^2) is considered on all floor of building except at roof level

7. Load combinations considered are as

   DL + LL

   DL ± EQ

   DL ± 0.8(LL+EQ)

   1.5DL + 1.5LL

   1.2(DL + LL ± EQ)

   1.5DL ± 1.5EQ

   0.9DL ± 1.5EQ

   All above combinations are as per the IS1893: (Part1)-2002 [25] and are shown in the Fig 3.10.

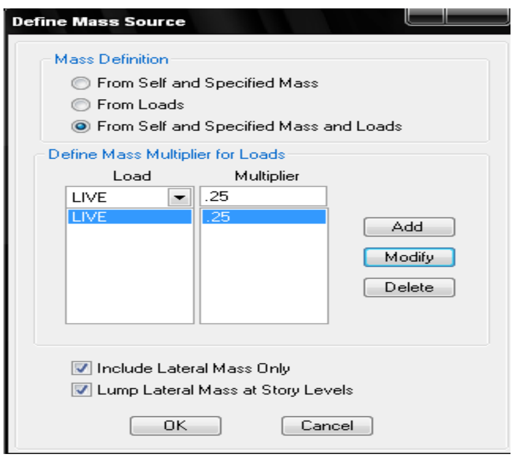

Fig. 3.9 Define mass source

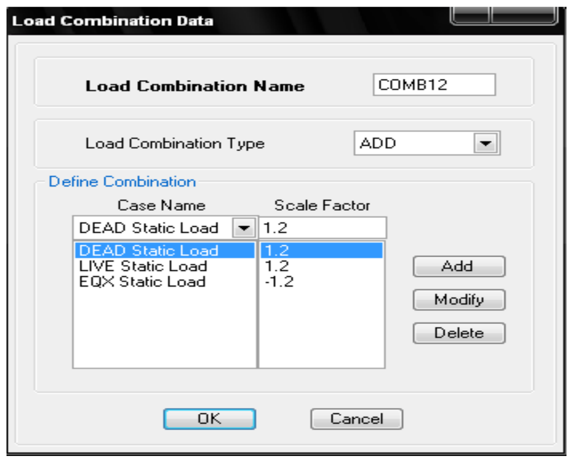

Fig. 3.10 Load combination

8. In building, slab is considered as a single rigid member during earthquake analysis. ETABS has a facility to create rigid diaphragm action for slab. For that, all slabs are selected first and apply diaphragm action for rigid or semi rigid condition.

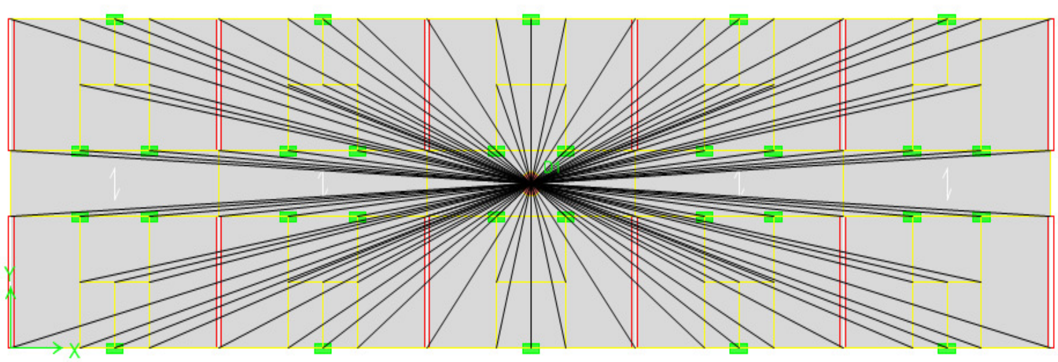

Fig. 3.11 Rigid diaphragm in plan

9. After application of rigid diaphragm, the entire shear wall is treated as a pier element in modeling. But for performance based analysis, shear wall is considered as a column element because ETABS has limitation to provide hinge properties in shear wall. Link beam is used for connecting center of column to beam element. Fig.3.12 shows the plan of building in ETABS.

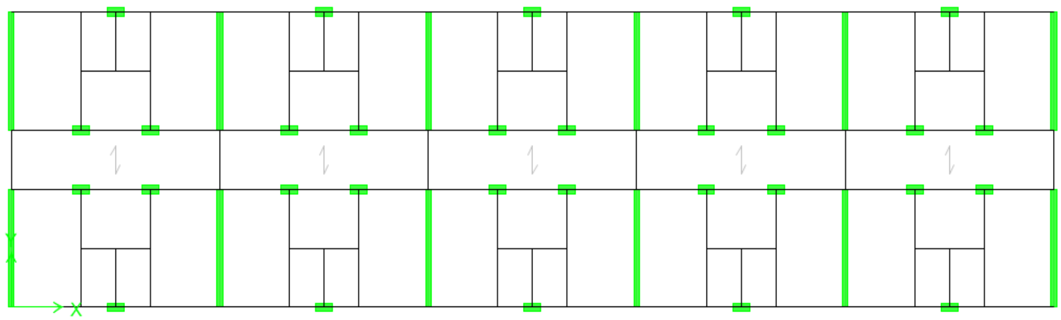

Fig. 3.12 Shear wall consider as a column

10. Linear analysis and design are carried out as per IS 456:2000[26]. Subsequently longitudinal reinforcement and hinge properties are defined as per FEMA – 273 [16] & ATC – 40 [13]. Detail description is given in subsequent section.

3.3 DEFINING NONLINEAR HINGE PROPERTIES

Inelastic behavior of element depends on hinge properties. Nonlinear moment-rotation and/or force-displacement relationship is very important for understanding the behavior of element. Practically hinge is developed in structure at certain distance form face of element. So, nonlinear hinges are assigned to an element at the distance equal to the plastic hinge length. These nonlinear hinges are only used during static nonlinear analysis. Otherwise in linear analysis the hinges behave as a rigid member.

Different types of nonlinear hinges used in ETABS such as axial hinge (P), shear hinge (V_2, V_3), torsion (T), moment hinge (M_2, M_3) and axial-moment hinge (P-M_2-M_3) as shown in Fig 3.13. The suffix 2, 3 indicates the direction of local axis of the member. In the present study three types of the Nonlinear hinges like Shear hinge (V_2), Moment hinge (M_3), Axial – Moment hinge (P–M_2–M_3) are used. For beam elements V_2 and M_3 hinge are assigned while for column element P-M_2-M_3 hinge is assigned.

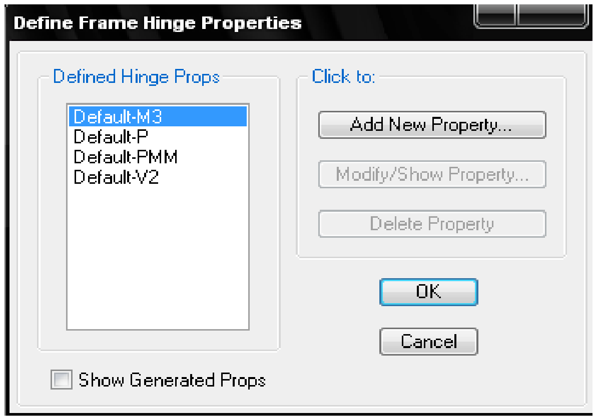

Fig.3.13 Default hinge type

3.3.1 Shear Hinge (V_2)

Shear resisting capacity of element depend on number of legs and spacing of stirrups. As the software doesn't have the data for stirrups so, yield shear capacity by default shear hinge cannot be used for analysis. Depending upon the grade of concrete, longitudinal reinforcement and stirrups provided in member, yield capacity is found and based on this relation between shear forces versus displacement as per ATC-40 [13] is derived. Derivation of shear hinge properties for beam and column are given in appendix A.

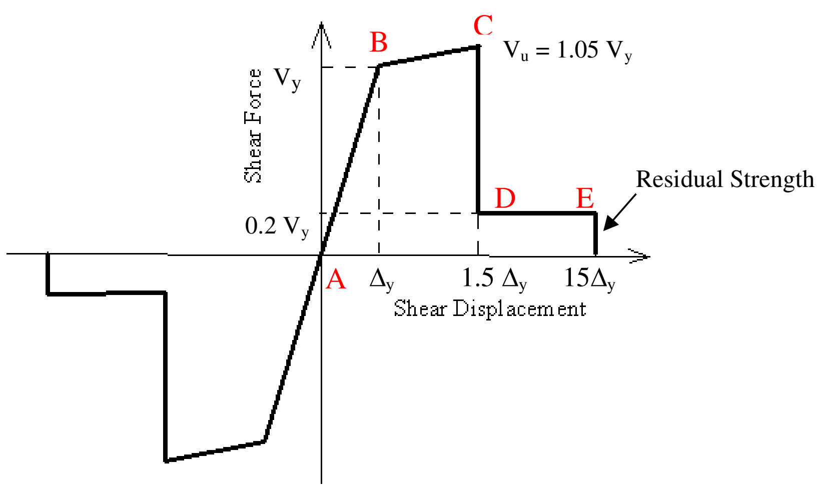

Fig. 3.14 Load – Displacement curve as per ATC - 40

In Fig. 3.14, Point A is starting point. A line up to point B shows yield condition of the hinge. As per ATC-40[13], Point C is the ultimate condition of the hinge. It is 5% more than the yield shear strength. The corresponding displacement is the ultimate displacement. After reaching to ultimate point the shear suddenly decreases and reaches to point D having some residual shear strength. For default hinge property the residual strength is taken as the 20% of the yield strength. Point E is the final deformation under residual strength.

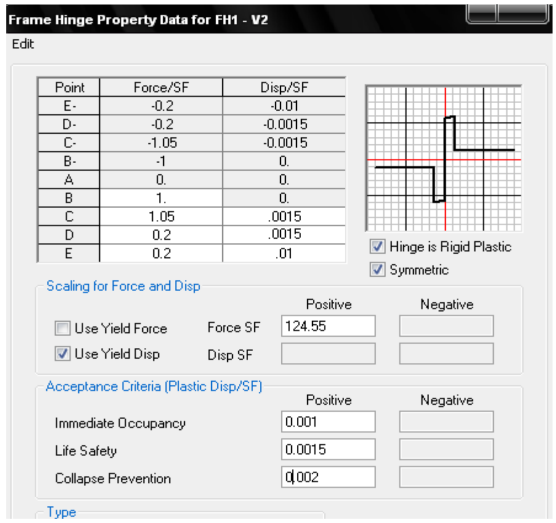

Fig. 3.15 User defined shear hinge

Fig. 3.15 shows user defined Nonlinear Shear (V_2) hinge. Yield force and Co-ordinate of shear hinge as per ATC 40 are assigned in tabular format.

3.3.2 Moment Hinge (M_3)

Fig. 3.16 (a) shows the moment versus rotation diagram. Moment hinges are developed based on the Moment–Rotation relationship. Moment hinges are depends on Flexural capacity of member which is directly related to size of member and tension reinforcement. Brief detail of moment hinges is given in ATC–40 for concrete member and FEMA–273 for steel member.

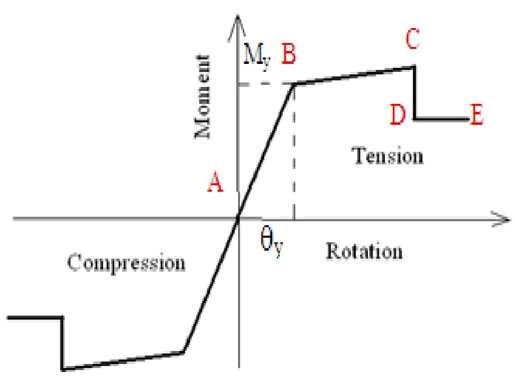

(a) Moment-Rotation curve as per FEMA-273

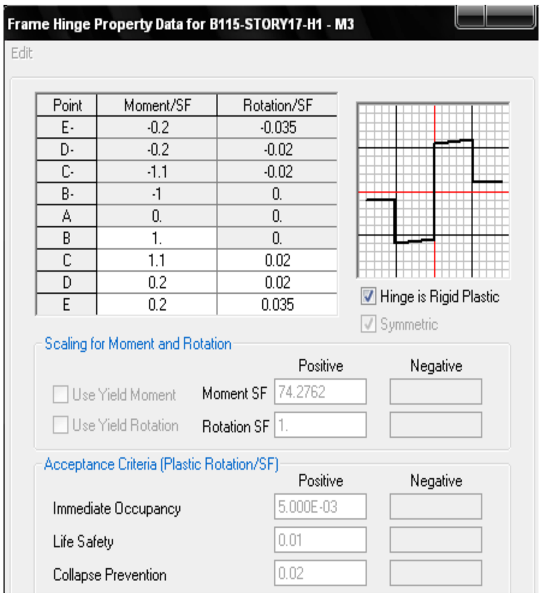

(b) Default moment hinge

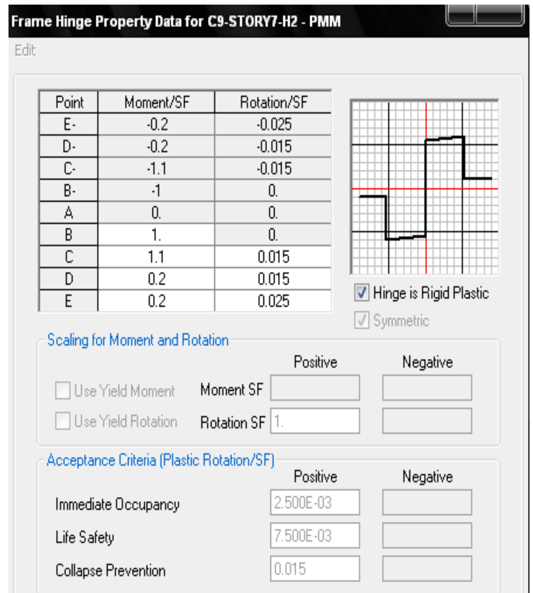

(c) Default P-M_2-M_3 hinge

Fig. 3.16 Moment hinge

For column member P-M_2-M_3 hinge is defined which is derived based on the P_u - M_u interaction curve. Immediate occupancy, life safety and collapse prevention limit are considered based on the FEMA 273 [16].

3.4 DEFINING LOAD APPLICATION

Loading can be applied in the form of any combination of primary Loads, Acceleration Loads, and Modal loads. A modal load is a specialized type of loading used for Pushover Analysis. The specified combination of loads is applied simultaneously. Normally the loads are applied incrementally from zero to the full specified magnitude. Loading is controlled by monitoring the displacement of structure

3.4.1 Load Application Control

Load control analysis is used when the magnitude of load acting on structure is known and the structure is expected to support that load. Under load control, all loads are applied incrementally from zero to the full magnitude. For a gravity loading, load controlled approach is used to find the capacity of structure as shown in Fig. 3.17(a).

3.4.2 Displacement Control

Displacement controlled approach is used when magnitude of loading is unknown. This is most useful for structures that become unstable and may lose load-carrying capacity during the lateral load analysis. Pattern for both the Load control and Displacement control approach applied to structure is determined by specialized combination of loads. Displacement control is an advanced feature for specialized purposes. Displacement control is simply used to measure the displacement that results from the applied loads, and to adjust the magnitude of the loading in an attempt to reach a certain measured displacement value. Procedure for selection of displacement control is shown in Fig. 3.17 (b).

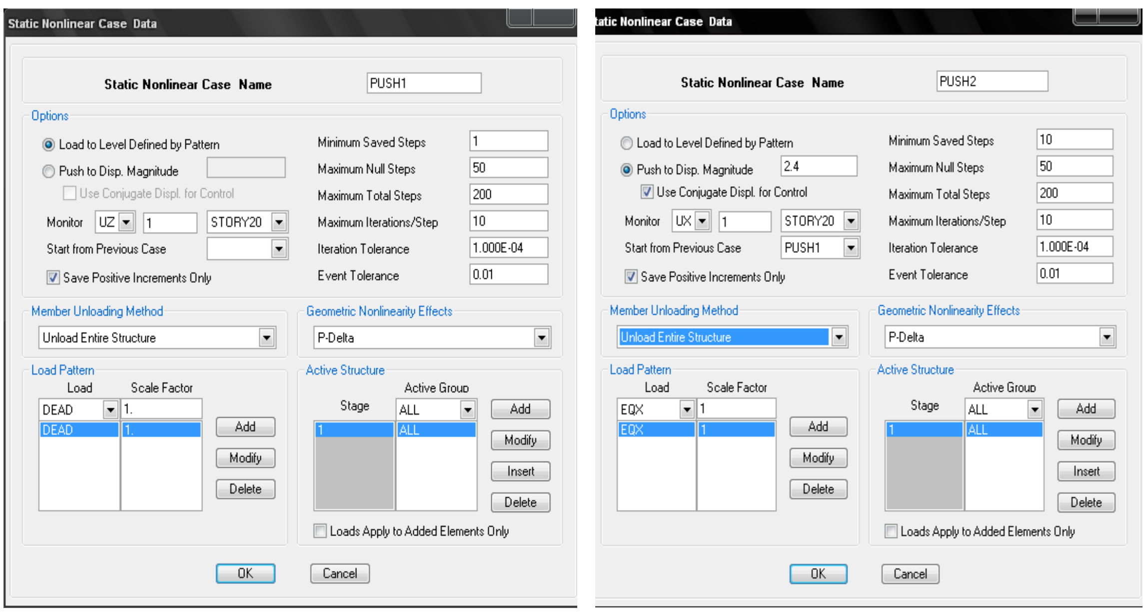

(a) Load controlled (b) Displacement controlled

Fig. 3.17 Load case for pushover analysis

3.5 HINGE UNLOADING METHOD

This option is used for Nonlinear Static Analysis (Pushover) during a hinge unloads. Hinge unloading occurs whenever the stress-strain (force-deformation or moment-rotation) curve shows a drop in capacity, as assumed from point C to point D or from point E to point F (complete rupture) as shown in Fig. 3.14.

Such unloading along a negative slope may be unstable in a static analysis, and a unique solution is not always mathematically possible. In dynamic analysis inertia provides stability and a unique solution. For Nonlinear Static Analysis, special methods are needed to solve this unstable problem. Different methods may work better with different problems. Different methods may produce different results with the same problem. ETABS Version 9.0.7 provides three different methods to solve this problem of hinge unloading as described below. If all stress-strain slopes are positive or zero, these methods are not used unless the hinge passes from point E and ruptures. Instability caused by geometric effects is not handled by these methods.

(1) Unload Entire Structure

(2) Apply Load Distribution

(3) Restart Using Secant Stiffness

3.5.1 Unload Entire Structure

When a hinge reaches a negative sloped portion of the stress-strain curve, the program continues to try to increase the applied load. If the strain tries to reverse, the program instead reverses the load on the whole structure until the hinge is fully unloaded to the next segment on the stress-strain curve. At this point the program reverts to increasing the load on the structure. Other parts of the building may now pick up the load that was removed from the unloading hinge. Whether the load must be reversed or not to unload the hinge depends on the relative flexibility of the unloading hinge compared with other parts of the structure that act in series with the hinge. This is very problem dependent, but it is automatically detected by the program. This method is the most efficient of the three methods available. It generally works well if hinge unloading does not require large reductions in the load applied to the structure. It will fail if two hinges compete to unload, i.e., where one hinges requires the applied load to increase while the other requires the load to decrease. In this case, the analysis will stop with the message "UNABLE TO FIND A SOLUTION", in which case one of the other two methods can be tried [19].

3.5.2 Apply Load Distribution

This method is similar to the first method, except that instead of unloading the entire structure, only the element containing the hinge is unloaded. When a hinge is on a negative-sloped portion of the stress-strain curve and the applied load causes the strain to reverse, the program applies a temporary, localized, self-equilibrating, internal load that unloads the element. This causes the hinge to unload. Once the hinge is unloaded, the temporary load is reversed, transferring the removed load to neighboring elements. This process is intended to imitate how local inertia forces might stabilize a rapidly unloading element.

This method is often the most effective of the three methods available, but usually requires more steps than the first method, including a lot of very small steps and a lot of null steps. The limit on null steps should usually be set between 40% and 70% of the total steps allowed. This method will fail if two hinges in the same element compete to unload, i.e., where one hinge requires the temporary load to increase while the other requires the load to decrease. In this case, the analysis will stop with the message "UNABLE TO FIND A SOLUTION". The *.LOG files to be checked for finding details of elements yielding [19].

3.5.3 Restart with Secant Stiffness

This method is quite different from the first two. Whenever any hinge reaches a negative sloped portion of the stress-strain curve, all hinges that have become nonlinear are reformed using secant stiffness properties, and the analysis is restarted. The Secant Stiffness for each hinge is determined as the secant from point O to point X on the stress strain curve, where: Point O is the stress-stain point at the beginning of the analysis case (which usually includes the stress due to gravity load); and Point X is the current point on the stress-strain curve. If the slope is zero or positive, or else it is the point at the bottom end of a negatively sloping segment of the stress-strain curve. When the load is reapplied from the beginning of the analysis, each hinge moves along the secant until it reaches point X, after which the hinge resumes using the given stress-strain curve [19].

3.6 PROCEDURE TO FIND OUT PERFORMANCE POINT

Performance based design (PBD) method has not been developed in detail previous section. In this section the use of nonlinear static procedure in general is emphasized with focus on capacity spectrum method. It provides a rigorous treatment of the reduction of seismic demand for increasing displacement. Two key element of a performance-based design procedure are demand and capacity. Demand is representation of the earthquake ground motion and Capacity is representation of the structure's ability to resist seismic demand. The performance is dependent on the capacity of structure which is able to handle the demand. Three primary elements considered for PBD are Capacity, demand and performance discussed in chapter 1.

3.6.1 Capacity spectrum method

Capacity spectrum method is also known as Acceleration-Displacement Response Spectrum (ADRS) method. This method requires both the capacity curve and the demand curve be represented in response spectra co-ordinates. Spectral reduction factor is given in term of effective damping and is calculated based on the shape of the capacity curve, the estimated displacement demand, and the resulting hysteresis loop. The capacity and demands is equal at which the capacity curve intersects the reduced demand curve, which is known as performance point.

To convert a response spectrum from the standard S_a vs T format found in the building code to ADRS format, it is necessary to determine the value of S_{di} for each point on the curve, where the S_{ai} and T meets. This can achieved using Eq. 3.1.

$$S_{di} = \frac{T_i^2}{4\pi} S_{ai} g \qquad \text{. . . . (3.1)}$$

Standard demand response spectra contain a range of spectral acceleration and a second range of constant spectral velocity (S_v). Spectral acceleration and displacement at period T_i are given by;

$$S_{ai} g = \frac{2\pi}{T_i} S_v \text{, and } S_{di} = \frac{T_i}{2\pi} S_v \qquad \text{. . . . (3.2)}$$

The resulting plot obtained from the above expressions is given in Fig.3.18

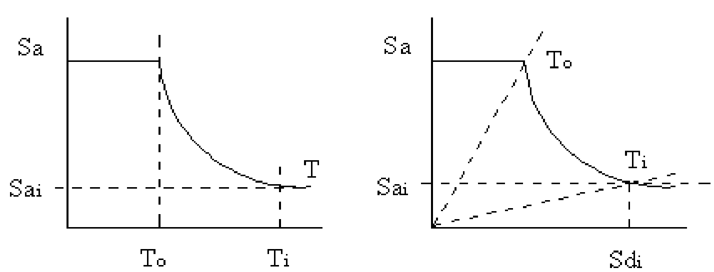

Standard Format (S_a vs T) ADRS Format (S_a vs S_d)

Fig. 3.18 Response spectrum conversion

The capacity spectrum can be developed from the pushover curve by a point conversion to the first mode spectral coordinates as shown in Fig.3.19. Any point V_i (Base shear) and δ_i (Roof Displacement) on the capacity or Pushover curve is converted in to the corresponding point S_{ai}, S_{di} on the capacity spectrum using Eq. 3.3 and 3.4.

$$S_{ai} = \frac{V_i / w}{\alpha_i} \qquad \text{. . . . (3.3)}$$

$$S_{di} = \frac{\delta}{PF_1 \times \phi_{1.roof}} \qquad \text{. . . . (3.4)}$$

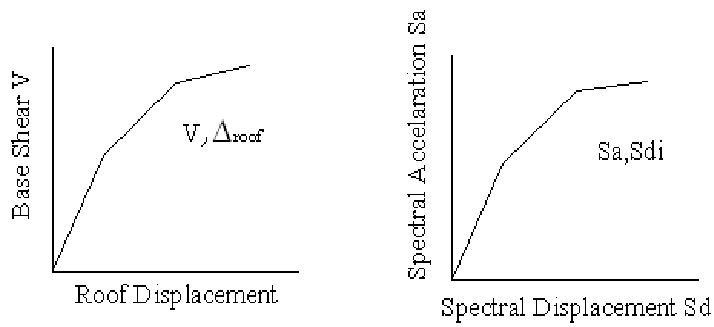

Capacity Curve   Capacity Spectrum

Fig. 3.19 Capacity spectrum conversion

Where α_i and PF_1 are the modal mass coefficient and participation factors for the first natural mode of the structure respectively. $\varnothing_{1,roof}$ is the roof level amplitude of the first mode.

The damping that occurs when the structure is pushed into the inelastic range can be viewed as a combination of viscous and hysteretic damping. Hysteretic damping can be representing as equivalent viscous damping. The total effective damping can be estimated by Eq. 3.5.

$$\beta_{eff} = k\beta_o + 0.05 \qquad \text{. . . . (3.5)}$$

The term k is damping modification factor considered as per Table 3.1 and β_0 is hysteretic damping calculated using Eq. 3.6.

$$\beta_0 = \frac{1}{4\pi} \frac{E_D}{E_{So}} \qquad \text{. . . . (3.6)}$$

Where E_D is the energy dissipated by damping and E_{So} is the maximum strain energy which is shown in Fig. 3.20. Derivation of E_D and E_{so} is given in ATC 40.

$$\beta_0 = \frac{0.637(a_y d_{pi} - d_y a_{pi})}{a_{pi} d_{pi}} \qquad \text{. . . . (3.7)}$$

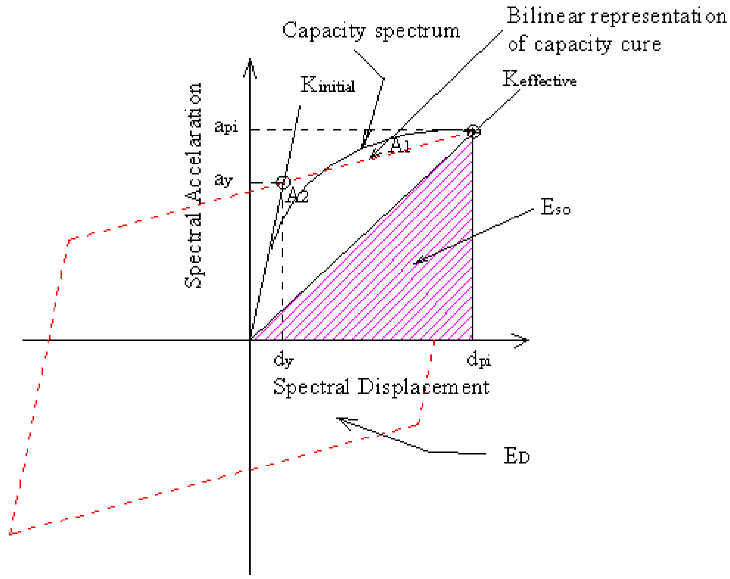

Fig. 3.20 Derivation of energy dissipated by damping

The reinforced concrete building that is not typically ductile structure. Therefore hysteresis loop area is imperfect compared to idealized hysteresis loop shown in Fig.3.20. Based on the type of new and existing structure damping modification factor is consider as per Table 3.1.

Table 3.1 Value for damping modification factor, k

Structure Behavior Type	β_0 (percent)	k
Type A	≤ 16.25	1.0
	≥ 16.25	$1.13 - \frac{0.51(a_y d_{pi} - d_y a_{pi})}{a_{pi} d_{pi}}$
Type B	≤ 25	0.67
	≥ 25	$0.845 - \frac{0.446(a_y d_{pi} - d_y a_{pi})}{a_{pi} d_{pi}}$
Type C	Any value	0.33

Classification of building based upon the shaking duration and condition of building is shown in Table 3.2.

Table 3.2 Structure Behavior Type

Shaking duration	Essentially New Building	Average Existing Building	Poor Existing Building
Short	Type A	Type B	Type C
Long	Type B	Type C	Type C

To account for the damping, the response spectrum is reduced by reduction factors SR_A and SR_V given by Eq. 3.8 and 3.9.

$$SR_A = \frac{3.21 - 0.68\,ln(\beta_{eff})}{2.12} \quad \text{. . . . (3.8)}$$

$$SR_V = \frac{2.31 - 0.41\,ln(\beta_{eff})}{1.65} \quad \text{. . . . (3.9)}$$

Both SR_A and SR_V must be greater than or equal to allowable value in Table 3.3

Table 3.3 Minimum allowable value for SR_A and SR_V

Structural Behavior Type	SR_A	SR_V
Type A	0.33	0.50
Type B	0.44	0.56
Type C	0.56	0.67

3.6.2 Procedure to obtain performance point

There are three methods to obtain performance point as discussed below:

Procedure A:

Add Strength or Stiffness or both to the building: As shown in Fig. 3.21, one of

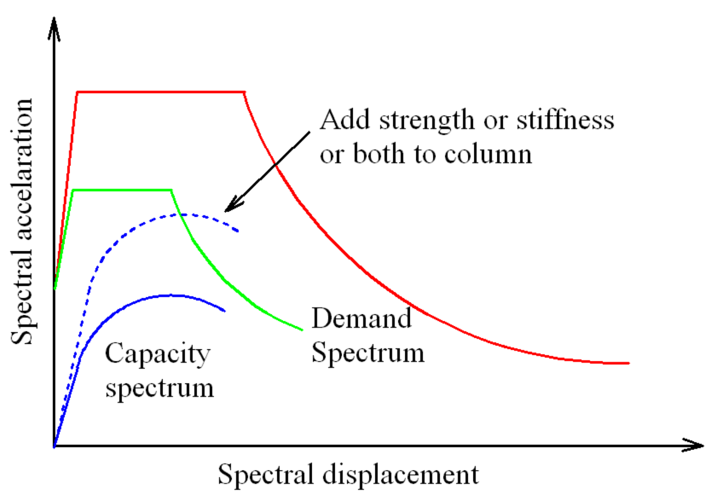

Fig. 3.21 Obtaining performance point by adding strength to system

the reasons for not getting performance point is that the demand is more and capacity is less. Adding strength or stiffness to the building raises the capacity of the building and subsequently the capacity curve of the building intersects the demand curve.

Procedure B:

Enhance System Ductility: Enhancing ductility in the building will increase the capacity of building to resist more loads in nonlinear range. As shown in Fig. 3.22 the capacity spectrum of this building will be elongated as it will be able to deform more under the constant load.

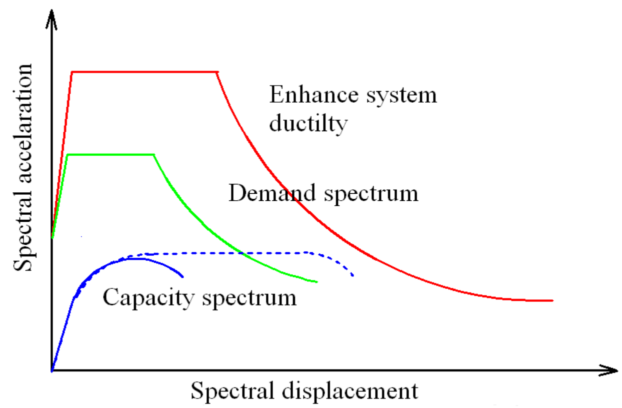

Fig. 3.22 Obtaining performance point by enhancing ductility to system

Procedure C:

Reduce Seismic Demand by adding Damping: Adding damping will reduce the demand as there will be more energy dissipation. This will bring down the demand curve as shown in Fig. 3.23.

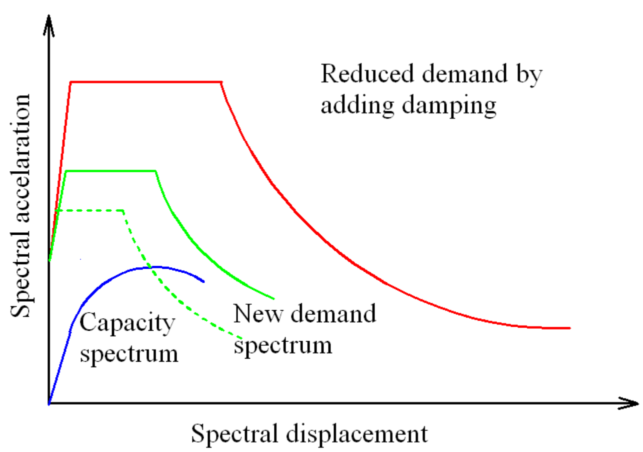

Fig. 3.23 Obtaining performance point by adding damping

3.6.3 Performance point on capacity and demand curve

Above three procedures are described in ATC-40 to find the performance point. The most transparent is the Procedure 'C'. To find the performance point using Procedure 'C' the following steps are followed:

1. Damped response spectrum (5% damping) appropriate for the site for the hazard level required for the performance objective is developed and converted to ADRS format using Eq.3.1 and 3.2.
2. The capacity curve as obtained from the nonlinear analysis is converted to a capacity spectrum using Eq. 3.3 and Eq. 3.4.
3. A trial performance point a_{pi}, d_{pi} is selected. This may be done using the equal displacement approximation (trial and error method to find maximum hysteresis loop area based on engineering judgment) as shown in Fig. 3.20.
4. The reduced demand spectrum is plotted together with the capacity spectrum in ADRS format.
5. A bilinear representation of capacity spectrum is developed such that the area under the capacity spectrum and the bilinear representation is the same. Bilinear representation depend on selection of starting point a_{pi},d_{pi} and ending point a_y,d_y.
6. If the reduced demand spectrum intersects the capacity spectrum at a_{pi},d_{pi} or if the intersection point d_p is within 5% of d_{pi}, then this point represents the performance point.
7. If the intersection point does not lie within acceptable tolerance (5% of d_{pi} or other) then select another point and repeat steps 4 to 7. The intersection point obtained in step 6 can be used as starting point for the next iteration.

The above procedure is represented graphically in Fig 3.24.

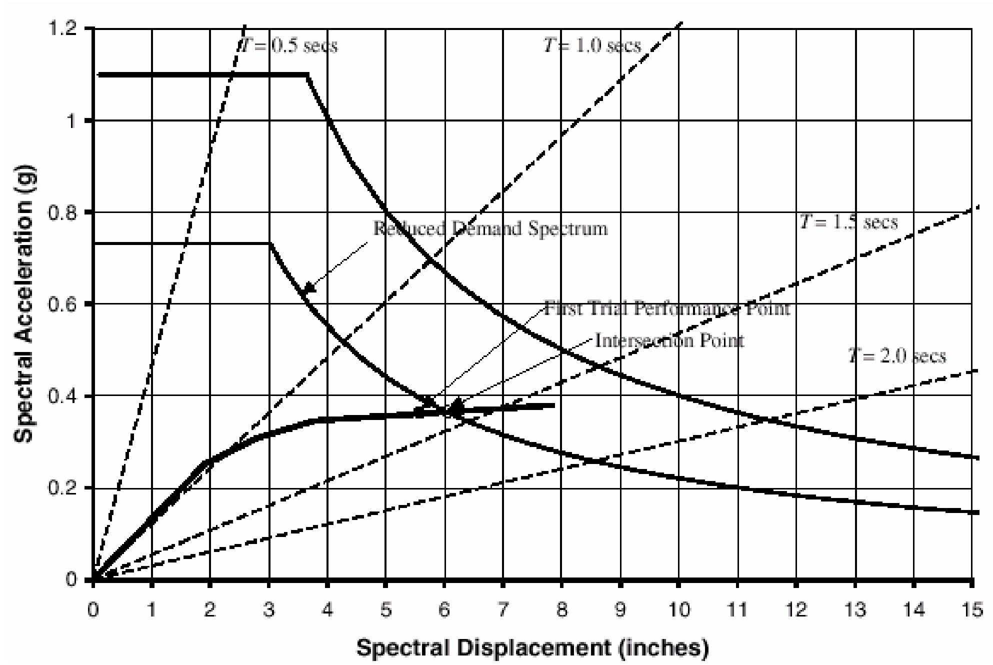

Fig 3.24 Performance point evaluation by procedure 'C'

3.7 SUMMARY

In this chapter step by step procedure of modeling structure using ETABS for performance based design is discussed. Inelastic properties of structural elements depend on the hinge formation. So implementation of hinge properties, load application and hinge unloading method are discussed for nonlinear static analysis.

Theoretical background for performance based analysis and procedures to obtain performance point are discussed.

4. EFFECTS OF PLASTIC HINGE PROPERTIES ON PUSHOVER ANALYSIS

4.1 GENERAL

The Nonlinear Static Analysis (Pushover) is an iterative procedure, in which loading is applied iteratively until the required displacement is achieved. The structure is capable of undergoing large deflections near-maximum load carrying capacity. This may save lives by giving warning of failure and preventing total collapse.

In implementation of pushover analysis, modeling is one of the important steps for providing nonlinear behavior of structural element. Modeling of structures for such analysis includes defining locations in structural components based on possibility of damage. Such locations, known as hinge, are classified depending on combinations of forces acting on it. Determination of nonlinear properties is quantified by strength and deformation capacities of each structural component in model. The ultimate deformation capacity of component depends on the ultimate curvature and plastic hinge length. In practice, FEMA 356 [14] and ATC 40 [13] documents specified default hinge properties are used due to convenience and simplicity, but one should be aware about the role of user defined hinge properties on results of pushover analysis. ETABS has already implemented these default nonlinear hinge properties.

This chapter aims to study the possible differences in result of pushover analysis due to default and user defined nonlinear hinge properties, using ETABS program.

4.2 MOMENT-CURVATURE RELATIONSHIP

The behavior of reinforce concrete section and influence of various parameter can be represented by relation between moment, curvature and axial force. Fig. 4.1 shows a straight element of Reinforced Concrete member with equal end moments and axial forces. The radius of Curvature R is measured from the neutral axis. The radius of Curvature R, neutral axis depth k_d, concrete strain in the extreme compression fiber ε_c, and tension steel strain ε_s, will vary along the member because between the cracks the concrete will be carrying some tension [17]. Considering only a small element of length dx of the member and using the notations of Fig. 4.1, the rotation between the ends of the element is given by,

$$\frac{dx}{R} = \frac{\varepsilon_c \times dx}{kd} = \frac{\varepsilon_s \times dx}{d(1-k)} \qquad \text{. . . . (4.1)}$$

$$\frac{1}{R} = \frac{\varepsilon_c}{kd} = \frac{\varepsilon_s}{d(1-k)} \qquad \text{. . . . (4.2)}$$

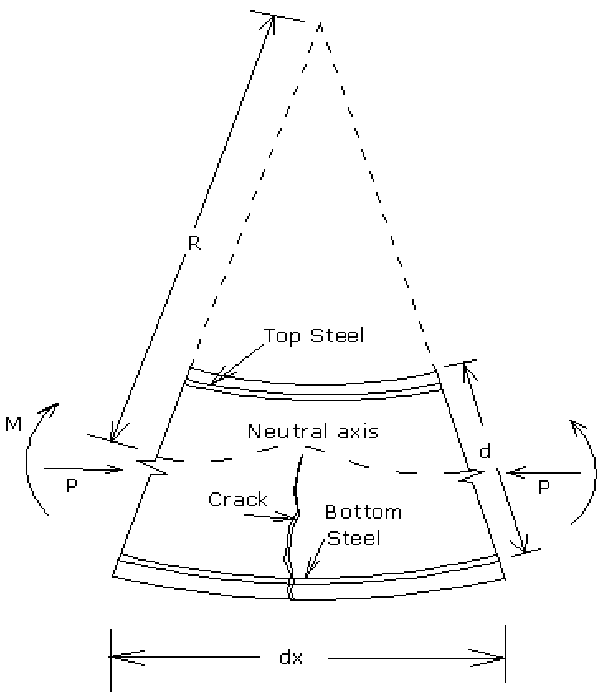

Deformation of a flexural member

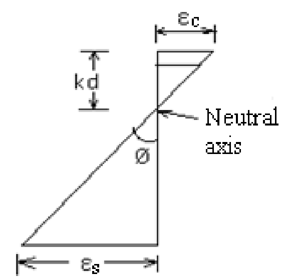

Strain Distribution

Fig.4.1 Deformation of a flexural member

Now $1/R$ is the curvature at the element (the rotation per unit length of member) and is given the symbol φ.

$$\varphi = \frac{\varepsilon_c}{kd} = \frac{\varepsilon_s}{d(1-k)} = \frac{\varepsilon_c + \varepsilon_s}{d} \qquad \text{. . . . (4.3)}$$

The curvature will actually vary along the length of the member because of the fluctuation of the neutral axis depth and the strains between the cracks. If the element length is small and over a crack, the curvature is given by Eq. 4.3 with ε_c and ε_s as the strains in concrete and steel at the cracked section.

If the strains at the critical section of a reinforced concrete beam are measured over a short gauge length as the bending moment is increased to failure, the curvature may be calculated from Eq. 4.3 permitting the Moment – Curvature relationship for the section to be obtained. Two such curves obtained from measurements on singly reinforced beams failing in tension and compressions are shown in Fig. 4.2. Both curves are linear in the initial stages, and the relationship between moment M and curvature Φ is given by the classical elastic equation,

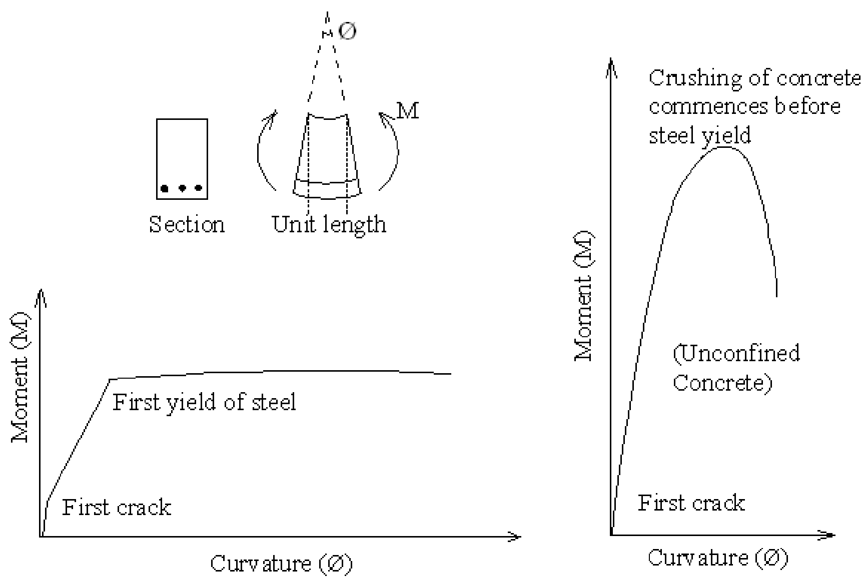

(a) Section Failing in Tension (b) Section Failing in Compression

Fig.4.2 Moment – Curvature relationships for reinforced concrete beam section

$$EI = MR = \frac{M}{\varphi} \quad \ldots . (4.4)$$

Where EI is the flexural rigidity of the section. With increase in moment, cracking of the concrete reduces the flexural rigidity of the sections, the reduction in rigidity being greater for the lightly reinforced section than for the more heavily reinforced section. The behavior of section after cracking is dependent mainly on the steel content. Lightly reinforced sections shows Fig. 4.2 (a) results in practically linear M–φ curve up to point of steel yielding. When steel yields, a large increase in curvature occurs at nearly constant bending moment, the moment rising slowly to a maximum due to an increase in the internal lever arm, then decreasing. In heavily reinforced sections shows in Fig. 4.2 (b), on the other hand, the M – φ becomes nonlinear when the concrete enters in inelastic part of stress – strain relationship, and failure can be quite brittle unless the concrete is confined by closed stirrups at close centers. If the concrete is not confined, the concrete crushes at a relatively small curvature before the steel yields, causing an immediate decrease in the moment–carrying capacity. To ensure ductile behavior in practice, steel contents less than the balanced design value are always used for beams [17].

4.3 DETERMINATION OF MOMENT, CURVATURE AND ROTATION

Under lateral load, the structures dissipate energy under severely imposed deformations through critical regions of the members, often termed as "plastic hinges". Location of plastic hinges in the structures is important, because plastic hinges cause excessive deformation. In plastic hinges regions, rotations of the member is very high which leads to failure.

Fig 4.3 (a) represent the general case of doubly reinforced rectangular section at first yield of the tension steel and at ultimate concrete strain. The curvature at first yield of tension steel Φ_y may be found from Eq. 4.5 in term of the strain in steel at yield for the steel contents considered. When the tension steel first reaches the yield strength, the stress in extreme fiber of the concrete may be appreciably less than the concrete stress [17].

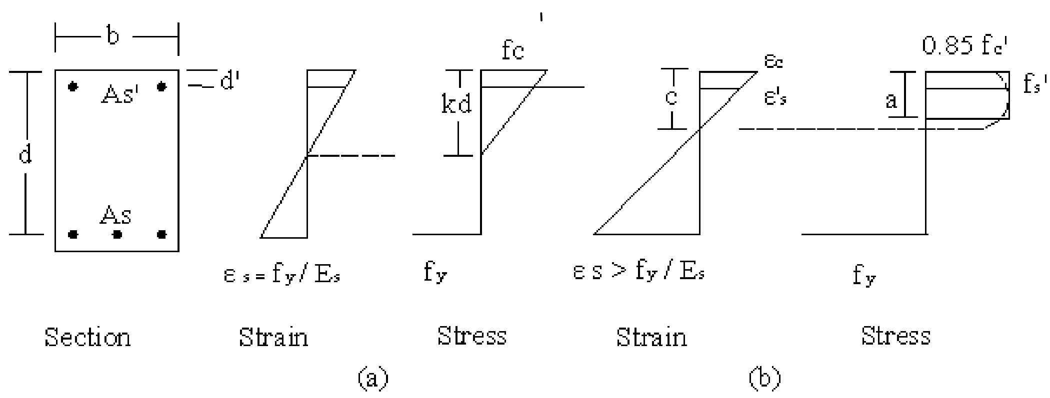

Fig. 4.3 Doubly reinforced beam section with flexure. (a) At first yield. (b) At ultimate.

The stress-strain curve for concrete is approximately linear up to 0.7 f_c'; hence if the concrete stress does not exceed this value when the steel reaches yield strength, the depth to neutral axis may be calculated using elastic theory formula. Once neutral axis depth factor k has been determined, the magnitude of force and the centroid of the compressive force in steel and the concrete can be found. The equation defining the moment and curvature at first yield are.

$$k = \left[(p_t + p_t')^2 n^2 + 2\left(p_t + \frac{p_t' d'}{d} \right) n \right]^{1/2} - (p_t + p_t')n \qquad \text{. . . . (4.5)}$$

$$M_y = A_s \ f_y \ jd \qquad \text{. . . . (4.6)}$$

$$\phi_y = \frac{f_y / E_s}{d(1-k)} \qquad \text{. . . . (4.7)}$$

Where

$n = E_s/E_c$

$p_t = A_s/bd$

$p_t' = A_s'/bd$

A_s = area of tension steel

A_s' = area of compression steel

b = width of section

d = effective depth of tension steel

d′ = distance from extreme compression fiber to centroid of compression steel

E_c = modulus of elasticity of concrete

E_s = modulus of elasticity of steel

f_y = yield strength of steel

jd = distance from centroid of compressive force in the steel and concrete to the centroid of tension

If the stress in extreme compression fiber of the concrete is greater than approximately 0.7 f_c', the neutral axis depth at first yield of tension steel should be calculated using the actual curved stress-strain curve from the concrete. However, an estimate may be obtained from the straight line formula even if the computed stress is as high as f_c'. Fig. 4.4 indicates that the value for k calculated from the straight line formula will be smaller than the actual value for k if concrete stress distribution is curve, which will lead to an underestimating of Φ_y and overestimation of M_y [17].

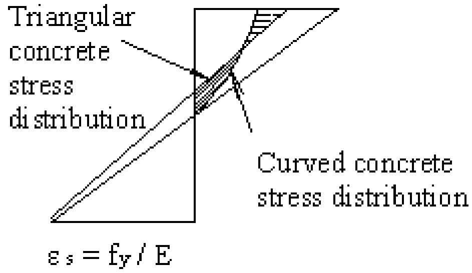

Fig. 4.4 Stress and strain distribution for same compressive force in concrete when steel reaches yield stress

The ultimate curvature and moment of doubly reinforced section are given by following equation.

$$a = \frac{A_s f_y - A_s' f_y}{0.85 f_c' b} \qquad \text{. . . . (4.8)}$$

$$M_u = 0.85 f_c' a b \left(d - \frac{a}{2} \right) + A_s' f_s' (d - d') \qquad \text{. . . . (4.9)}$$

$$\phi_u = \frac{\varepsilon_c}{c} \qquad \text{. . . . (4.10)}$$

4.4 PLASTIC HINGE ZONES

In R.C. member, the plastic hinge is defined as that section of the beam, where plastification of concrete in compression and yielding of steel in tension zone has occurred causing rotation of the section under constant ultimate moment.

Location of plastic hinge in beams must be clearly identified since special detailing requirements are needed in inelastic regions of beams of frames subjected to earthquake forces. In capacity design concept, potential plastic hinges regions within structure are clearly defined. These are designed to have dependable flexural strengths as close as practicable to the required strength.

Subsequently, these regions are carefully detailed to ensure that estimated ductility demands in these regions can be reliably achieved. This is obtained primarily by closely-spaced and well anchored transverse reinforcement.

4.4.1 Types of Plastic Hinges

Two types of plastic hinge develop in structure element based on the locations as:

I. Positive plastic hinges.

II. Negative plastic hinges.

I. Positive plastic hinges.

Positive plastic hinges are generally formed in the long span beams, which is dominating by gravity load, where the tension reinforcement is at the bottom and compression at top fiber as shown in Fig.4.5. If the plastic hinges are formed at column faces, the hinge plastic rotations is θ. Positive plastic hinges formed at the distance l_1 from right end of beam. Therefore rotation of the positive plastic hinges $\theta' = (l/l_1)\,\theta$ as shown in Fig.4.5

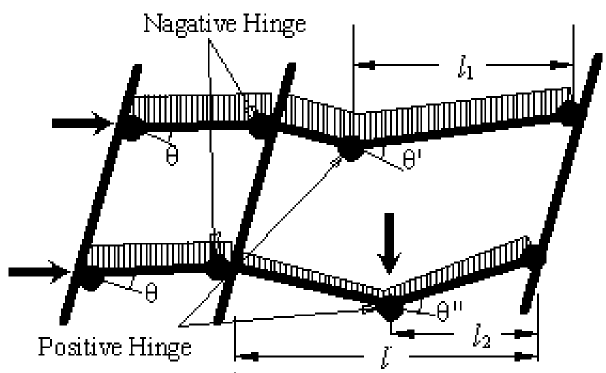

Fig. 4.5 Beam hinge pattern

II. Negative Plastic Hinge

Negative plastic hinges are generally formed in short span of beam, which is dominated by seismic actions or lateral force, where the tension at top and compression at bottom occurs. This hinges are formed adjacent to the face of the column or at the maximum negative moment regions. As shown in Fig. 4.5 the plastic hinges formed at the adjacent side of the column, rotation of the beams at the plastic hinges is θ.

4.4.2 Plastic Hinge Length

M.J.N Priestly and T. Paulay [22] described the equation for hinge length as,

$$L_p = 0.08L + 0.022 \times f_y \times d_{bl}$$

Where, L_p is the potential plastic hinge length, L is the distance from the critical section to the point of contraflexure, f_y is the yield strength of the beam longitudinal bars of diameter d_{bl} [22].

The special detailing of the transverse reinforcement should be required in *2h* length of plastic hinge. Where, h is the depth of the section. When critical section of the plastic hinge is at the face of the supporting column, this length is measured from the critical section towards the span as shown in Fig.4.6.

Where the critical section of the plastic hinge is not at the face of a column and is located at a distance not less than the beam depth *h* away from a column, the length should be assumed to begin between the column face and the critical sections, at least *0.5×h* from the critical section, and to extend at least *1.5×h* past critical section towards mid span. At positive plastic hinges where the shear force is zero at the critical sections, such as at *C* shown in Fig. 4.6, the length should extended by h in both directions from the critical sections.

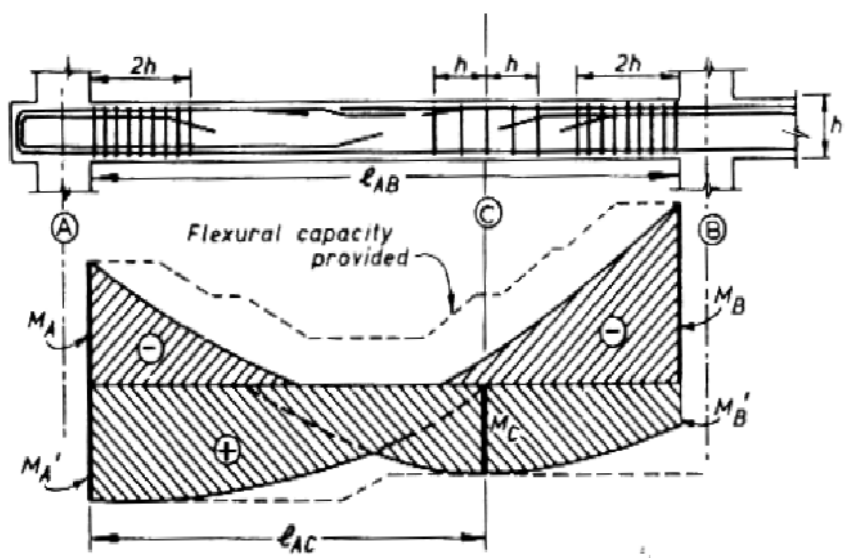

Fig. 4.6 Locations of Potential plastic hinges where special detailing is required

Redistribution of moments and shear forces relies entirely on rotation within plastic hinges in the beams. The apparent redistribution of moments and shear forces between individual columns also relies on plastic hinge rotations in the beam only. It is recommended that in any span of a continuous beam in a ductile frame, the maximum moments may be decreased, if so desired, by up to 30% of the absolute maximum moments derived for that span from elastic analysis, for any combination of seismic and gravity loading. This limit is placed to ensure that plastic hinges do not occur prematurely under a moderate earthquake, and that the beam rotational ductility demand is not increased excessively.

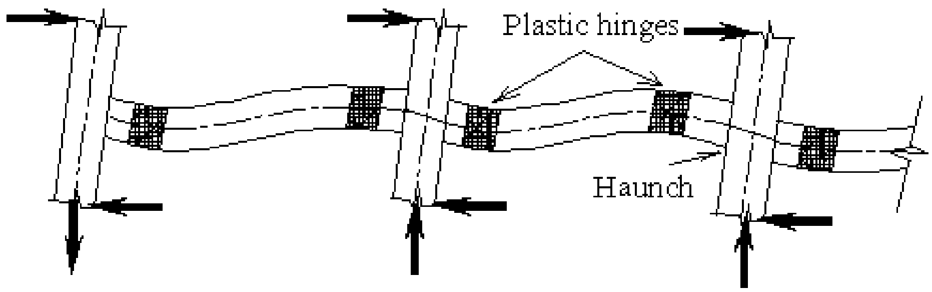

Fig. 4.7 Beams with relocated plastic hinges

4.5 ANALYSIS AND DESIGN OF 3D FRAME IN ETABS

A three dimensional reinforced concrete (RC) frame structure is considered for nonlinear analysis as shown in Fig. 4.8. All beams are of 250×400 mm size and columns are 400×400 mm size with 150 mm slab thickness. 3 kN/m^2 live load and 1 kN/m^2 floor finish load are considered.

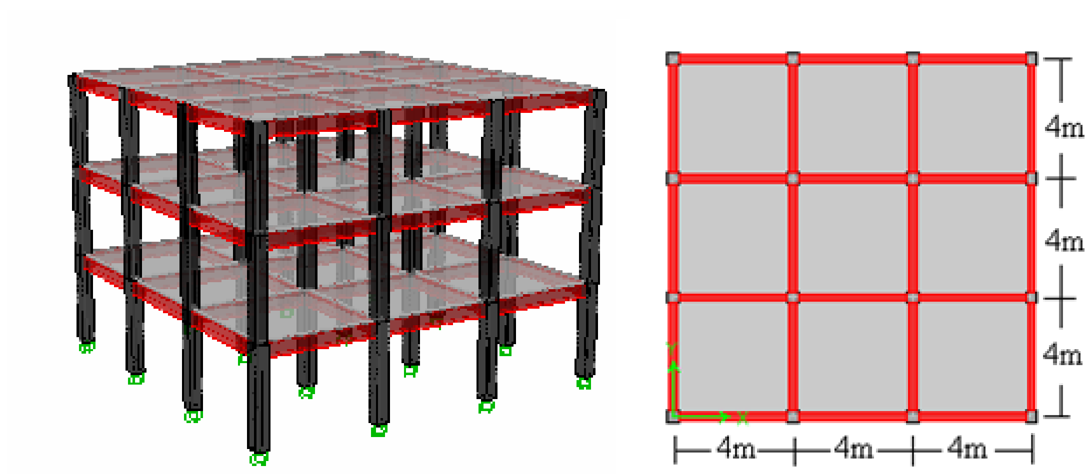

Fig. 4.8 3D Frame of building

Earthquake parameters considered are medium soil, Zone V and response reduction factor 5. Story height is taken 3m. Material properties are assumed as M25 concrete and Fe 415 longitudinal and transverse reinforcement.

Design is carried out using ETABS software as per IS 456-2000. Reinforcement in beam and column are shown in Fig. 4.9.

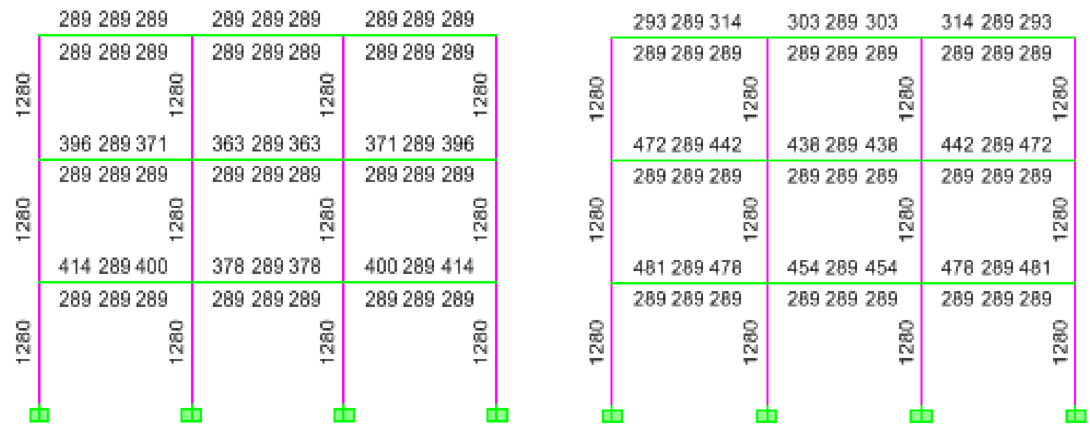

(a) Outer Frame (b) Inner Frame

Fig. 4.9 Reinforcement (mm^2) detailing in Element

Based on the size of member and percentage of reinforcement in beam, moment rotation relationships are derived at yield condition using Eq. 4.6 and Eq. 4.7 and at ultimate condition using Eq. 4.9 and Eq. 4.10. An EXCEL sheet is developed to calculate moment curvature relationship as shown in Fig. 4.10.

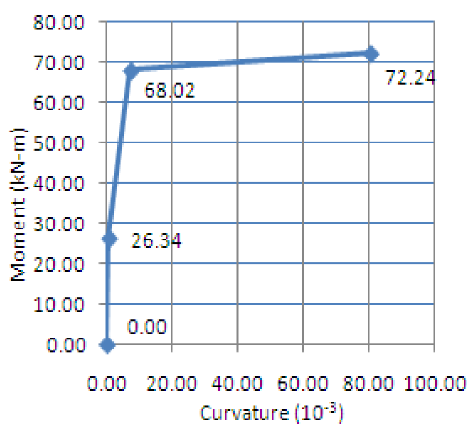

Fig. 4.10 Moment curvature relationship

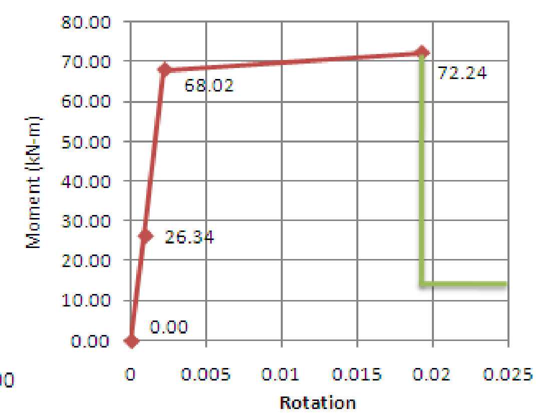

Fig. 4.11 Moment rotation relationship

The pushover analysis consists of the application of gravity loads and a representative lateral load pattern. The frames are subjected to gravity analyses and simultaneously lateral loading. Gravity loads are in place during lateral loading. In all cases, lateral forces are applied monotonically in a step-by-step in nonlinear static analysis. The applied lateral forces are proportional to the product of mass and the first mode shape amplitude at each story level under consideration. Moment rotation relationship is most important to understand the behavior of structural element. This relation is derived using EXCEL sheet as a user defined hinge properties. Moment versus curvature relationship is shown in Fig. 4.10. ETABS has a facility to consider the user defined hinge properties. User defined moment versus rotation relationship as given in ETABS is shown in Fig. 4.11.

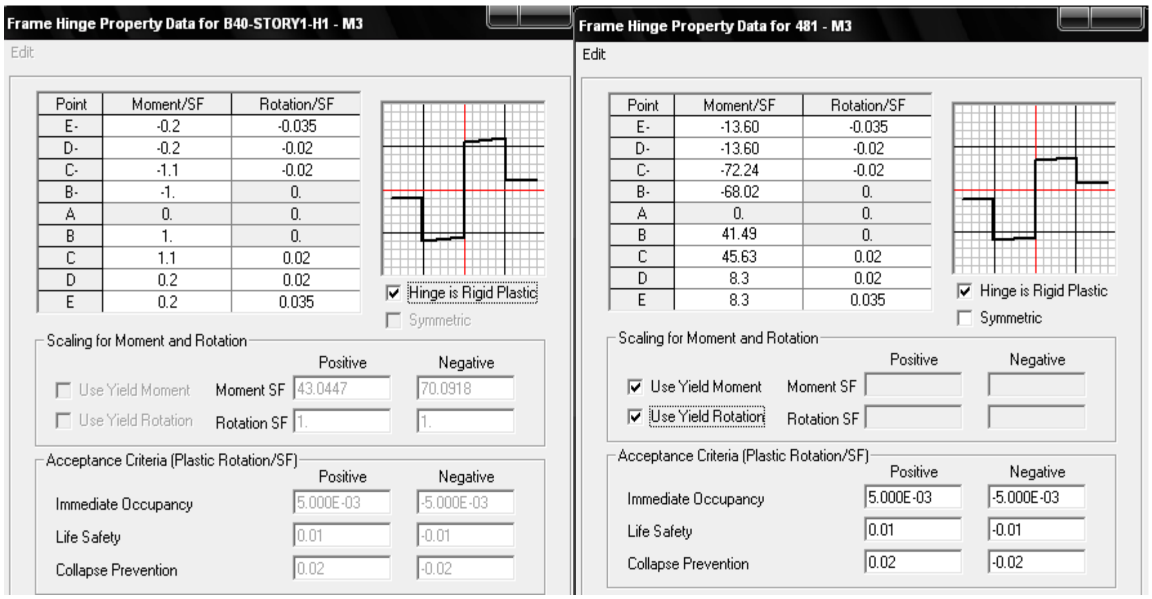

(a) Default moment hinge properties (b) User defined moment hinge properties

Fig. 4.12 Moment hinges in ETABS

Default hinge properties are based upon a simplified set of assumptions that may not be appropriate for all structures. One may want to use default properties as a starting point, and explicitly override properties as needed during the development of model. This study defines three points corresponding to 10% for immediately occupancy, 50% for life safety, and 90% for collapse prevention for plastic hinge deformation capacity. Moment versus rotation relationship based on default hinge properties is shown in Fig. 4.12 (b).

4.6 RESULT AND DISCUSSION

The hinge patterns are plotted at yielding point (top displacement is 0.0241 m) as shown in Fig. 4.13 and at a near to collapse point (top displacement is 0.072 m) as shown in Fig. 4.14.

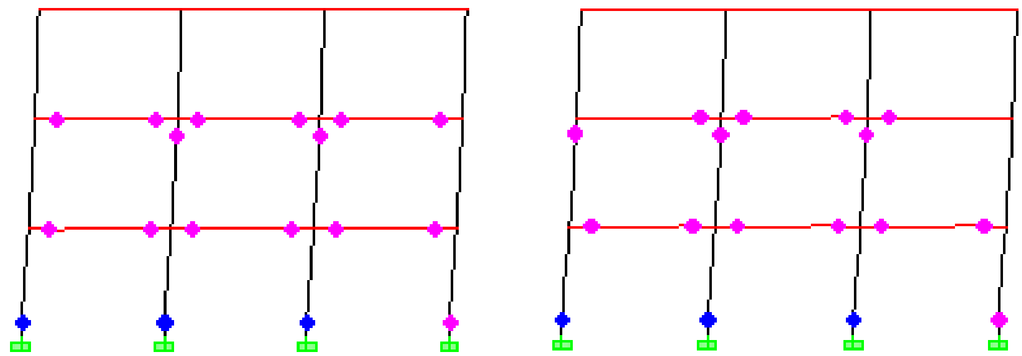

Default hinge properties User defined hinge properties

(a) Outer Frame

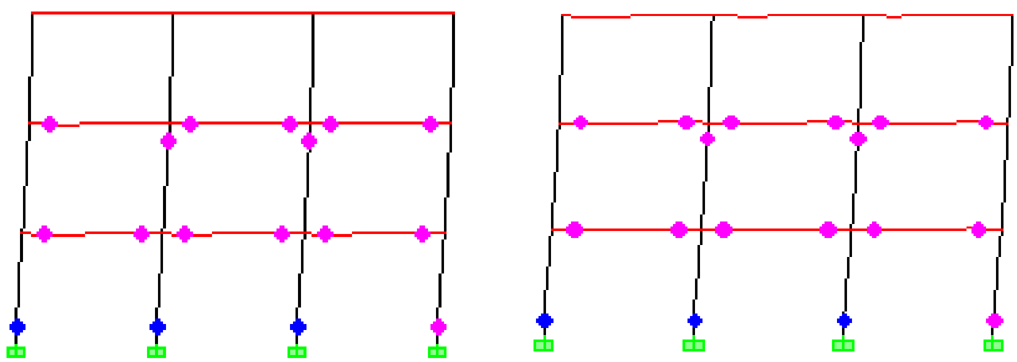

Default hinge properties User defined hinge properties

(b) Inner Frame

Fig. 4.13 Hinge formation at yielding point

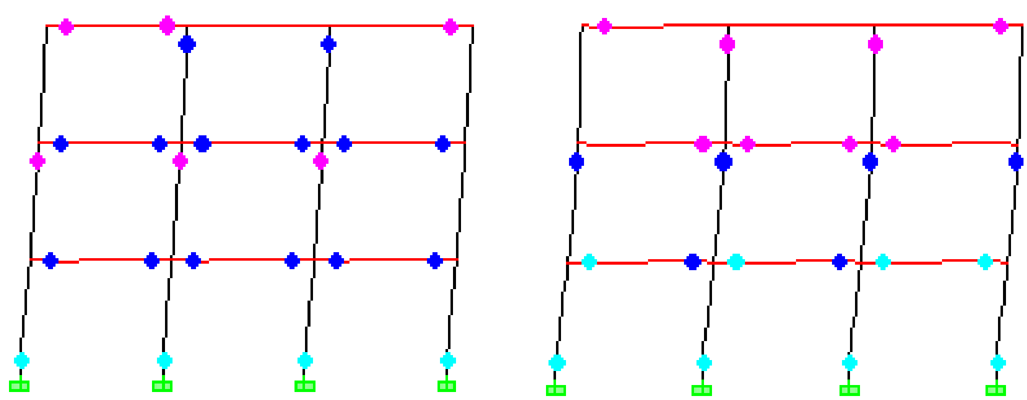

Default hinge properties User defined hinge properties

(a) Outer Frame

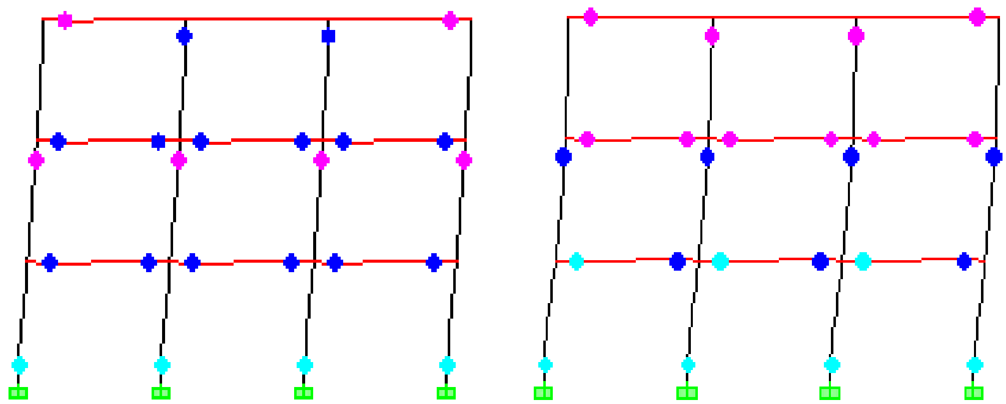

Default hinge properties User defined hinge properties

(b) Inner Frame

Fig. 4.14 Hinge formation at near to collapse point

Before carrying out nonlinear analysis, nonlinear static load cases are to be defined. Two load cases are defined one having gravity load pattern (PUSH1) and second having lateral load pattern in X dir. (PUSH2). For push over analysis first apply the gravity loading and then use lateral displacement in sequence for derive capacity curve and demand curve. Development of hinges during pushover analysis considering user defined and default hinge properties are shown in Fig. 4.15 and 4.16.

PUSHOVER CURVE

File

Step	Displacement	Base Force	A-B	B-IO	IO-LS	LS-CP	CP-C	C-D	D-E	>E	TOTAL
0	0.0000	0.0000	228	12	0	0	0	0	0	0	240
1	0.0095	467.2738	208	32	0	0	0	0	0	0	240
2	0.0116	525.6688	184	56	0	0	0	0	0	0	240
3	0.0187	604.6731	170	58	12	0	0	0	0	0	240
4	0.0242	630.8166	160	64	16	0	0	0	0	0	240
5	0.0303	648.9831	152	72	16	0	0	0	0	0	240
6	0.0313	650.3314	144	24	56	16	0	0	0	0	240
7	0.0719	669.3606	142	22	60	16	0	0	0	0	240
8	0.0752	670.8160	118	46	60	0	0	0	4	12	240
9	0.0752	416.1241	118	46	60	0	0	0	2	14	240
10	0.0766	416.2316	118	30	76	0	0	0	0	16	240
11	0.0568	406.2360	240	0	0	0	0	0	0	0	240

Fig. 4.15 Tabular format of pushover curve considering default hinge properties

PUSHOVER CURVE

File

Step	Displacement	Base Force	A-B	B-IO	IO-LS	LS-CP	CP-C	C-D	D-E	>E	TOTAL
0	0.0000	0.0000	236	4	0	0	0	0	0	0	240
1	0.0092	450.3966	206	34	0	0	0	0	0	0	240
2	0.0115	519.7038	188	52	0	0	0	0	0	0	240
3	0.0180	594.0006	170	58	12	0	0	0	0	0	240
4	0.0255	632.7687	150	74	16	0	0	0	0	0	240
5	0.0327	653.0224	148	76	16	0	0	0	0	0	240
6	0.0358	656.3423	148	36	26	30	0	0	0	0	240
7	0.0718	678.7350	148	36	0	44	0	12	0	0	240
8	0.1000	696.3104	148	36	0	40	0	2	14	0	240
9	0.0878	63.1814	240	0	0	0	0	0	0	0	240

Fig. 4.16 Tabular format of pushover curve considering user defined hinge properties

If capacity curve and demand curve are generated in same spectrum co-ordinate than the performance point can be found for user defined hinge properties model and default hinge properties model. Comparison of capacity and demand curve for both models is shown in Fig. 4.17.

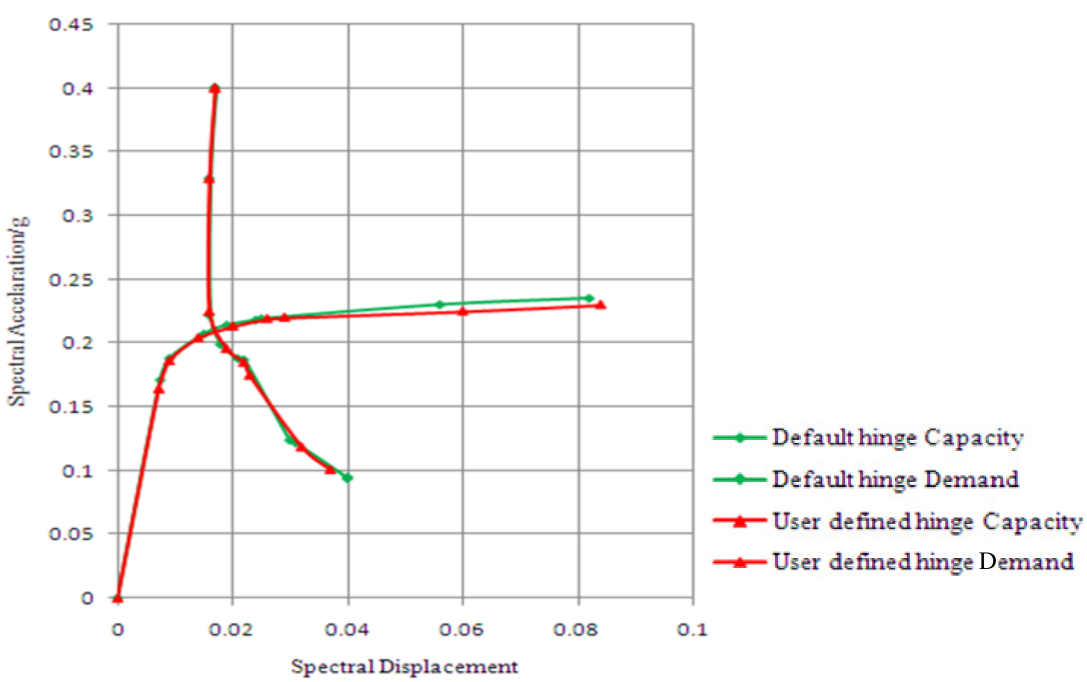

Fig. 4.17 Comparison of capacity and demand curve in spectrum
co-ordinate as per different hinge properties

From above study following findings are observed:

- The base shear capacity of models with the default hinges and with the user-defined hinges properties are similar. The variation in the base shear capacity is less than 1%. Thus, the base shear capacity does not depend on whether the default or user-defined hinge properties are used.
- Comparison of hinging patterns indicates that both models with default hinges and the user-defined hinges estimate plastic hinge formation at the yielding point quite well. However, there are significant differences in the hinging patterns at near to collapse point.
- Capacity curve and demand curve is nearly matched in both models. So, hinge properties considered based on stress-strain relationship and default hinge properties based on ATC 40 and FEMA 356 are nearly same.

4.8 SUMMARY

In this chapter derivation of moment-curvature and moment-rotation relationship are presented. One 3D frame example is considered for nonlinear static analysis using default hinge properties and user defined hinge properties. The result of base shear for each push displacement and the hinge formation pattern at yield state and near to collapse state are compared. The capacity and demand curve for user define and default hinge properties are presented.

5. PUSHOVER ANALYSIS CONSIDERING SITE SPECIFIC RESPONSE SPECTRA AND TIME HISTORY

5.1 GENERAL

The pushover analysis is used for determination of the nonlinear response behavior of structure at different level of lateral displacement, ranging from initial elastic response through development of failure mechanism and initiation of collapse. The response behavior is gauged by measurement of strength of structure, at various increment of lateral displacement or lateral force. There are several methods for estimating seismic demands for performance-based design of buildings. The accuracy of design is based on applied pattern of loads inducing deformation in the structure which should be similar to that induced by the earthquake ground motion.

In present chapter an attempt is made to find a more realistic lateral load distribution pattern for derivation of seismic demand using site specific response spectra and acceleration time history. At three sites of Ahmedabad city, site specific response spectra and time history are obtained to calculate lateral force on building for static pushover analysis. Site specific time history and response spectra are obtained using ProSHAKE software considering soil profiles at a site. Acceleration time history recorded during 26th January 2001 Bhuj earthquake is used for obtaining site specific response. In addition IS 1893 response spectrum is also considered for seismic demand. A three dimensional reinforced concrete (RC) frame structure with different no. of story is considered for study. Time history and response spectra analysis of structure is carried out using ETABS software. The result of pushover analysis in term of capacity, demand and performance point are compared as obtained from inverted triangular distribution of lateral load pattern based on codal formula, and lateral load distribution generated from site specific response spectra and acceleration time history.

5.2 RESPONSE SPECTRUM ANALYSIS METHODOLOGY

The procedure to compute the peak response of an N storey building to an earthquake motion characterized by a response spectrum or design spectrum is

Summarized in following step [22].

1. Define the structural properties.
   a. Determine the mass matrix |m| and lateral stiffness matrix |k|.
   b. Estimate the modal damping ratio ζ_n.
2. Determine the natural frequencies ω_n by solving Eq. 5.1.

$$\left| k-\omega_n^2 m \right| = 0 \qquad \text{. . . . (5.1)}$$

   Substituting natural frequency value in Eq. 5.2 find out natural modes.

$$\left| k-\omega_n^2 m \right| \phi_n = 0 \qquad \text{. . . . (5.2)}$$

3. The maximum deformation and pseudo accelerations corresponding to the periods are determined for each normal mode from design spectrum or earthquake response spectrum.
4. The effective modal masses M_n are determined for each normal mode and from these maximum inertia forces F_{jn} for each mode are determined.

$$L_n^h = m_1\,\phi_{1n} + m_2\,\phi_{2n} + m_3\,\phi_{3n} + \cdots\cdots\cdots + m_j\,\phi_{jn}$$
$$M_n = m_1\,\phi_{1n}^2 + m_2\,\phi_{2n}^2 + m_3\,\phi_{3n}^2 + \cdots\cdots\cdots + m_j\,\phi_{jn}^2 \qquad \text{. . . . (5.3)}$$

   For *n*th mode $\quad F_{1n} = m_1\phi_{1n}\dfrac{L_n^h}{M_n}A_n$

$$F_{2n} = m_2\phi_{2n}\frac{L_n^h}{M_n}A_n$$
$$F_{jn} = m_j\phi_{jn}\frac{L_n^h}{M_n}A_n \qquad \text{. . . . (5.4)}$$

   For the three dimensional unsymmetrical building, it is required to determine inertia force in X, Y and in torsional direction.
   For nth mode and storey j, inertia force in torsional direction is given by,

$$M_{jn} = m_j\phi_{wj,n}\frac{L_n^h}{M_n}A_n \qquad \text{. . . . (5.5)}$$

5. The maximum values of the response parameters (moment, shear, displacements and so on) are determined through a static analysis for the maximum inertia forces of every normal mode.
6. Determine the peak value *r* of any response quantity by considering the SRSS rule if the natural frequencies are well separated. The CQC (complete quadratic combination) rule should be used if the natural frequencies are closely spaced.

5.3 TIME HISTORY ANALYSIS METHODOLOGY

Time-history analysis is used to determine time-dependent response of the structure which can be obtained through direct numerical integration and differential equation of ground acceleration $\ddot{u}_g(t)$ appears on the right side of the Eq.5.6 governing the response of an MDF system to earthquake excitation.

$$\ddot{q}_n + 2\zeta_n \omega_n \dot{q}_n + \omega_n^2 q_n = \Gamma_n \ddot{u}_g(t) \qquad \text{. . . . (5.6)}$$

Where *q, q′ and q″ are* displacement, velocity and accelerations of structure ζ_n is damping ration, ω_n is natural frequency.

The response of an N-story building with symmetric plan about two orthogonal axes of earthquake ground motion along an axis of symmetry can be computed as a function of time by the procedure given below [22].

1. Define the ground acceleration $\ddot{u}_g(t)$ numerically at every time step Δt.
2. Define the structural properties.
   a. Determine the mass matrix |m| and lateral stiffness matrix |k|.
   b. Estimate the modal damping ratio ζ_n.
3. Determine the natural frequencies ω_n by solving Eq. 5.7.

$$\left| k - \omega_n^2 m \right| = 0 \qquad \text{. . . . (5.7)}$$

   Substituting natural frequency value in Eq. 5.8 find out natural modes.

$$\left| k - \omega_n^2 m \right| \phi_n = 0 \qquad \text{. . . . (5.8)}$$

4. Determine the modal components S_n of the effective earthquake distribution by following Eq. 5.9.

$$S_n = \Gamma_n m_j \phi_{jn} \qquad \text{. . . . (5.9)}$$

$$L_n^h = \sum_{j=1}^{N} m_j \phi_{jn}$$

$$M_n = \sum_{j=1}^{N} m_j \phi_{jn}^2$$

$$L_n^\theta = \sum_{j=1}^{N} h_j m_h \phi_{jn}$$

$$\Gamma_n = L_n^h / M_n$$

5. Compute the response contribution of the n^{th} mode by the following steps, which are repeated for all modes, n= 1,2,3……..N.

   a. Perform static analysis of the building subjected to lateral force S_n. To determine r_n^{st}, the modal static response for each desired response quantity r formulas given in Table 5.1 can be used.

   b. Determine the pseudo-acceleration response $A_n(t)$ of the n^{th}-mode SDF system to $\ddot{u}_g(t)$, using numerical time-stepping methods.

   $$A_n(t) = \omega^2 D_n(t) \qquad \text{. . . . (5.10)}$$

   Peak values of $D_n(t)$ and $A_n(t)$ can be determined directly from the time history of the ground motion.

   c. Determine $r_n(t)$ from Eq. 5.6.

   $$r_n(t) = r_n^{st} A_n(t) \qquad \text{. . . . (5.11)}$$

6. Combination of the modal contributions $r_n(t)$ to determine the total response using Eq. 5.7.

$$r(t) = \sum_{n=1}^{N} r_n(t) = \sum_{n=1}^{N} r_n^{st} A_n(t) \qquad \text{. . . . (5.12)}$$

Steps 5 and 6 can be easily understood by following table.

Table 5.1 Modal Static Responses

Response, r	**Modal Static response, r_n^{st}**
V_i	$V_{in}^{st} = \sum_{j=1}^{N} S_{jn}$
M_i	$M_{in}^{st} = \sum_{j=1}^{N} (h_j - h_i) S_{jn}$
V_b	$V_{bn}^{st} = \sum_{j=1}^{N} S_{jn} = \Gamma_n L_n^h \equiv M_n^*$
M_b	$M_{bn}^{st} = \sum_{j=1}^{N} h_j S_{jn} = \Gamma_n L_n^\theta \equiv h_n^* M_n^*$
u_j	$u_{jn}^{st} = (\Gamma_n / \omega_n^2) \phi_{jn}$
Δ_j	$\Delta_{jn}^{st} = (\Gamma_n / \omega_n^2)(\phi_{jn} - \phi_{j-1,n})$

This procedure can be extended to multistory buildings with arbitrary plan with no axis of symmetry. In this case the system has 3 of dynamic degrees of freedom. They are in each of the three modes generally contains coupled x-lateral, y-lateral, and torsional motions and is excited by ground motion in the x or y direction. For n^th^ mode and storey j, modal components S_n of the effective earthquake distribution in torsional direction is given by Eq. 5.13.

$$S_n = M_j \phi_{wj,n} \frac{L_n^h}{M_n} \qquad \text{. . . . (5.13)}$$

The contribution of the *n*th mode to dynamic response is obtained by multiplying the result of two analyses: (1) static analysis of the structure with applied force S_n, and (2) dynamic analysis of the *n*th-mode SDF system excited by $\ddot{u}_g(t)$. Thus modal analysis requires dynamic analysis of N different SDF systems. Combining the modal responses gives the earthquake response of the structure.

Table 5.2 Conceptual explanation of modal analysis

Mode	Static Analysis of Structure	Dynamic Analysis of SDF System	Modal Contribution to Dynamic Response
1	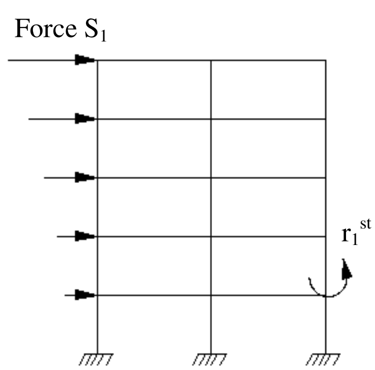	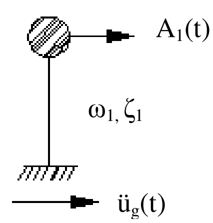	$r_1(t) = r_1^{st} A_1(t)$
2	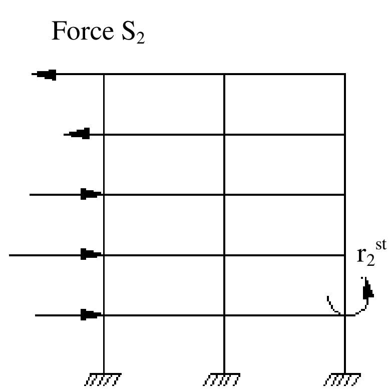	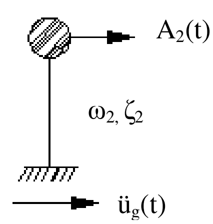	$r_2(t) = r_2^{st} A_2(t)$

* * *	* * *	* * *	* * *
N	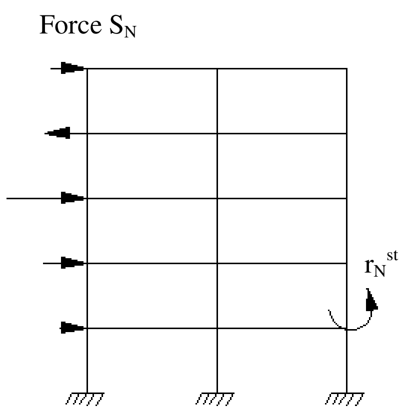	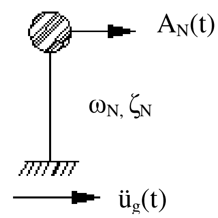	$r_N(t) = r_N^{st}\, A_N(t)$
Total Response			$r(t) = \sum_{n=1}^{N} r_n(t) = \sum_{n=1}^{N} r_n^{st}\, A_n(t)$

5.4 RESPONSE SPECTRUM AND TIME HISTORY AT AHMEDABAD SOIL SITES

For engineering purpose the time variation of ground acceleration is the most useful way of defining the shaking of the ground during an earthquake. The ground acceleration $\ddot{u}_g(t)$ appears on the right side of the differential equation given by Eq. 5.6, which govern the response of structure to earthquake excitation. Thus, for ground acceleration the problem to be solved is defined completely for a single degree of freedom (SDOF) system with known mass, stiffness and damping properties.

The ground motion recorded at ground floor of passport office building during Bhuj earthquake on 26th January 2001 is used to develop the ground motion at the rock or hard soil level which is considered at 15 m below ground level. This artificial developed acceleration time history at 15 m depth at passport office is used as an input motion at other sites for the development of acceleration time history on ground. This acceleration time history developed at various site using one dimensional ground response analysis software ProSHAKE are shown in

Fig. 5.1. For the development of artificial time history, longitudinal direction is considered because it is critical compared to other directions.

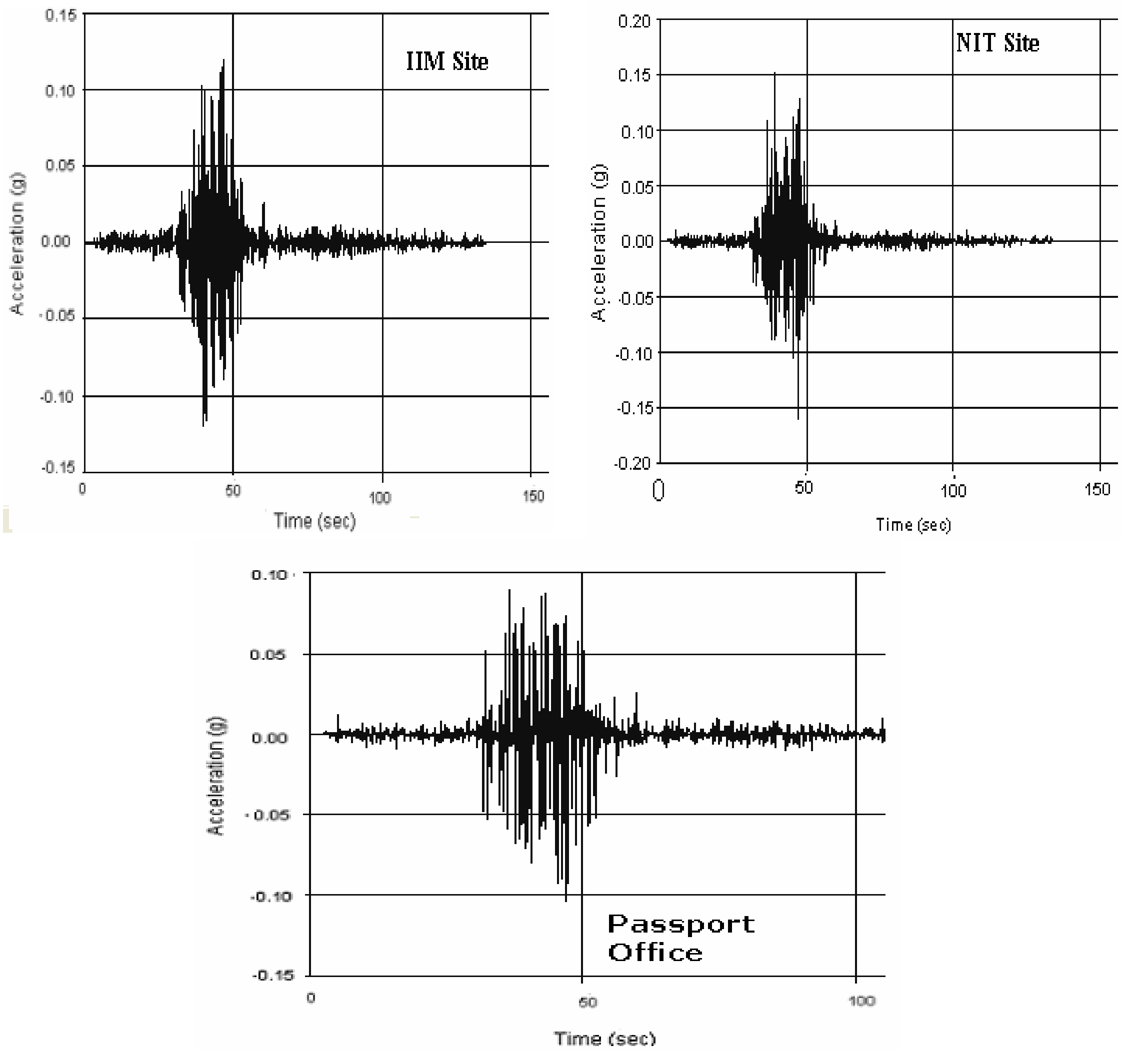

Fig. 5.1 Acceleration Time History plots on ground surface at various sites

Response spectrum analysis is widely used in the field of structural engineering for design. Site specific response spectrum for three sites of Ahmedabad city is derived using ProSHAKE software. From the available data of sub-soil strata and input motion of acceleration time history, the response spectrum is obtained by plotting the spectral accelerations against the time periods of vibrations for 5% damping. The plots of response spectra obtained for three sites are presented in the Fig. 5.2.

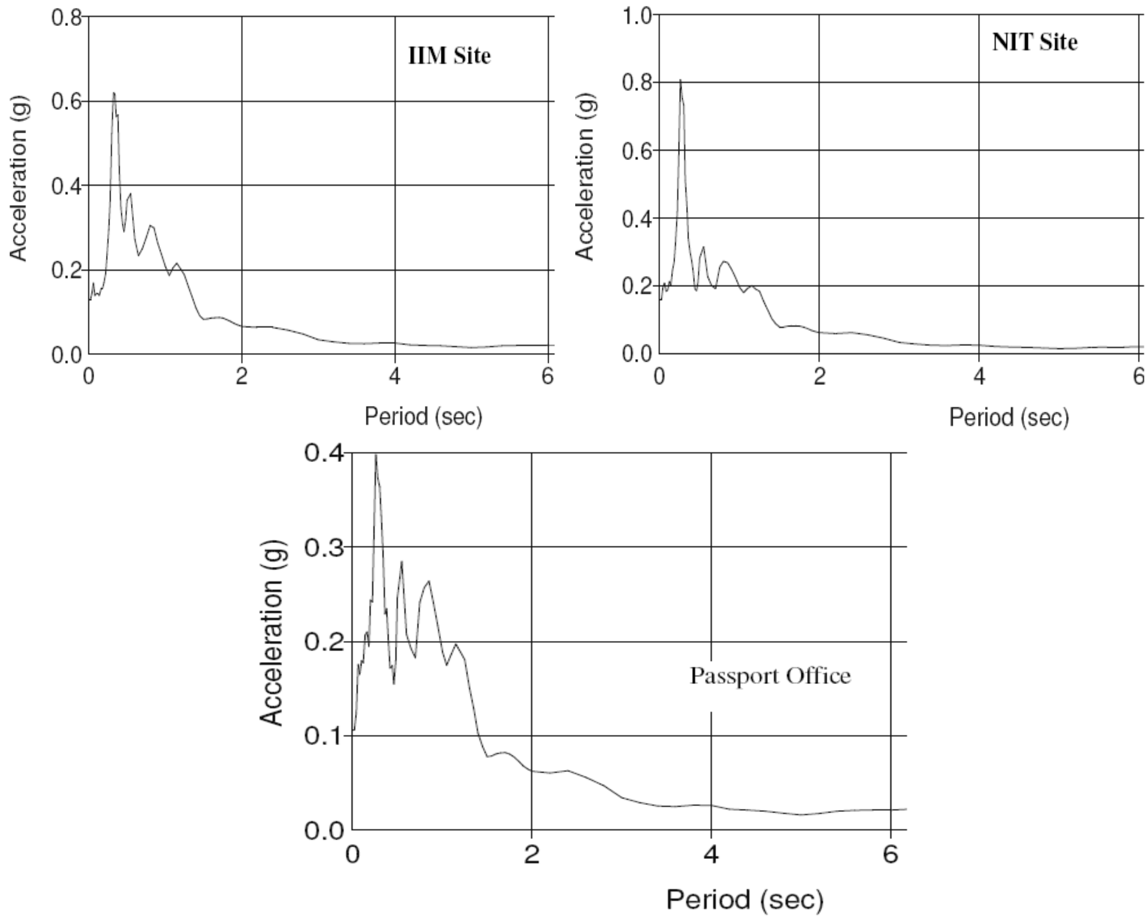

Fig. 5.2 Response spectra plots on ground surface at various sites

5.5 TIME HISTORY ANALYSIS USING ETABS

Time history analysis is a step-by-step analysis for dynamic response of structure to specified loading that may vary with respect to time. Site specific acceleration time history analysis is obtained for various sites of Ahmedabad city using ProSHAKE software. ProSHAKE software generates a file consisting of ground acceleration at different time interval and is used to carry out site specific time history analysis using ETABS.

The procedure to define time history load case for analysis of building in ETABS is illustrated as follows:

From the **Define** menu, **Static load case** is selected. In static load case various loads are defined such as Dead Load, Live Load, Super Imposed Dead Load and Floor Finish Dead Load are to be assigned as shown in Fig. 5.3. Dead Load is calculated in ETABS based on the material properties and cross section dimensions of member.

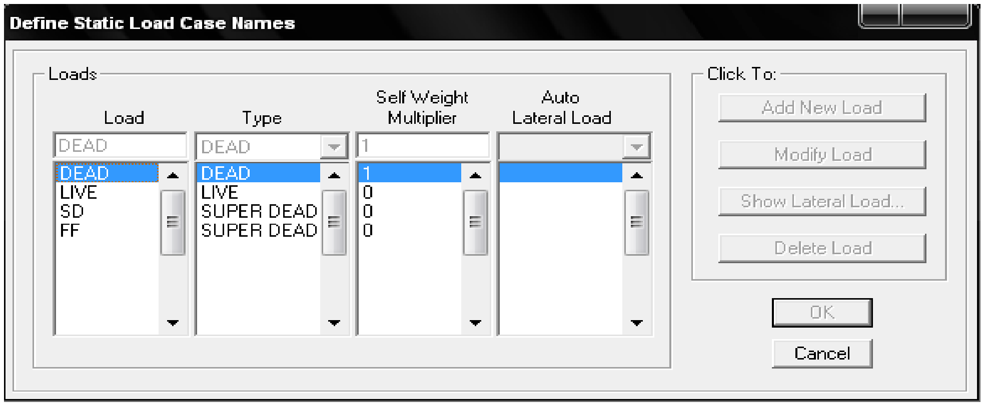

Fig. 5.3 Static Load Case

All slabs are selected using area curser and assign Live Load, Super Imposed Dead Load in form of uniform load over the slab as shown in Fig. 5.4.

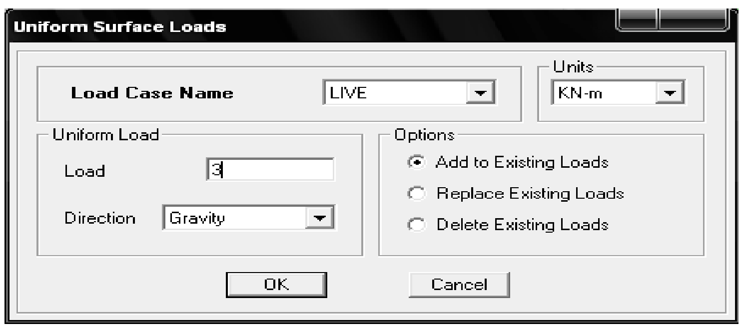

Fig. 5.4 Uniform Surface Loads

For the dynamic analysis **mass source** is an important factor that is to be considered and is assigned as illustrated in Fig. 5.5. In this study live load is taken as 3 kN/m^2 so as per IS: 1893-2002 25% of Live load is considered.

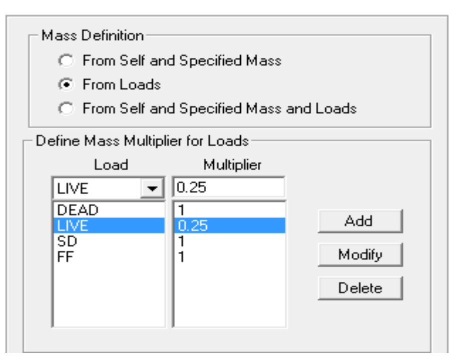

Fig. 5.5 Mass Source Definition

The design acceleration time history for three sites are given as input in **Define menu** -> **Time History Function.** The time history load cases are defined from the **Time History Cases** option as shown in the Fig. 5.6. The acceleration time history of IIM site as defined in ETABS is shown in Fig. 5.7.

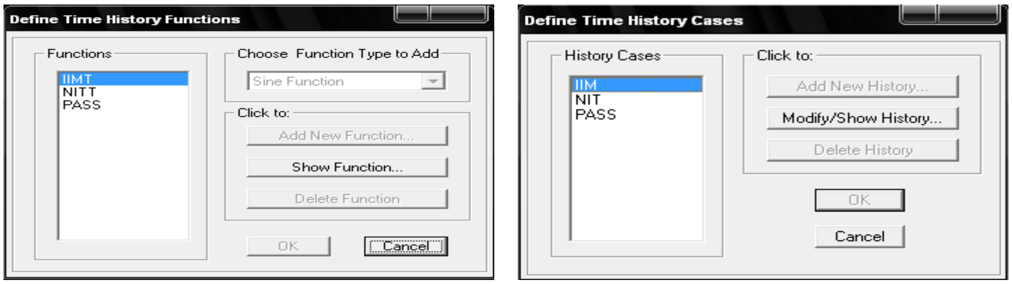

Fig. 5.6 Time History Options

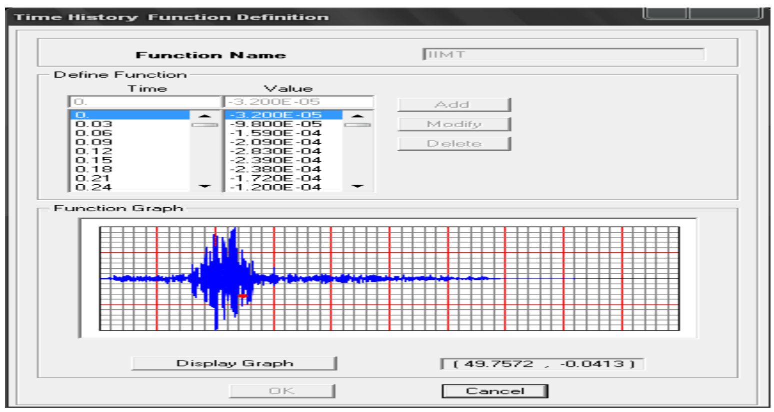

Fig. 5.7 Time History Graphs

Time history case data is defined for simplicity of analysis. Number of output time steps is 300. Linear analysis case and two direction acceleration load case are considered. The scale factor 9.81 i.e. gravitational acceleration (m/sec^2) and 5% damping are defined as shown in Fig 5.8.

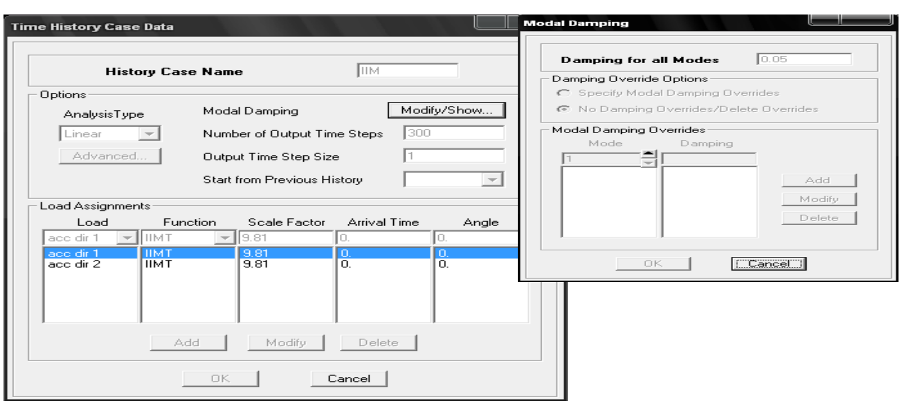

Fig. 5.8 Time History Case Data

After assigning all the steps, **Run analysis** command used to carry out the analysis of building. The results are obtained in the form of shear forces, axial forces, bending moments, story shear forces and base shear in graphical and tabular form in display menu as shown in Fig. 5.9.

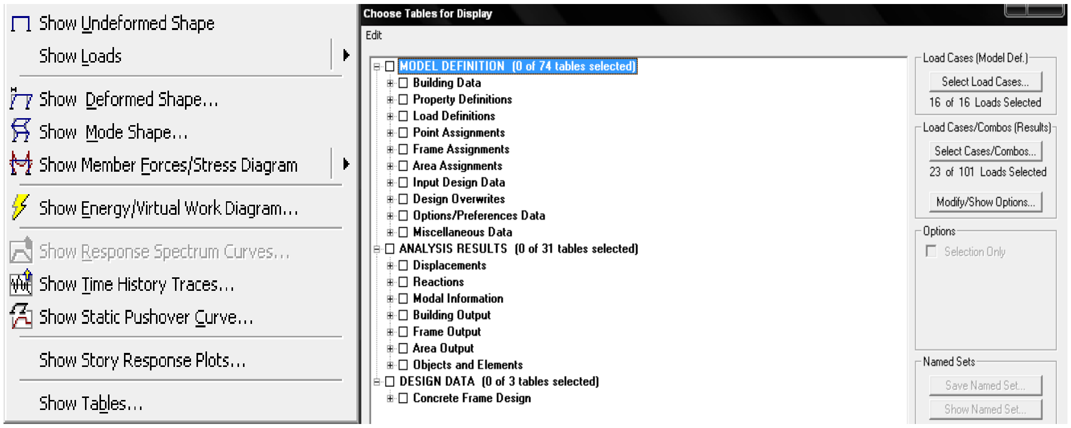

Fig. 5.9 Output Data of Analysis and Design

5.6 SITE SPECIFIC RESPONSE SPECTRUM ANALYSIS

The procedure of assigning dead and live load case, different load combinations, defining mass source, and assigning the rigid diaphragms to all storeys are same as Time history analysis method, explained in section 5.5. The procedure to define and to assign Response spectra load case for analysis of building is illustrated as follows:

The design response spectra developed using ProSHAKE software for three sites are given as input in the **Define menu -> Response Spectrum Functions.** Response spectra load cases are defined in **Response Spectrum cases** as shown in Fig 5.10.

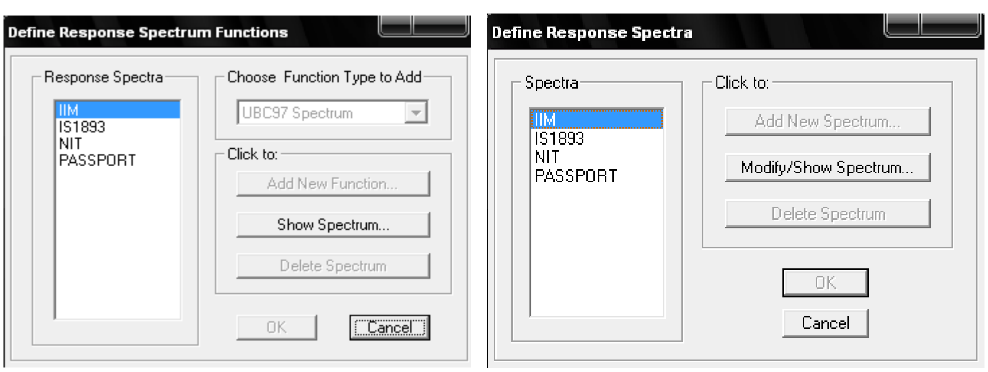

Fig. 5.10 Response Spectra Options

Site specific response spectrum curve of IIM site and IS 1893 response spectrum curve for zone III are shown in Fig. 5.11. The damping value of 5% is specified to generate the response spectrum curve. The scale factor of 9.81 (i.e. g) is assigned as shown in Fig. 5.12.

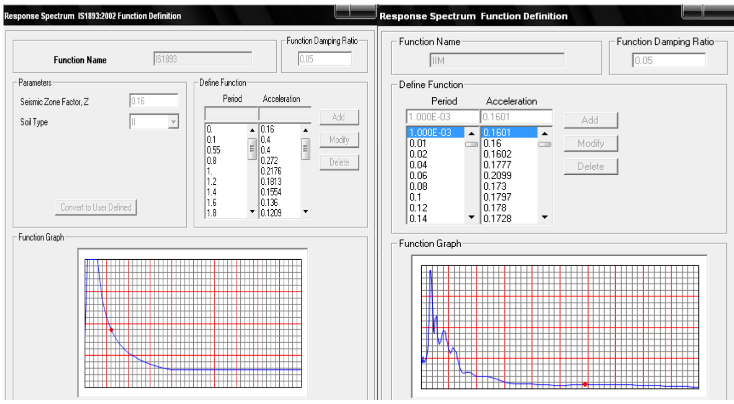

(a) IS: 1893-2002 (b) IIM site

Fig. 5.11 Response Spectra Graphs

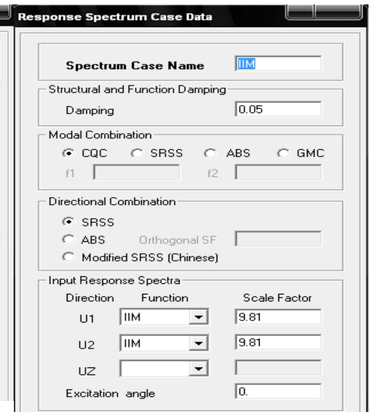

Fig. 5.12 Response Spectra Case Data

After defining the load cases to the frame structure, load combinations are generated for three site specific response spectra and IS 1893 response spectra. In ETABS, the program has facility to generate default combination and user define combination according to IS: 1893(Part1) - 2002. Load combination used only during the design of building but analysis part, the serviceability load is considered.

After completing the above steps, **Run analysis** command is used to carry out the analysis of building. After the analysis is performed various results are displayed. The results are obtained in the form of shear forces, axial forces, bending moments, story shear forces and base shear in graphical and tabular form through display menu as shown in Fig. 5.9.

5.7 LATERAL FORCE FOR PUSHOVER ANALYSIS

Lateral forces and vertical downward forces are considered during the analysis and design of building structures. Vertical force or gravity force can be easily calculated. But lateral force is randomly generated on the building during the earthquake and so it is difficult to calculate. Many codes give different lateral load distribution pattern for earthquake design, but still it is not realistic for all types of building structures. It is accurate only if the applied pattern of loads induces a pattern of deformation in the structure that is similar to that which will be induced during the earthquake ground motion.

The effect of acceleration time history and site specific response spectra analysis on lateral load pattern is discussed in this section. A three dimensional reinforced concrete (RC) frame structure is considered for pushover analysis. All beam sizes are 250×500 mm and column sizes are given in Table 5.3. The slab thickness is considered as 150 mm. The loading considered on building are:

- 3 kN/m^2 live load
- 3 kN/m^2 super imposed dead load for partition wall
- 1 kN/m^2 floor finish load
- 12.5 kN/m for periphery wall

Story height is taken 3m. Material properties are assumed as M25 concrete and Fe 415 longitudinal and transverse reinforcement. Parametric study is carried out considering force in X-Direction.

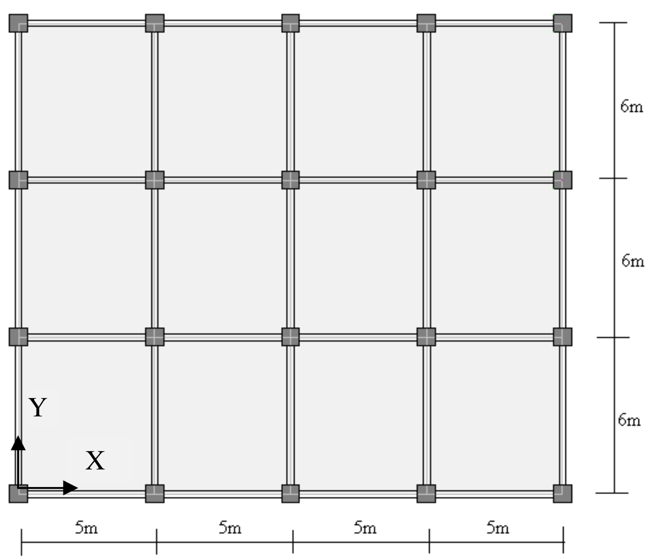

Fig. 5.13 Reinforced Concrete Frame Structure

Table 5.3 Column sizes

No. of Story	Size of Column
10	650×650
15	800×800
20	900×900
25	1000×1000
30	1200×1200

5.7.1 Fundamental Time Period

The seismic response of structure is depends upon its fundamental time period. The time period are determined by eigen value analysis as per ETABS and compared with time period based on codal formula. The fundamental time period of structures as per code is evaluated from the empirical expression given in Clause. 7.6.1 of IS: 1893 (Part I)-2002 which is expressed in Eq. 5.14.

$$T_s = 0.075\, H^{0.75} \qquad \text{. . . . (5.14)}$$

Where, T_s is fundamental time period and H is height of building in m.

Comparison of time period using IS: 1893 (Part I)-2002 and dynamic analysis is shown in Fig 5.14.

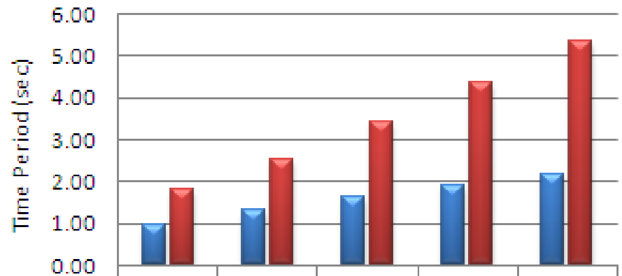

No. of Story	10	15	20	25	30
IS:1893-2002	0.96	1.30	1.62	1.91	2.19
Dynamic analysis	1.81	2.51	3.41	4.36	5.34

Fig. 5.14 Comparison of Time period of multi storey building

5.7.2 Lateral force distribution

In Pushover analysis, lateral loads are applied such that it represents approximately the relative inertial forces generated at each floor level. It includes pushing the structure under lateral loads to displacements that are larger than the maximum displacements expected in design basis earthquakes. The pushover analysis provides a shear Force versus Displacement relationship which indicates the behavior of structure in inelastic limit as well as lateral load capacity of the structure [24].

As discussed earlier pushover analysis is load controlled and displacement controlled. Load control pushover is based on the distribution of inertial forces along the height. The simplified loading patterns are considered for static analysis is based on the Eq. 5.15 given in cause 7.7.1 of IS: 1893 (Part I)-2002. This equation indicates the inverted triangular force distribution and is nearly similar to 1st mode vibration of structure. But it may be different while considering dynamic analysis using time history and site specific response spectra. Inverted triangular is the most common load distribution pattern.

$$Q_i = V_B \frac{W_i h_i^2}{\sum_{j=1}^{n} W_j h_j^2} \qquad \text{. . . . (5.15)}$$

Where,

Q_i = Design lateral force at each floor i

V_B = Design base Shear

W_i = Seismic weight of floor i

hi = Height of floor measured from base

n = number of story at which mass is located

Lateral forces at each story level is calculated considering Site specific time history and response spectra using ETABS software and the resulting force distribution along the height of structure is compared for each case. Comparison of story forces given by IS 1893 static and dynamic analysis, site specific time history and response spectra for 10 story building are shown in Fig. 5.15.

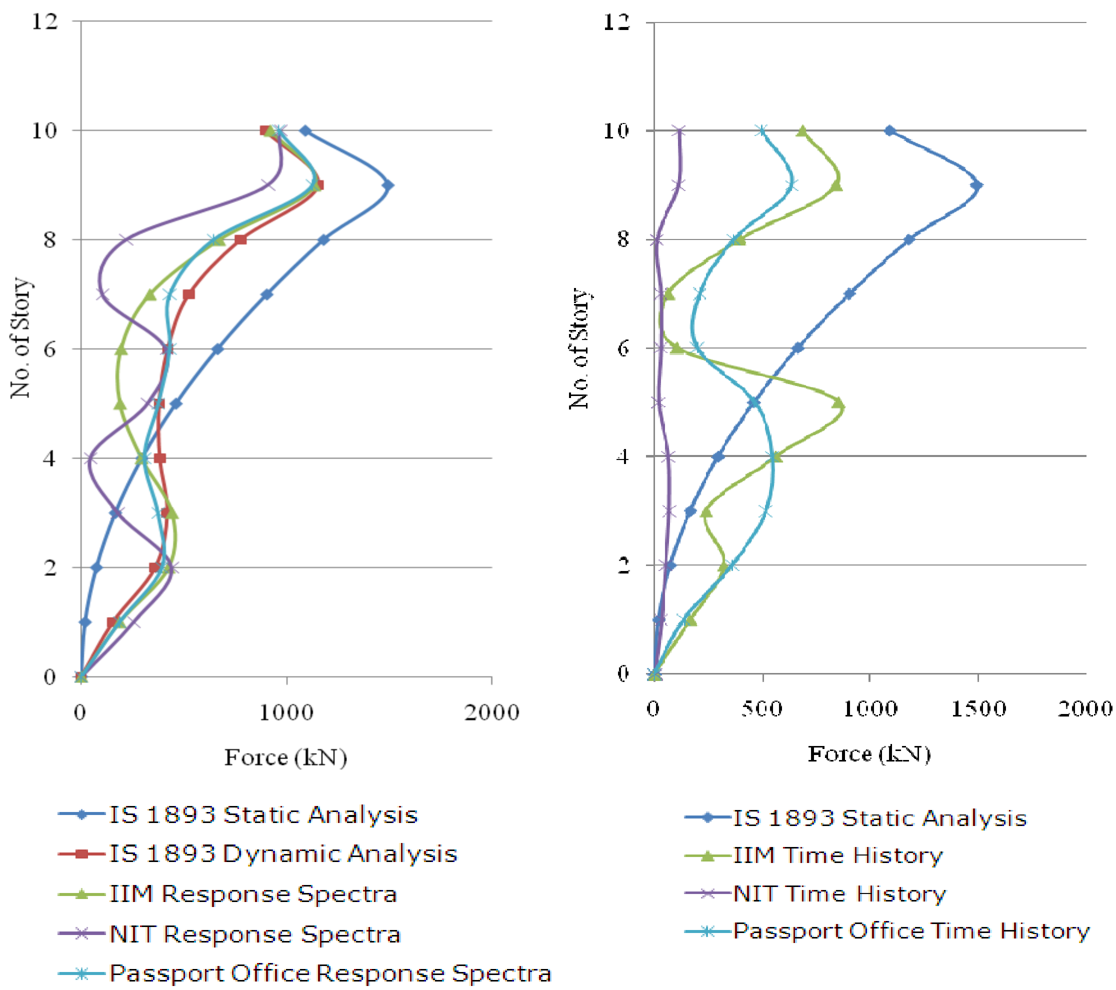

(a) Response spectrum analysis (b) Time history analysis

Fig. 5.15 Earthquake force distribution for 10 storey building

Similarly static and dynamic analysis as per IS 1893, site specific response spectrum and time history analysis are carried out for 15, 20, 25 and 30 story buildings. Comparison of seismic force along height is presented in Fig. 5.16 to 5.19.

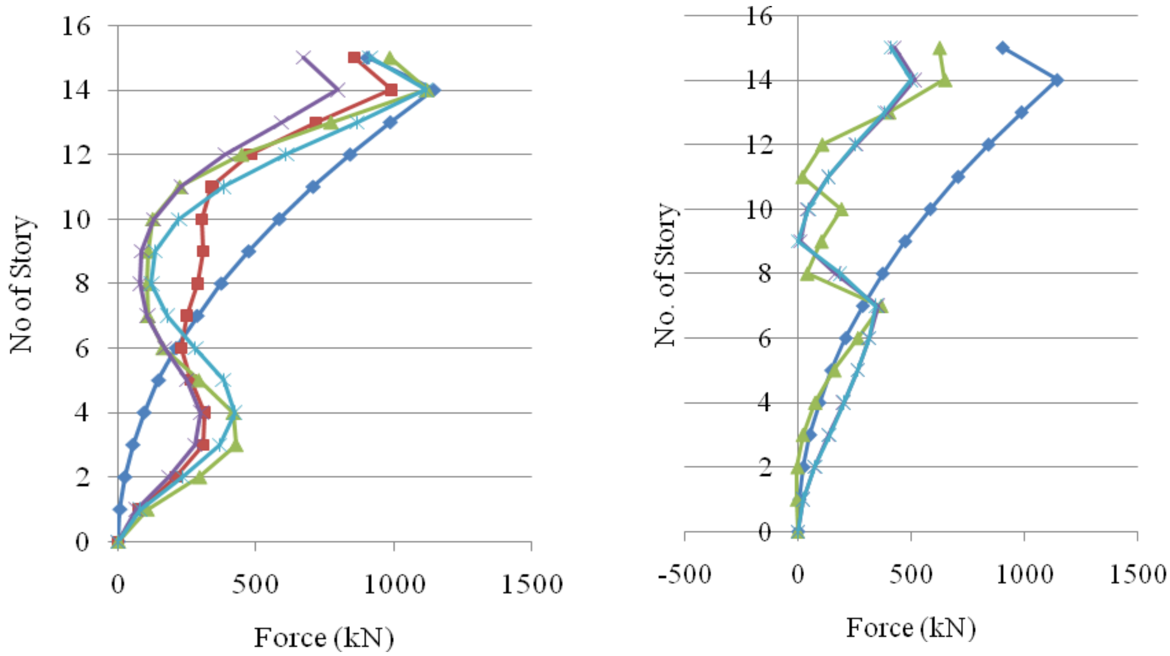

(a) Response spectrum analysis (b) Time history analysis

Fig. 5.16 Earthquake force distribution for 15 story building

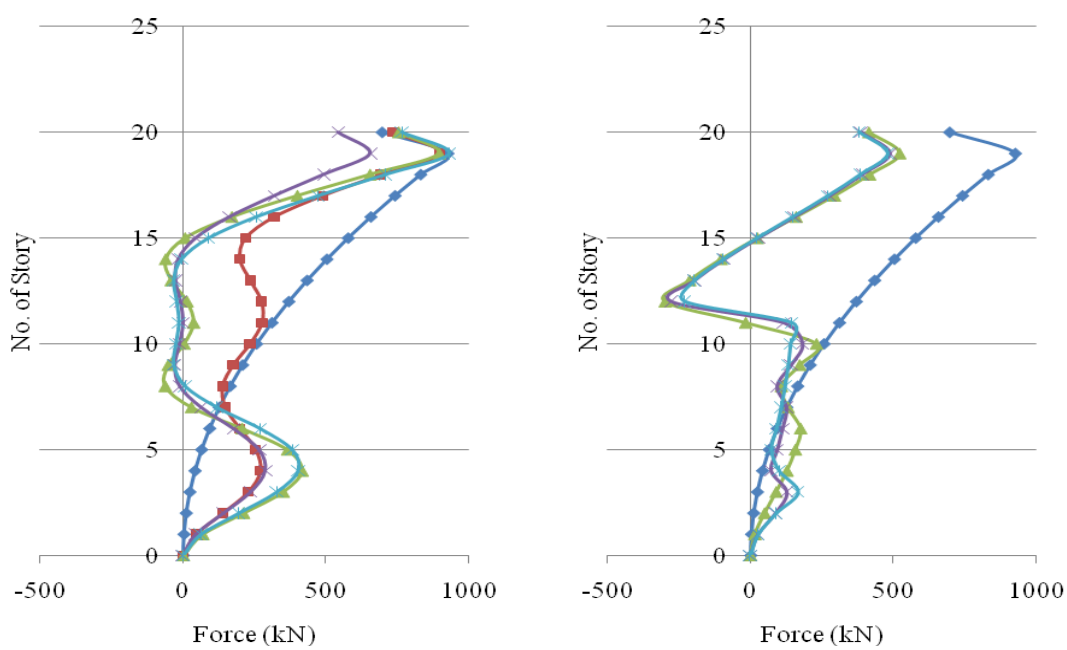

(a) Response spectrum analysis (b) Time history analysis

Fig. 5.17 Earthquake force distribution for 20 storey building

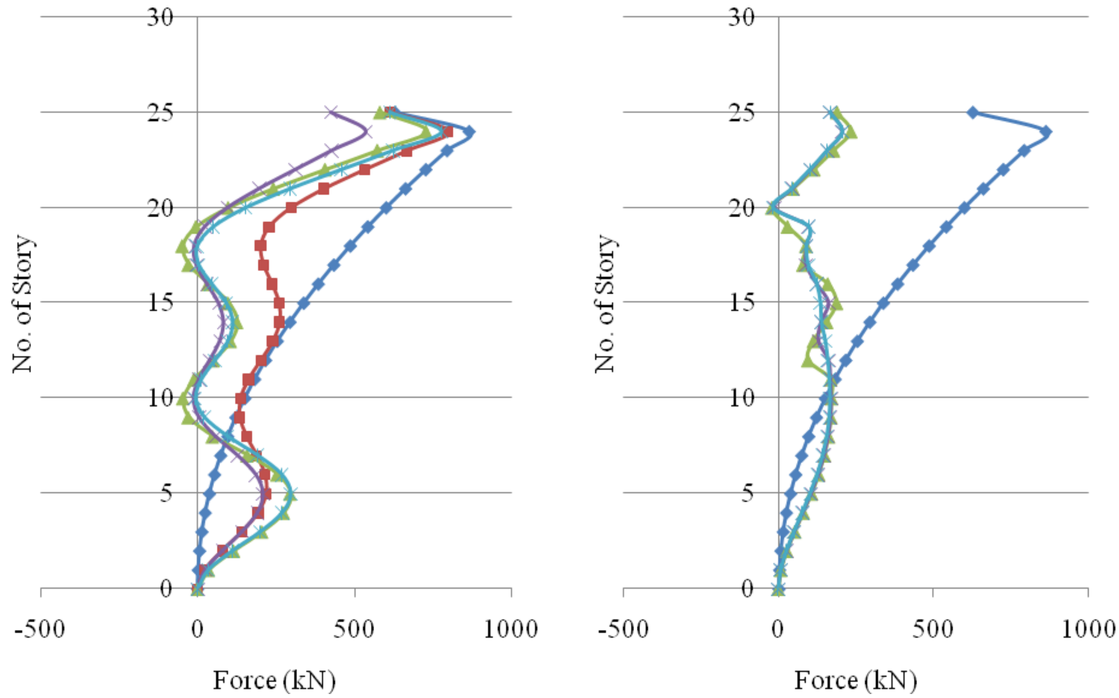

(a) Response spectrum analysis (b) Time history analysis

Fig. 5.18 Earthquake force distribution for 25 storey building

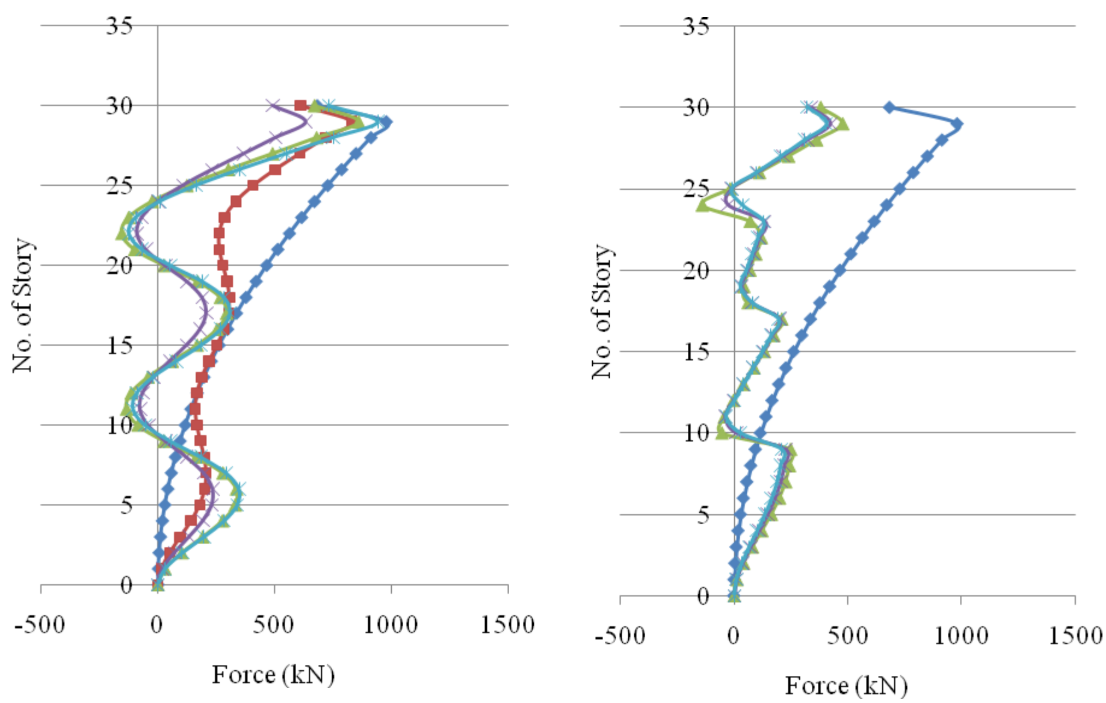

(a) Response spectrum analysis (b) Time history analysis

Fig. 5.19 Earthquake force distribution for 30 storey building

Total base shear of building obtained by various analysis is presented in Table 5.4.

Table 5.4 Comparison of Base Shear (MCE, R=1) (kN)

No. of Story	IS 1893		IIM Site specific		NIT Site specific		Passport office Site specific	
	Static	Dynamic	Response spectra	Time history	Response spectra	Time history	Response spectra	Time history
10	6329.40	5428.27	4755.81	4224.16	3758.73	515.61	5189.90	3917.17
15	6816.14	5915.64	5670.45	3015.12	4279.47	3271.47	6289.40	3259.12
20	7000.48	6145.74	4329.99	2454.29	3337.44	2344.84	4833.16	2368.31
25	7955.84	6711.48	4235.38	2871.51	3272.23	2849.64	4838.46	2837.92
30	9976.23	8685.86	5302.57	3715.90	4097.10	3619.77	6104.05	3532.63

Note: Above forces are converted to DBE forces for Building design considering scale factor as 2 and Important factor and Response reduction factor based on IS 1893.

Pushover analysis is widely used for Performance based design. It gives two controlling parameter i.e. lateral load and lateral displacement to estimate strength of building. Hinge formation in pushover analysis depends on monotonically increasing displacement or lateral load. In this chapter, Force control approach based on site specific time history and response spectra is followed for pushover analysis and the results in term of capacity, demand and base shear at performance point are compared.

5.8 PUSHOVER ANALYSIS USING ETABS

The steps followed in performing a nonlinear static pushover analysis are as:

1. Create a model as shown in Fig. 5.13 and defining the load cases that are required to perform a pushover analysis using **Define > Static load cases command**.

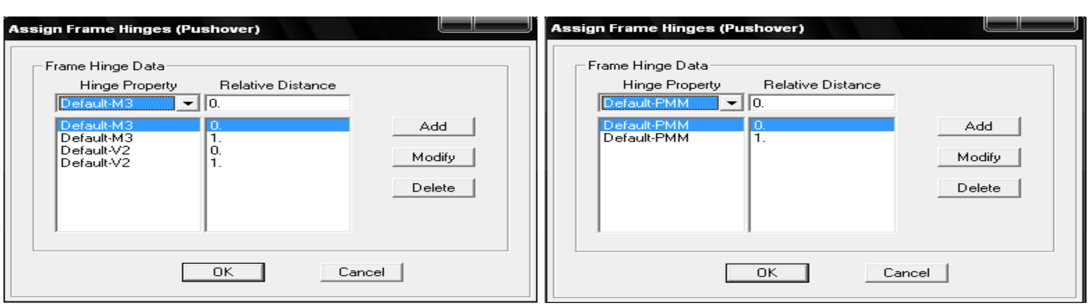

(a) Define Beam Hinges (b) Define Column Hinges

Fig. 5.20 Define Hinge Properties

2. Analysis and Design is carried out based on IS: 456-2000 and defining the default hinge properties for beam and column from **Assign > Frame/Line > Frame nonlinear Hinges**. Moment and shear (M & V) hinges are considered for beam element and axial with biaxial moment (P-M-M) hinges are considered for column element as shown in Fig. 5.20.

3. Defining static nonlinear load cases (Define > Static Nonlinear/Pushover command). For push over analysis first apply the gravity loading as PUSHDOWN shown in Fig. 5.21 and subsequently use lateral displacement or lateral force as PUSH 2 in sequence to derive capacity curve and demand curve as shown in Fig. 5.22. Start from previous pushover case as PUSHDOWN for gravity loads is considered for lateral loading as PUSH 2.

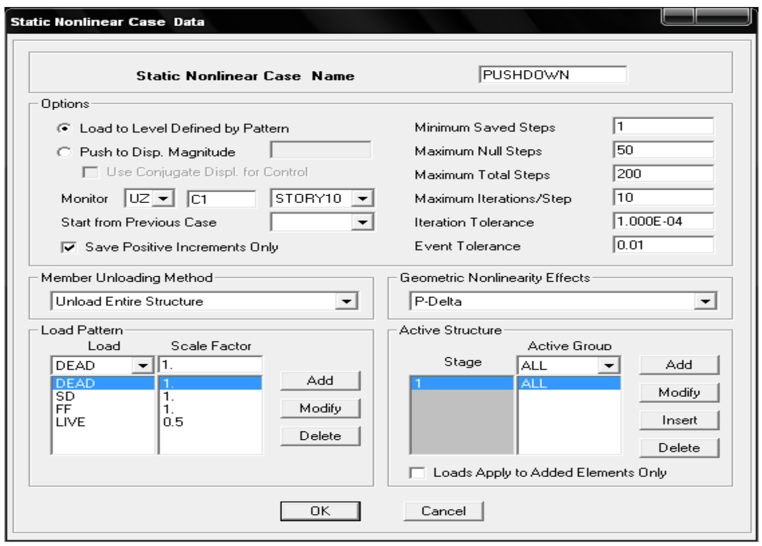

Fig. 5.21 Pushdown a gravity load cases

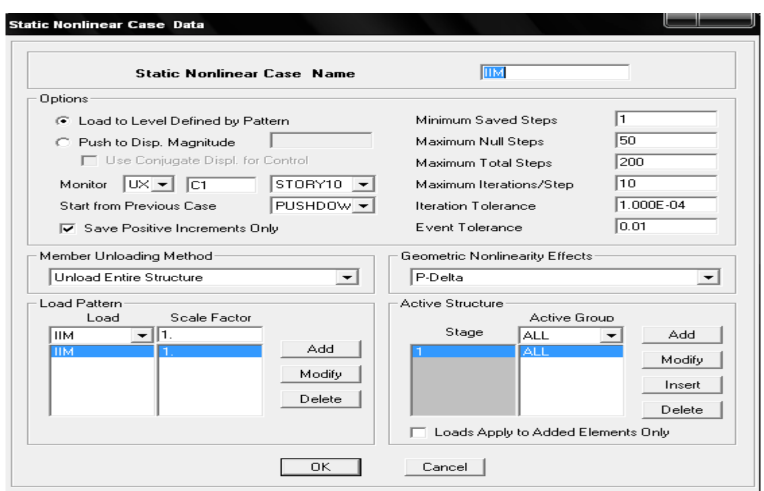

Fig. 5.22 Push lateral load cases

4. Run the Pushover analysis from **Analysis > Run Static Nonlinear Analysis command**.

5. Review the pushover analysis results from **Display > Show Static Pushover Curve command**. Base shear versus displacement can be observed as show in the Fig. 5.23. To obtain Spectrum demand curve shown Fig. 5.24 and change the value of C_a, C_v, damping percentage and Structure behavior factor β as per Indian code. The value of C_a and C_v is shown in Table 5.4 and derivation of this table is shown in Appendix B.

Table 5.5 Coefficient of Acceleration and Coefficient of Velocity

Seismic Coefficient C_a				
Soil	Zone II	Zone III	Zone IV	Zone V
Type I	0.10	0.16	0.24	0.36
Type II	0.10	0.16	0.24	0.36
Type III	0.10	0.16	0.24	0.36
Seismic Coefficient C_v				
Type I	0.100	0.160	0.240	0.360
Type II	0.138	0.220	0.330	0.495
Type III	0.168	0.268	0.402	0.603

Capacity curve is show in Fig. 5.23. Capacity spectrum, demand spectrum and performance point are shown in Fig. 5.24 for IIM site specific response spectra.

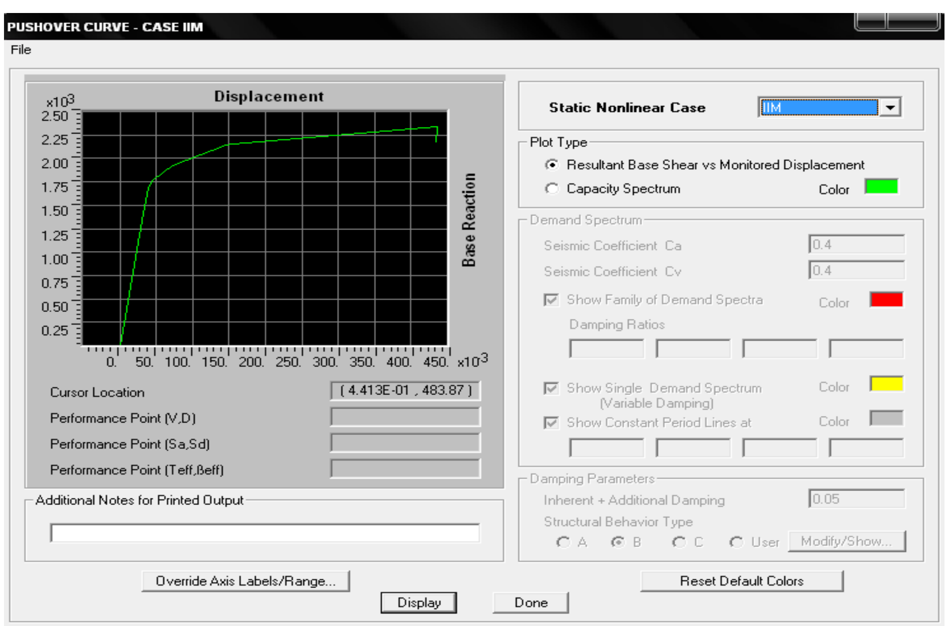

Fig. 5.23 Capacity curve of frame structure

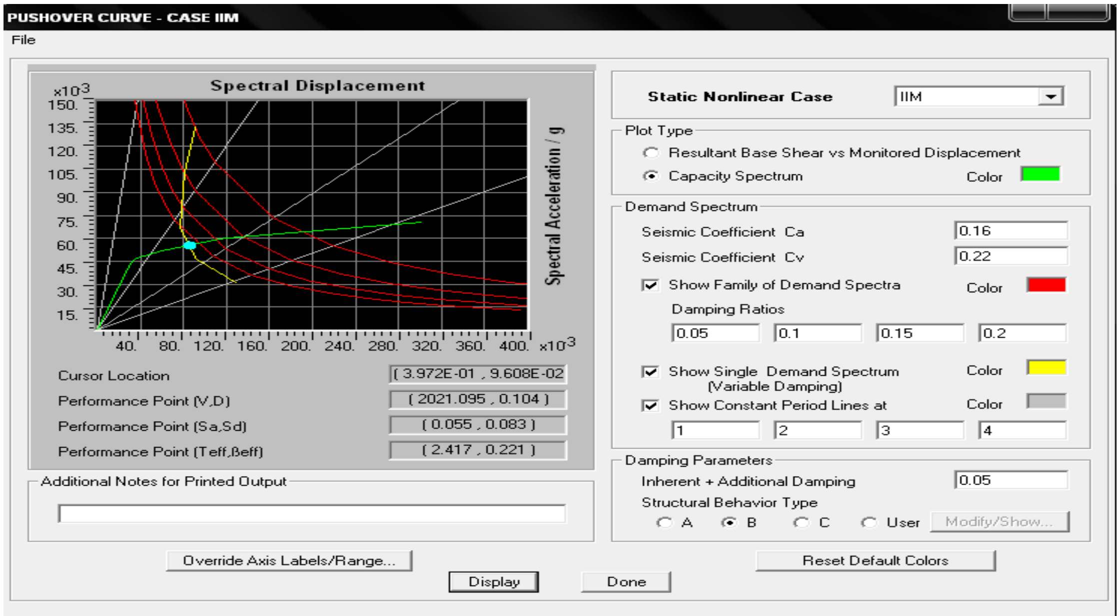

Fig. 5.24 Capacity and Demand spectrum curve of frame structure

5.9 RESULTS AND DISCUSSION

Pushover analysis of multistory frame structure is carried out using ETABS software. The results are obtained in term of capacity, demand, base shear and top displacement at performance point considering IS 1893:2002 specified response spectrum, site specific response spectrum and site specific time history. Further comparison of results for 10, 15, 20, 25 and 30 story frame structure is carried out in this section.

5.9.1 Comparison of Capacity Curve

The response behavior of structure is gauged by measurement of capacity of structure, at various increment of lateral displacement or lateral force. Comparison of capacity curve using IS 1893:2002 Static and Dynamic analysis for MCE (Maximum Considering Earthquake) and DBE (Design Based Earthquake consider reduction factor is 5) are shown in Fig. 5.25. Capacity curve considering site specific response spectra of three sites are shown in Fig. 5.26. The capacity curves obtained considering site specific time history of three sites are shown in Fig. 5.27.

5.9.2 Comparison of Demand Spectrum

The comparison of capacity and demand spectrum using site specific response spectrum and time history curve shown in Fig. 5.28 and Fig. 5.29

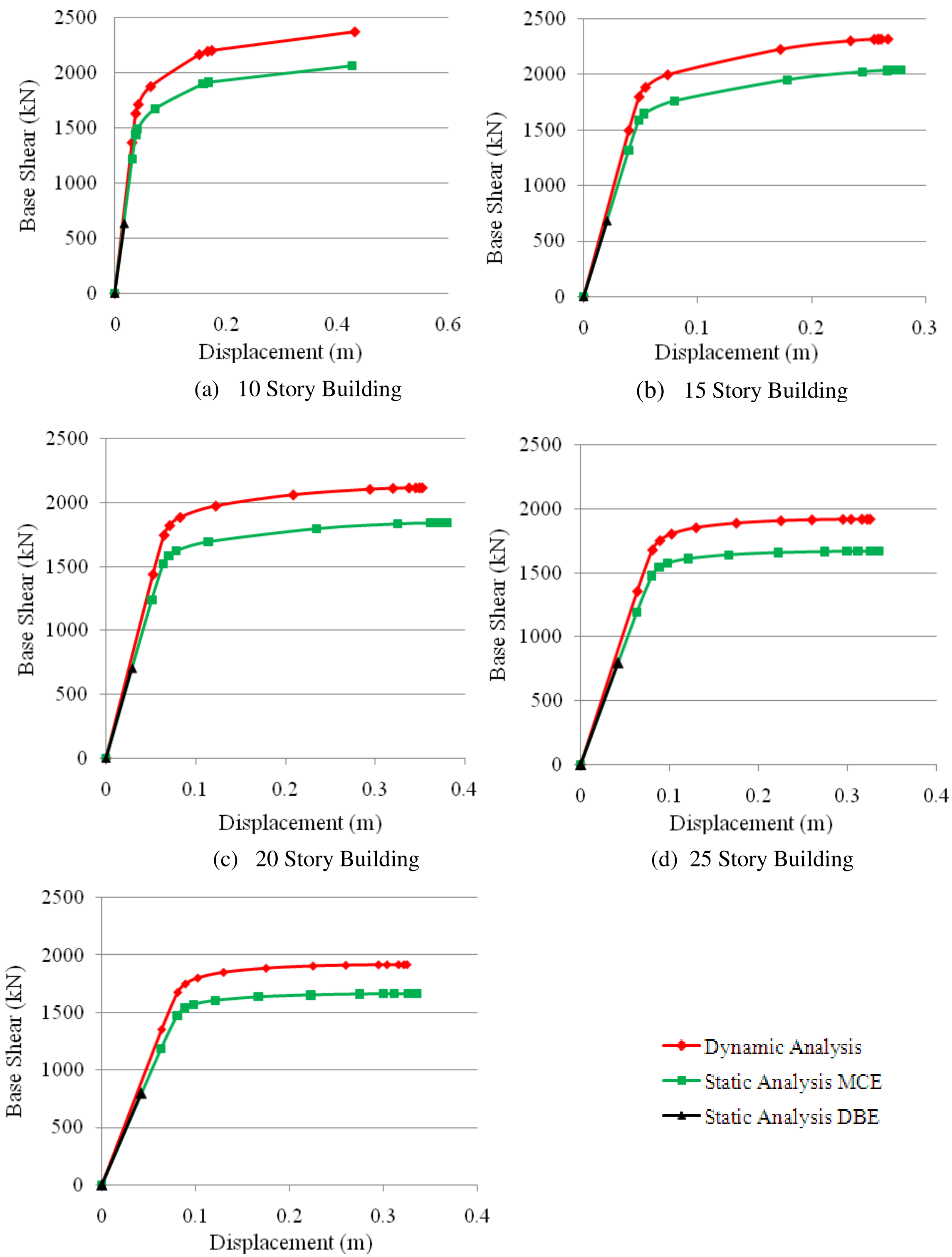

(a) 10 Story Building

(b) 15 Story Building

(c) 20 Story Building

(d) 25 Story Building

(e) 30 Story Building

Fig. 5.25 Capacity curve using IS 1893 response spectra

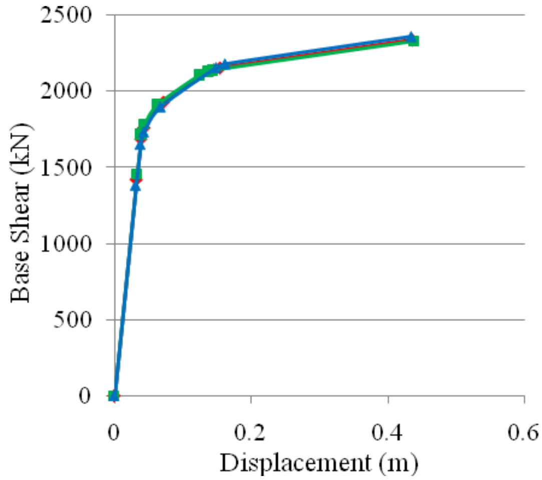

(a) 10 Story Building

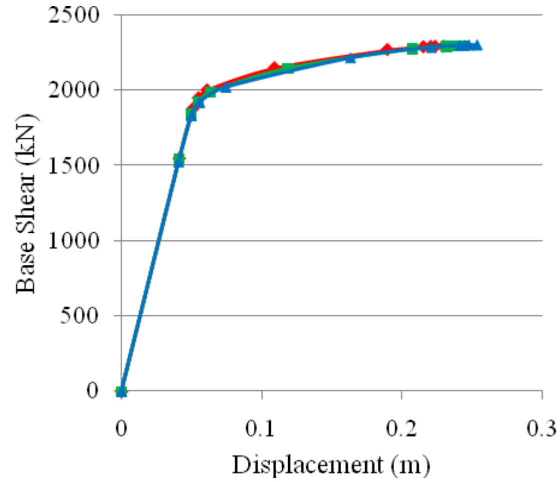

(b) 15 Story Building

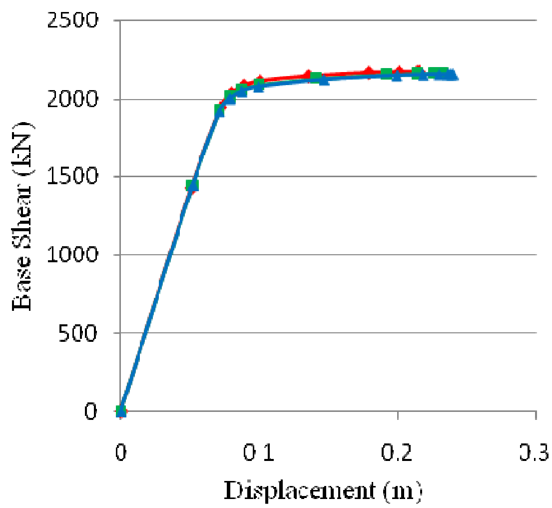

(c) 20 Story Building

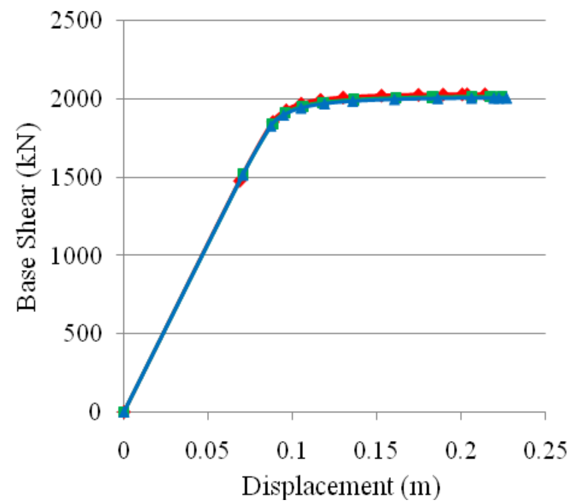

(d) 25 Story Building

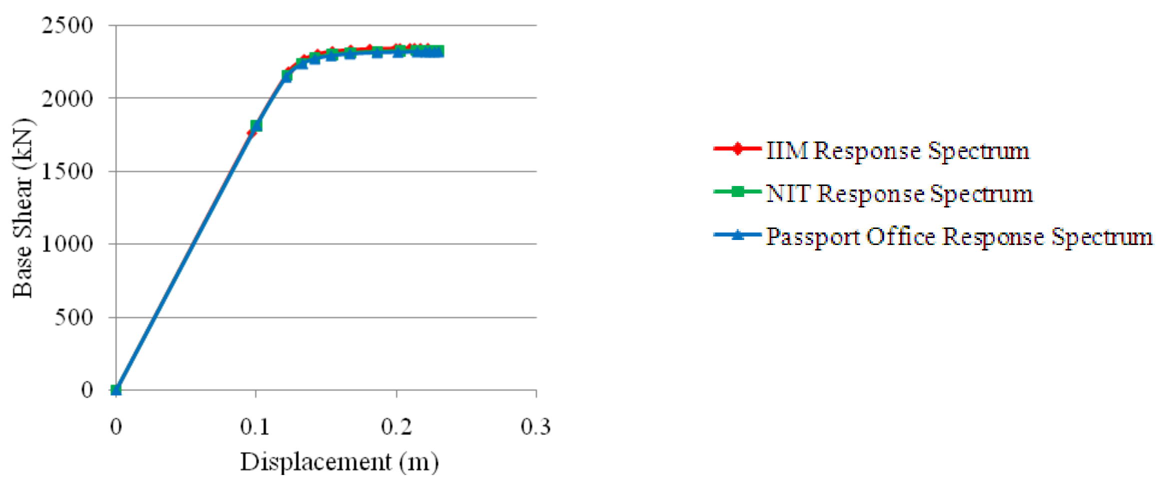

(e) 30 Story Building

Fig. 5.26 Capacity curve using site specified response spectra

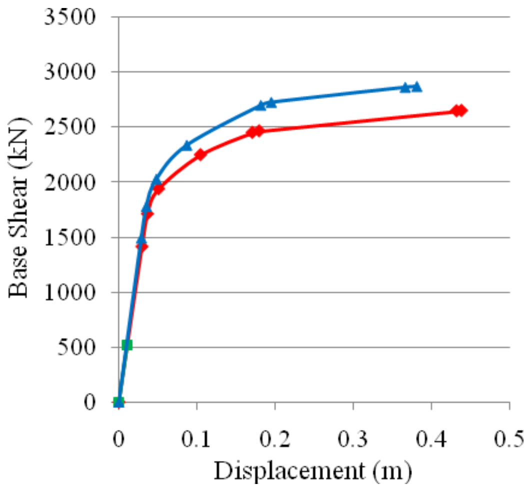

(a) 10 Story Building

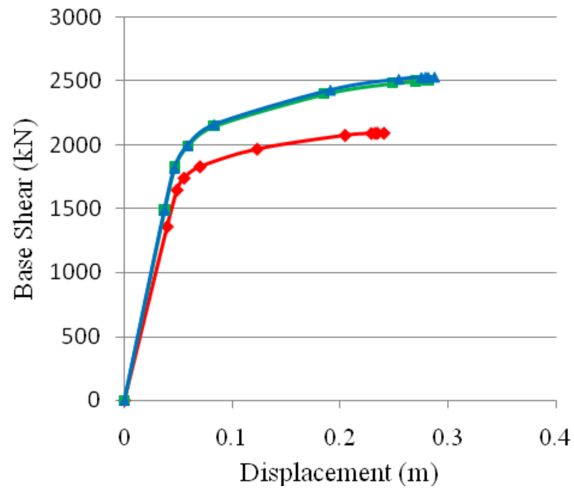

(b) 15 Story Building

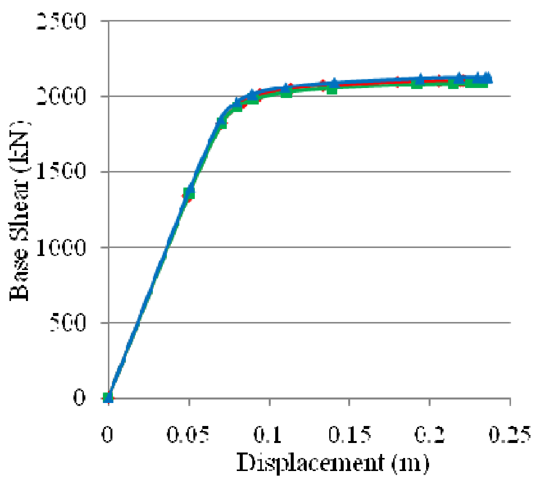

(c) 20 Story Building

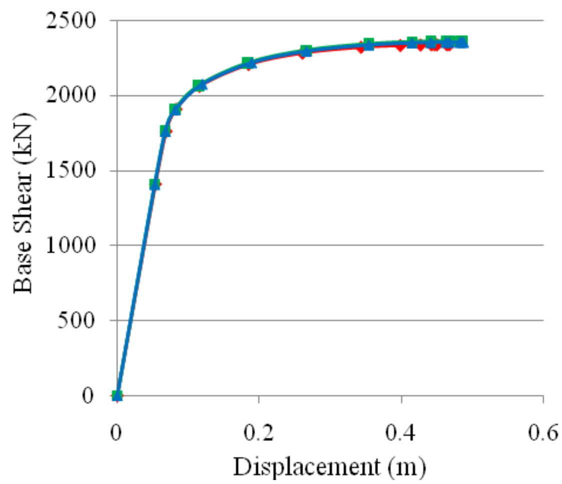

(d) 25 Story Building

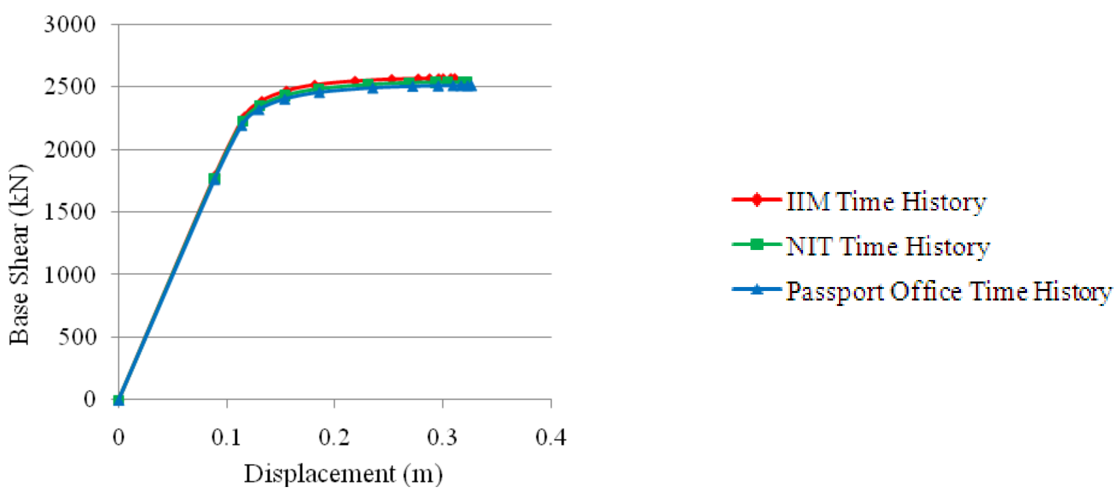

(e) 30 Story Building

Fig. 5.27 Capacity curve using site specified time history

(Unit kN-m)

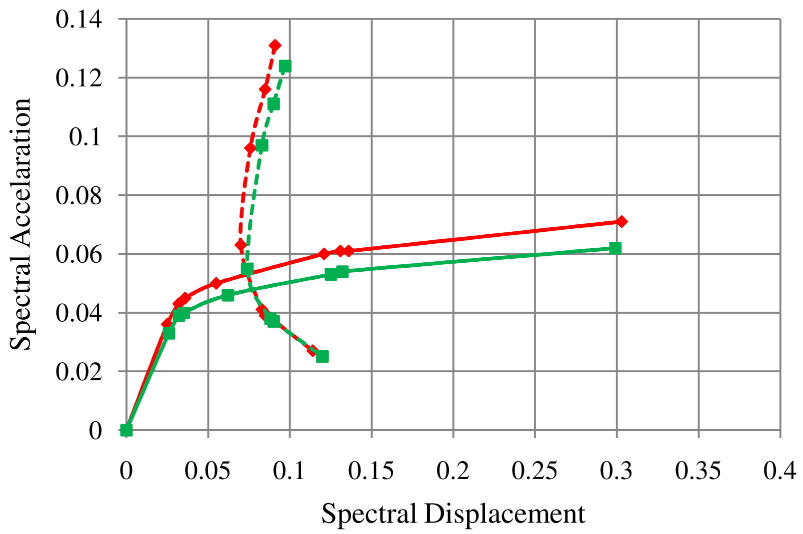

10 Story building

Dynamic Analysis

Performance point (V, D)	2267.75	0.089
Performance point (S_a, S_d)	0.053	0.073

Static Analysis

Performance point (V, D)	1736.47	0.095
Performance point (S_a, S_d)	0.048	0.078

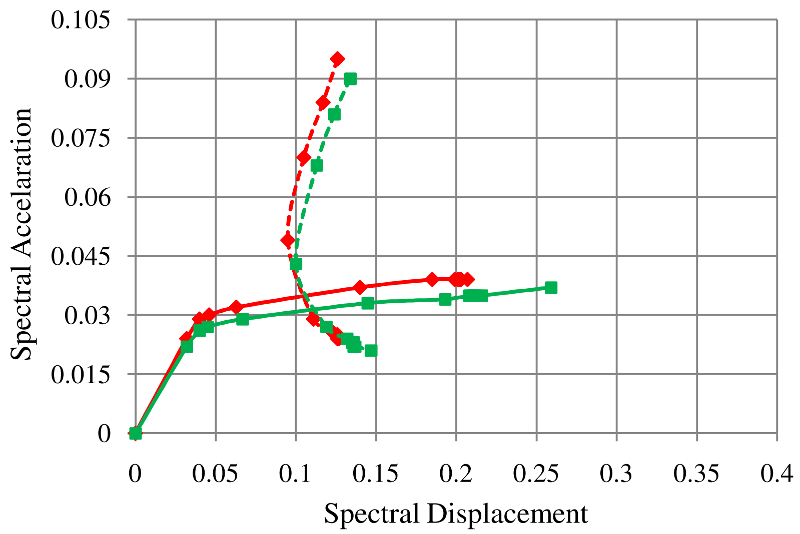

15 Story building

Dynamic Analysis

Performance point (V, D)	2119.18	0.126
Performance point (S_a, S_d)	0.035	0.104

Static Analysis

Performance point (V, D)	1865.51	0.136
Performance point (S_a, S_d)	0.031	0.111

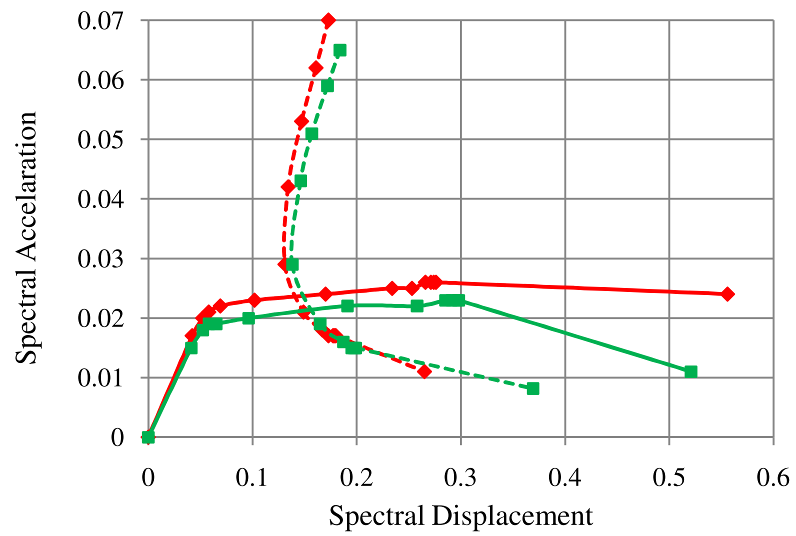

20 Story building

Dynamic Analysis

Performance point (V, D)	2023.14	0.172
Performance point (S_a, S_d)	0.024	0.214

Static Analysis

Performance point (V, D)	1759.19	0.189
Performance point (S_a, S_d)	0.021	0.155

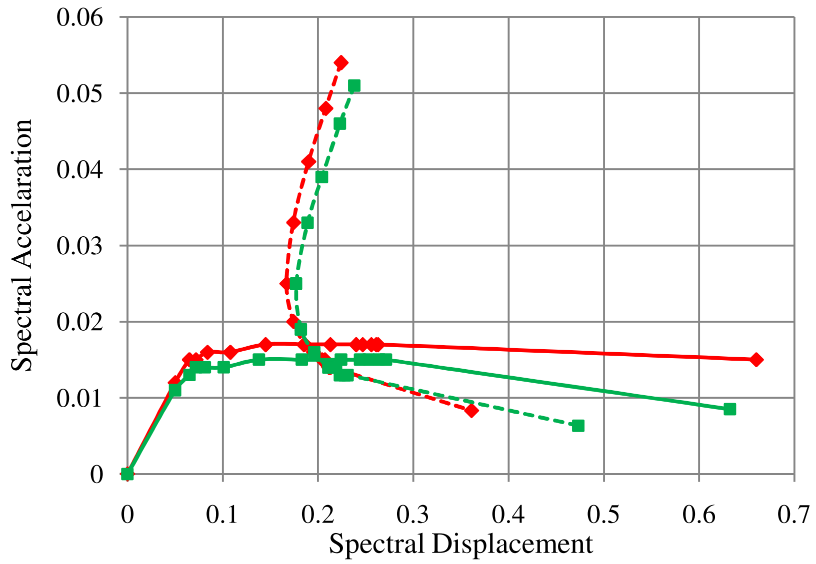

25 Story building

Dynamic Analysis

Performance point (V, D)	1906.4	0.226
Performance point (S_a, S_d)	0.017	0.186

Static Analysis

Performance point (V, D)	1659.61	0.248
Performance point (S_a, S_d)	0.015	0.203

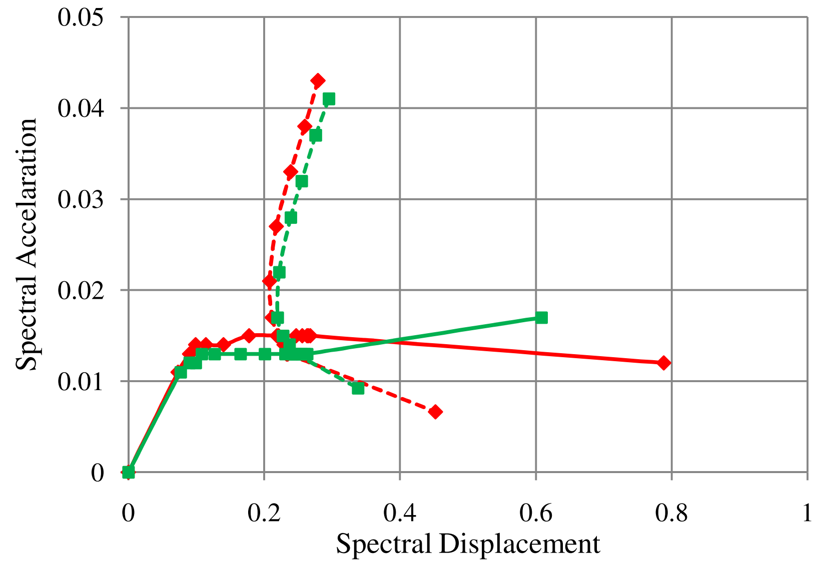

30 Story building

Dynamic Analysis

Performance point (V, D)	2195.2	0.277
Performance point (S_a, S_d)	0.015	0.222

Static Analysis

Performance point (V, D)	1924.9	0.301
Performance point (S_a, S_d)	0.013	0.239

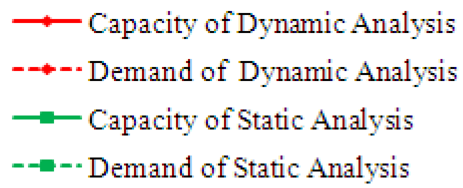

Fig 5.28 Performance point using IS1893 specified response spectrum

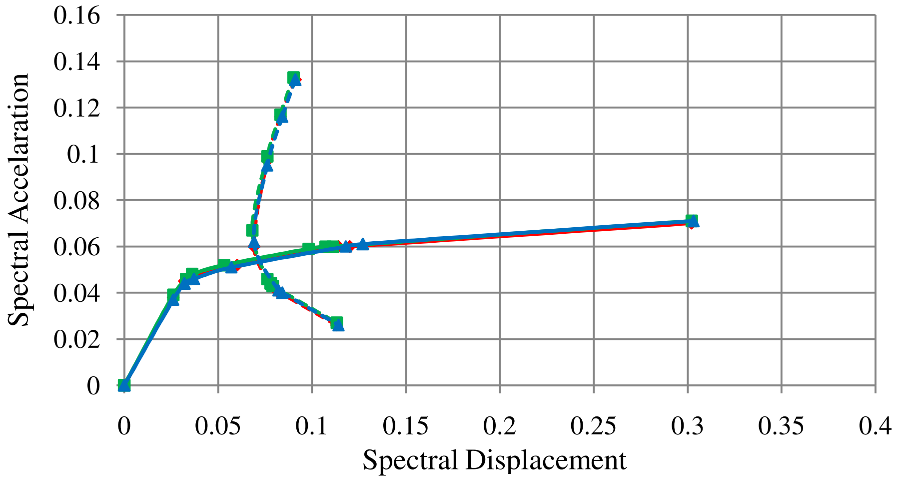

10 Story building

IIM Response Spectrum		
Performance point (V, D)	1975.80	0.088
Performance point (S_a, S_d)	0.054	0.072
NIT Response Spectrum		
Performance point (V, D)	1992.85	0.089
Performance point (S_a, S_d)	0.055	0.071
Passport Office Response Spectrum		
Performance point (V, D)	1964.49	0.089
Performance point (S_a, S_d)	0.053	0.073

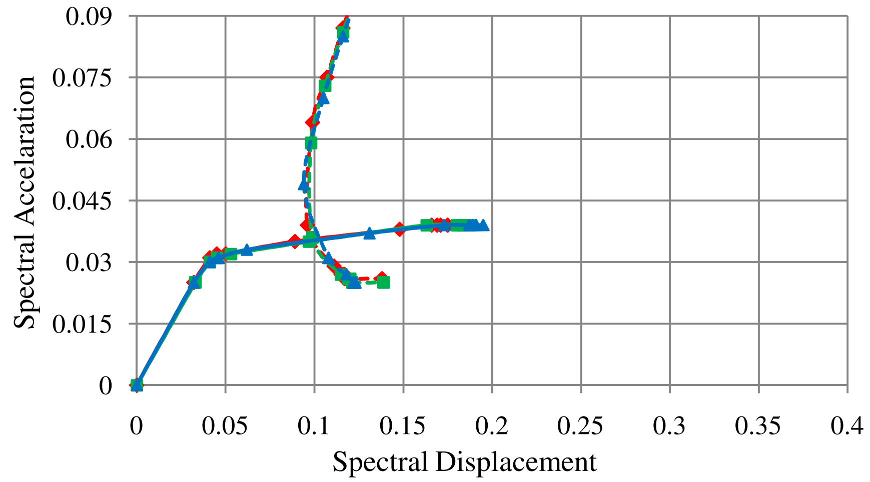

15 Story building

IIM Response Spectrum		
Performance point (V, D)	2168.55	0.123
Performance point (S_a, S_d)	0.036	0.099
NIT Response Spectrum		
Performance point (V, D)	2165.55	0.122
Performance point (S_a, S_d)	0.036	0.100
Passport Office Response Spectrum		
Performance point (V, D)	2135.48	0.126
Performance point (S_a, S_d)	0.035	0.103

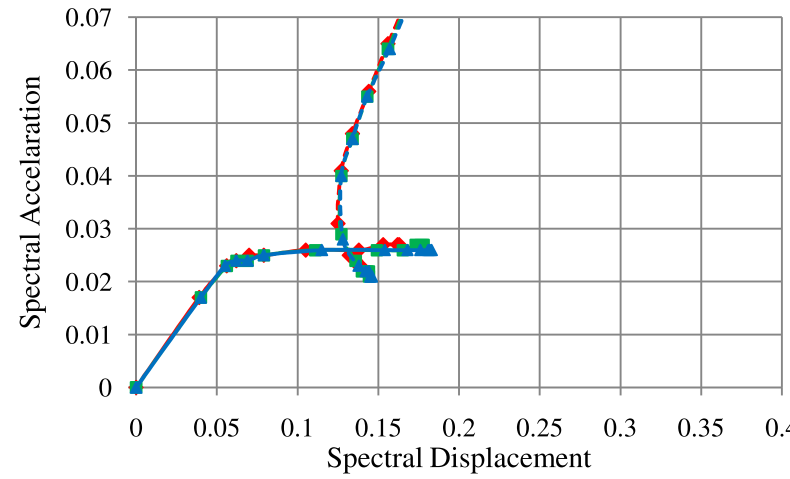

20 Story building

IIM Response Spectrum		
Performance point (V, D)	2155.96	0.169
Performance point (S_a, S_d)	0.0266	0.130
NIT Response Spectrum		
Performance point (V, D)	2136.87	0.170
Performance point (S_a, S_d)	0.026	0.132
Passport Office Response Spectrum		
Performance point (V, D)	2129.91	0.170
Performance point (S_a, S_d)	0.026	0.132

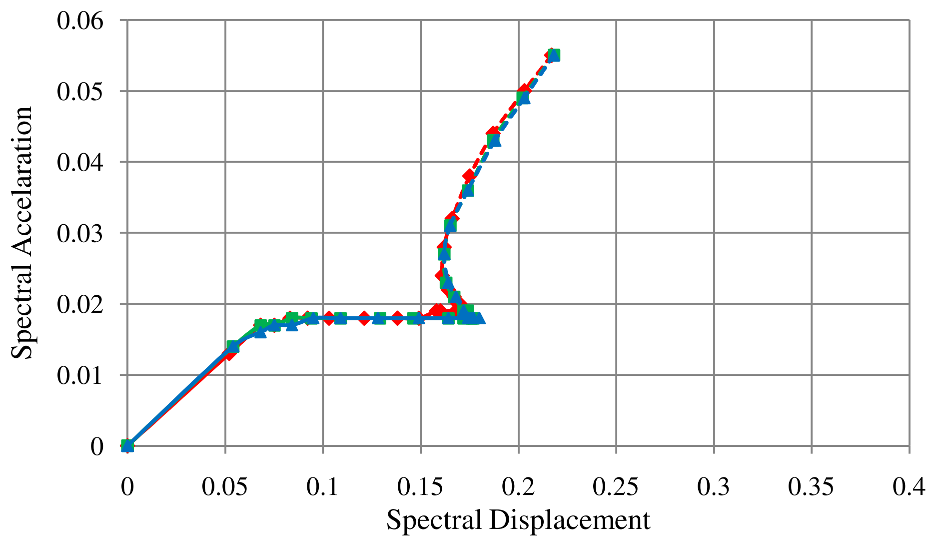

25 Story building

IIM Response Spectrum		
Performance point (V, D)	-	-
Performance point (S_a, S_d)	-	-
NIT Response Spectrum		
Performance point (V, D)	2014.28	0.221
Performance point (S_a, S_d)	0.018	0.175
Passport Office Response Spectrum		
Performance point (V, D)	2007.83	0.221
Performance point (S_a, S_d)	0.018	0.176

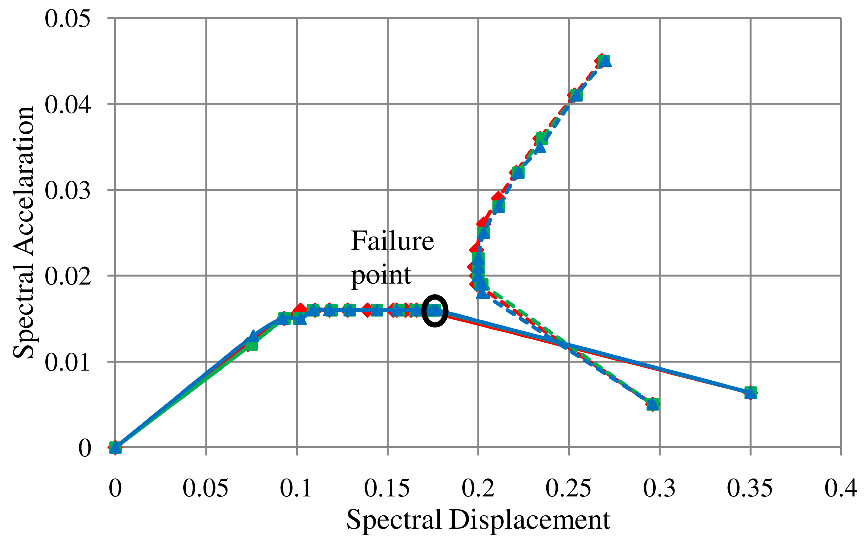

30 Story building

IIM Response Spectrum		
Performance point (V, D)	-	-
Performance point (S_a, S_d)	-	-
NIT Response Spectrum		
Performance point (V, D)	-	-
Performance point (S_a, S_d)	-	-
Passport Office Response Spectrum		
Performance point (V, D)	-	-
Performance point (S_a, S_d)	-	-

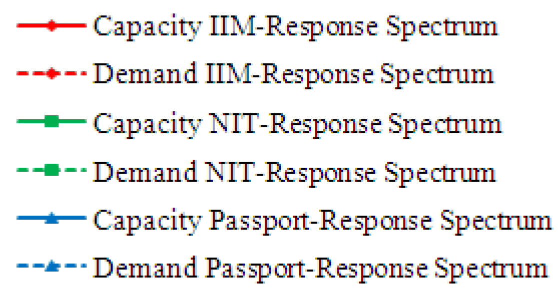

Fig. 5.29 Performance point using site specified response spectrum analysis

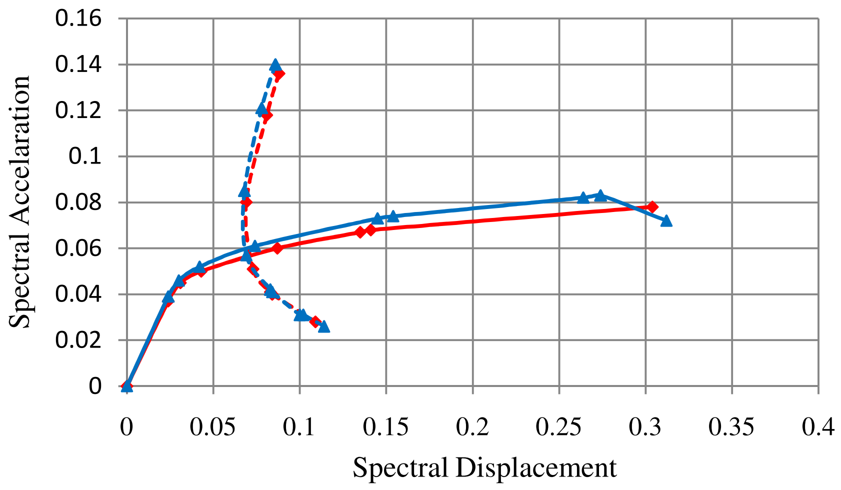

10 Story building

IIM Time History		
Performance point (V, D)	2142.22	0.086
Performance point (S_a, S_d)	0.056	0.072
NIT Time History		
Performance point (V, D)	-	-
Performance point (S_a, S_d)	-	-
Passport Office Time History		
Performance point (V, D)	2284.77	0.080
Performance point (S_a, S_d)	0.059	0.069

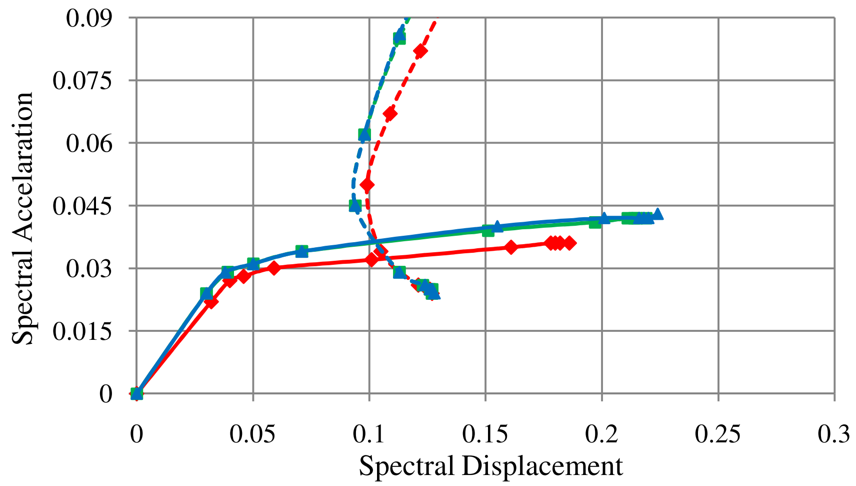

15 Story building

IIM Time History		
Performance point (V, D)	1979.88	0.131
Performance point (S_a, S_d)	0.033	0.107
NIT Time History		
Performance point (V, D)	2241.29	0.122
Performance point (S_a, S_d)	0.036	0.101
Passport Office Time History		
Performance point (V, D)	2258.31	0.121
Performance point (S_a, S_d)	0.036	0.101

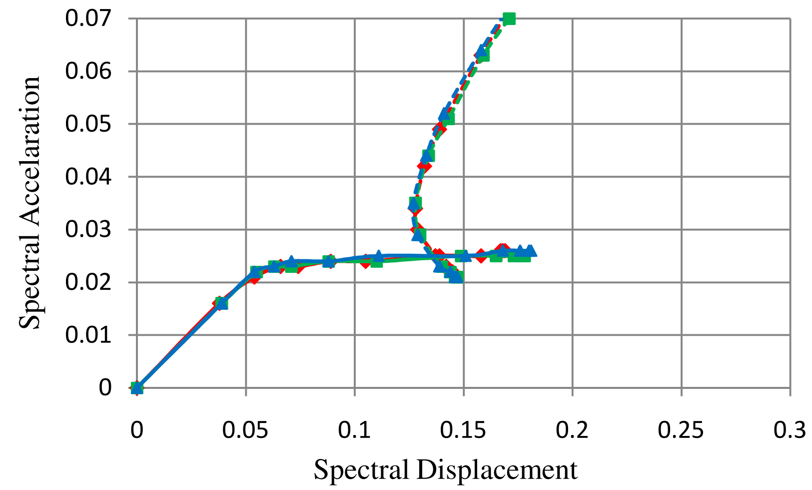

20 Story building

IIM Time History		
Performance point (V, D)	2092.82	0.175
Performance point (S_a, S_d)	0.025	0.136
NIT Time History		
Performance point (V, D)	2070.13	0.180
Performance point (S_a, S_d)	0.030	0.140
Passport Office Time History		
Performance point (V, D)	2106.98	0.173
Performance point (S_a, S_d)	0.025	0.135

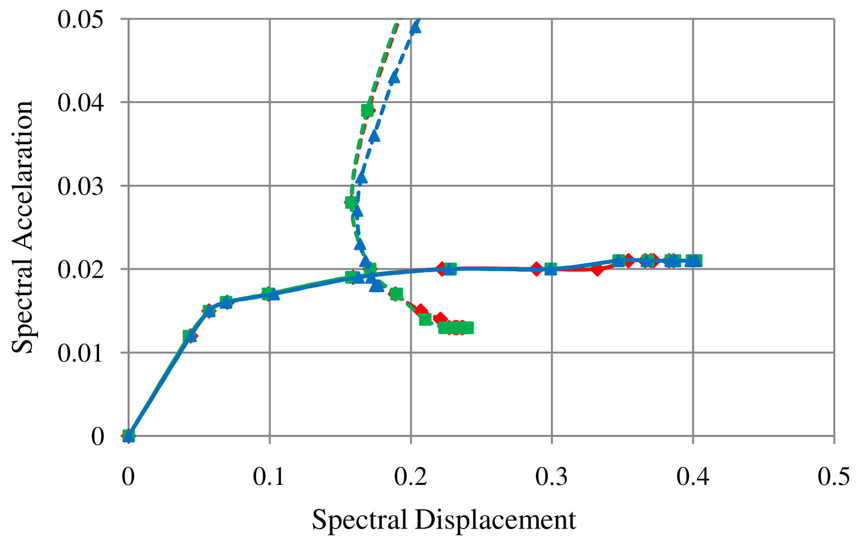

25 Story building

IIM Time History		
Performance point (V, D)	2227.10	0.205
Performance point (S_a, S_d)	0.019	0.176
NIT Time History		
Performance point (V, D)	2237.69	0.204
Performance point (S_a, S_d)	0.019	0.176
Passport Office Time History		
Performance point (V, D)	2230.74	0.205
Performance point (S_a, S_d)	0.019	0.176

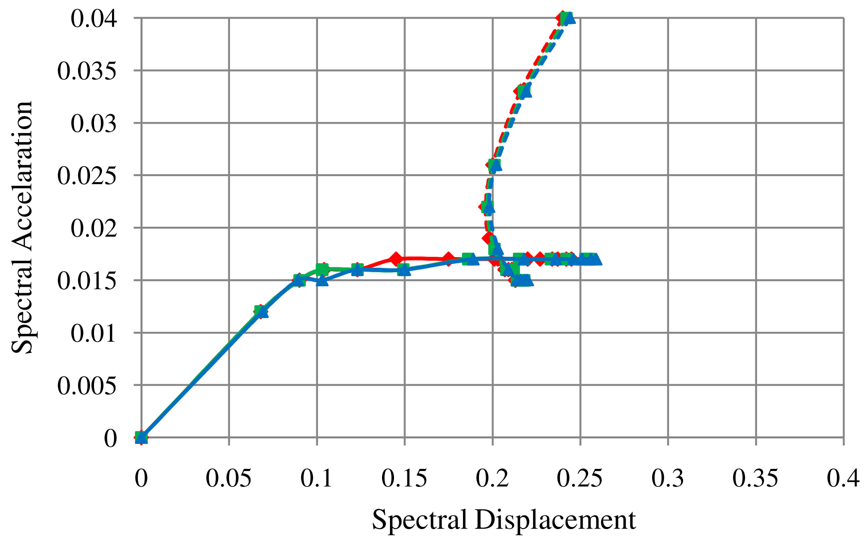

30 Story building

IIM Time History		
Performance point (V, D)	2561.73	0.256
Performance point (S_a, S_d)	0.017	0.204
NIT Time History		
Performance point (V, D)	2531.01	0.257
Performance point (S_a, S_d)	0.017	0.206
Passport Office Time History		
Performance point (V, D)	2499.36	0.258
Performance point (S_a, S_d)	0.017	0.207

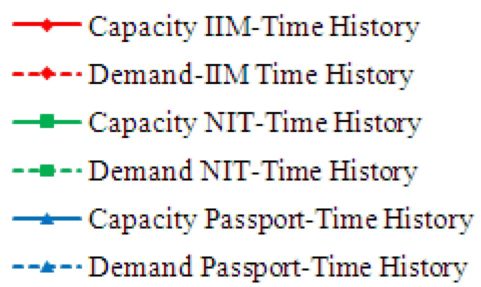

Fig. 5.30 Performance point using site specified time history analysis

Comparison of base shear and top displacement at performance point is shown in Table 5.6.

Table 5.6 Base shear and top displacement at performance point (kN,m)

	Type of Analysis	Quantity	**IIM Site**	**NIT Site**	**Passport Office Site**	**IS 1893**	
						Static Analysis	**Dynamic Analysis**
10	Site Specific Response Spectra	Base Shear	1975.80	1992.85	1964.49	1736.47	2267.75
		Top Displacement	0.088	0.089	0.089	0.095	0.089
	Site Specific Time History	Base Shear	2142.22	-	**2284.77**		
		Top Displacement	0.086	-	0.08		
15	Site Specific Response Spectra	Base Shear	2168.55	2165.55	2135.48	1865.51	2119.18
		Top Displacement	0.123	0.122	0.126	0.136	0.126
	Site Specific Time History	Base Shear	1979.88	2241.29	**2258.31**		
		Top Displacement	0.131	0.122	0.121		
20	Site Specific Response Spectra	Base Shear	**2155.96**	2136.87	2129.91	1759.19	2023.14
		Top Displacement	0.169	0.17	0.17	0.189	0.172
	Site Specific Time History	Base Shear	2092.82	2070.13	2106.98		
		Top Displacement	0.175	0.18	0.173		
25	Site Specific Response Spectra	Base Shear	-	2014.28	2007.83	1659.61	1906.4
		Top Displacement	-	0.221	0.221	0.248	0.226
	Site Specific Time History	Base Shear	2227.10	2237.69	**2230.74**		
		Top Displacement	0.205	0.204	0.205		
30	Site Specific Response Spectra	Base Shear	-	-	-	1924.86	2195.17
		Top Displacement	-	-	-	0.301	0.277
	Site Specific Time History	Base Shear	**2561.73**	2531.01	2499.36		
		Top Displacement	0.256	0.257	0.258		

5.9.3 Hinge Formation Pattern

It is observed that first hinge form in beam element as per strong column and week beam assumption and subsequently hinge form in beam and column elements. Initially hinges are in B-IO stage and subsequently proceeding to IO-LS and LS-CP stage. On further pushing of buildings the hinges formed initially moved to higher stage of hinge property. The intersection of capacity curve and demand curve in spectrum co-ordinate is called performance point. It represents the damages on structure for the given earthquake ground motion. Fig. 5.30 and Fig. 5.31 is shows the hinge formation in frame structure at performance point. At intermediate story level hinges are in higher stage which is due to maximum story drift at that level.

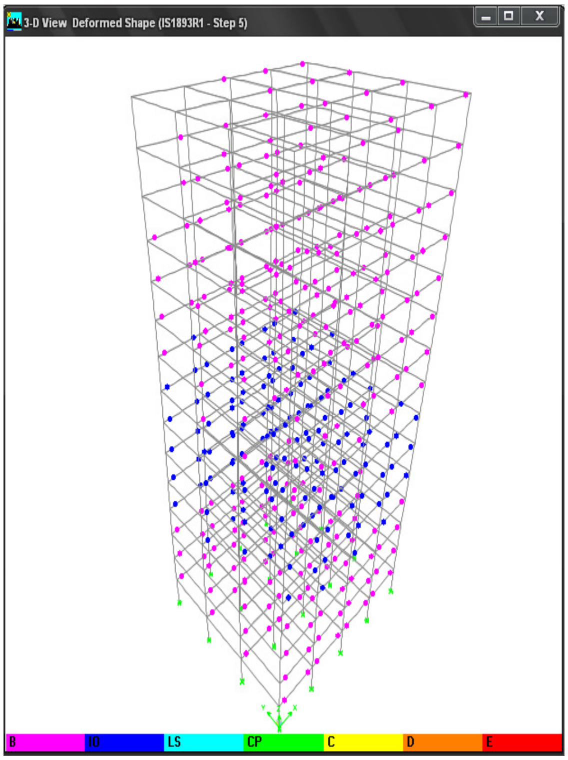

IS 1893 Static analysis

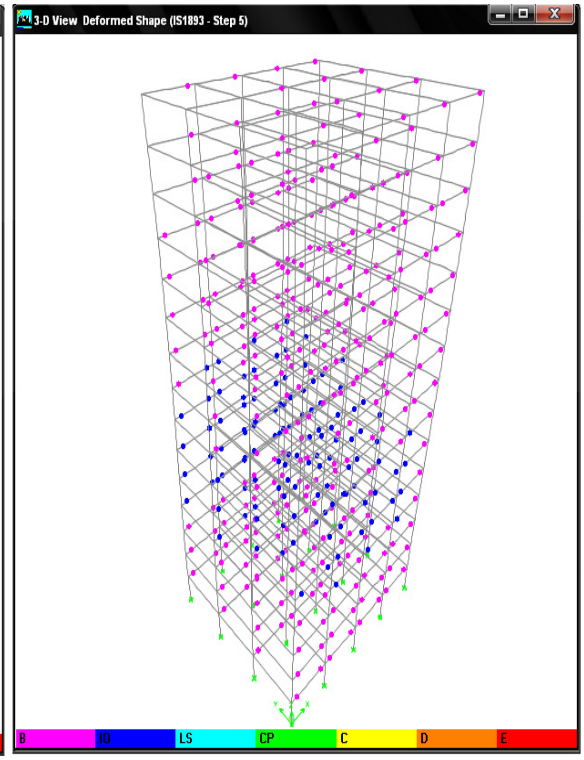

IS 1893 Dynamic analysis

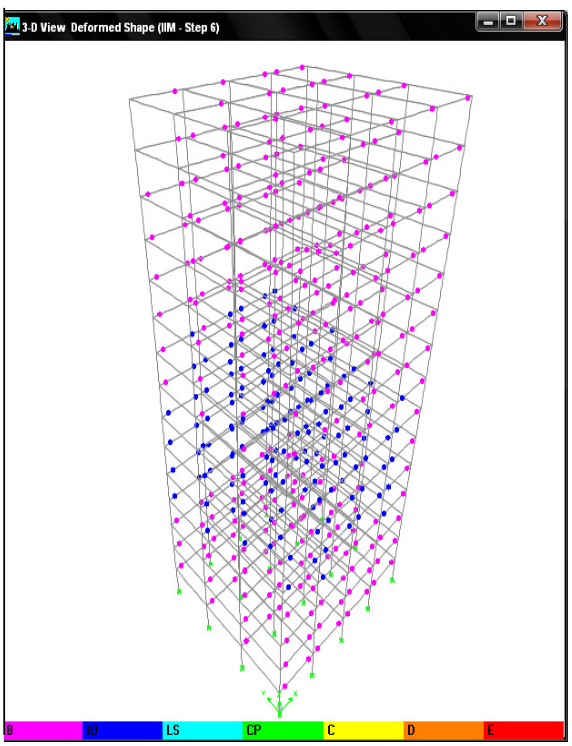

IIM Response Spectrum Analysis

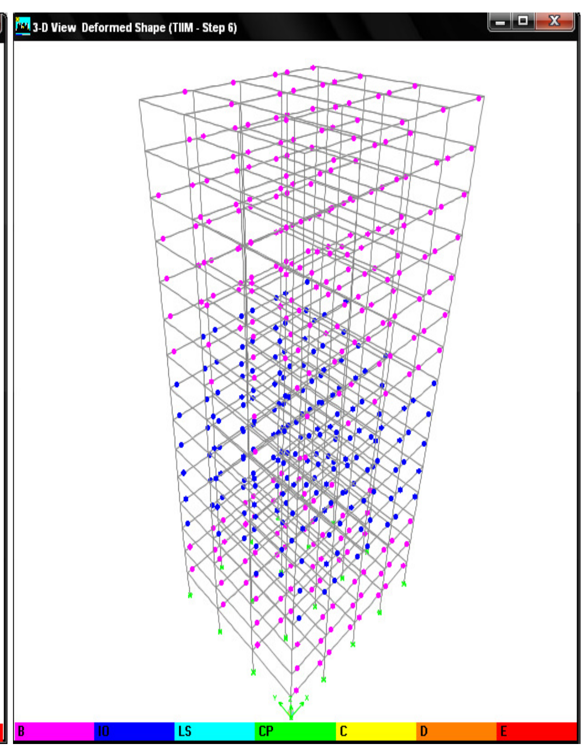

IIM Time History Analysis

Fig. 5.31 Hinge Formation at Performance Point

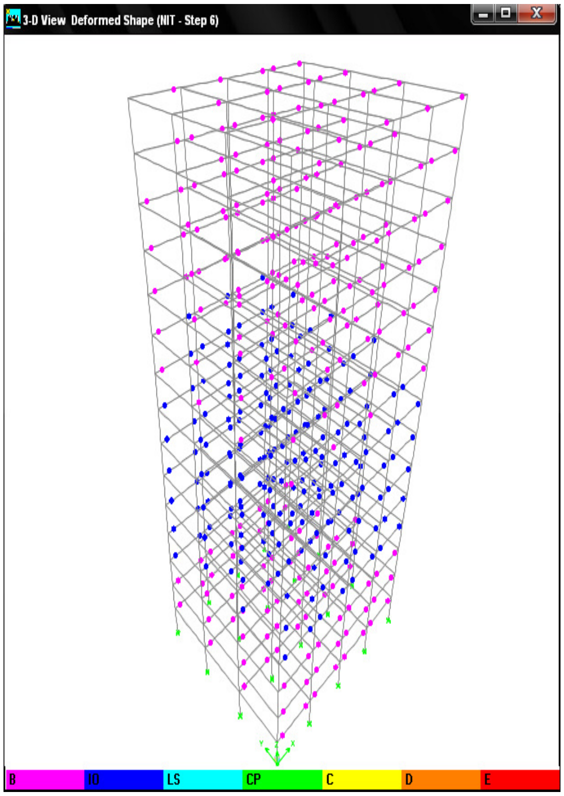

NIT Response Spectrum Analysis

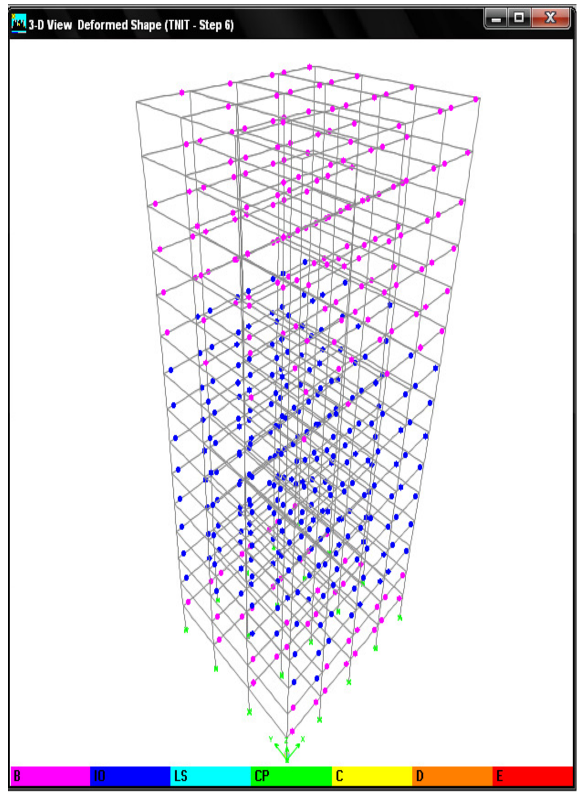

NIT Time History Analysis

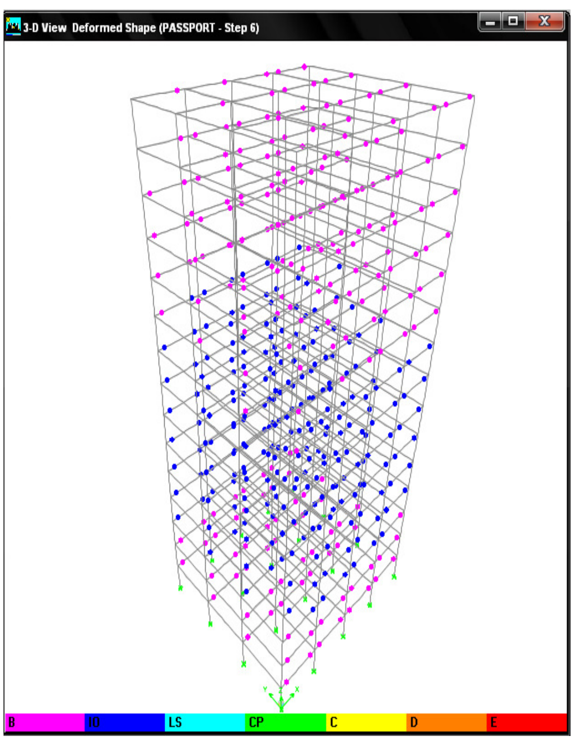

Passport Office Response Spectrum Analysis

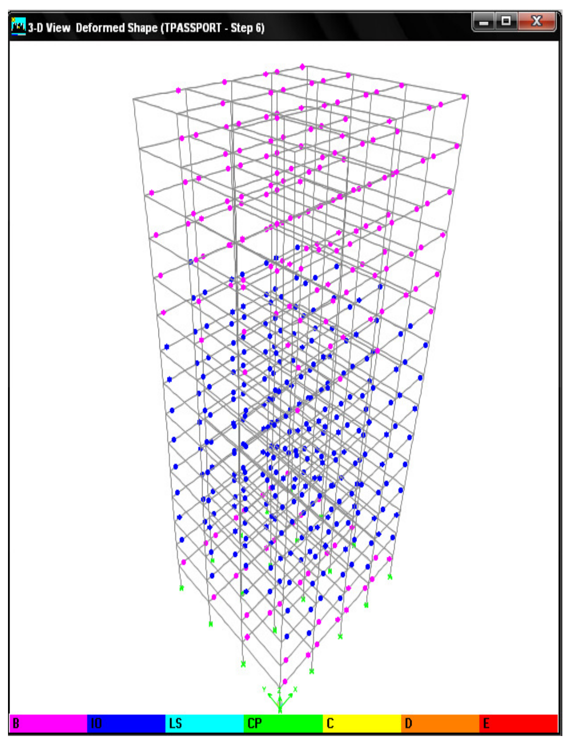

Passport Office Time History Analysis

Fig. 5.32 Hinge Formation at Performance Point

Based on above study, the following findings are observed:

1. Static analysis as per IS: 1893-2002 considers only first mode shape of building but time history analysis considers higher mode shape of building. So large variation in force along the height of structure is observed in 25 story building considering time history analysis compared with IS: 1893-2002.
2. Performance point cannot be obtained in 30 story building in site specific response spectrum. So this indicates that building is not capable to meet demand and increase in size of element or increase in percentage of reinforcement are required to meet the capacity and demand curve.
3. Base shear at performance point in static analysis and dynamic analysis is quite more compared to difference in base shear considering time history and site response spectra analysis.
4. Higher stage hinge formations are observed in time history analysis indicating the importance of higher mode shape.

5.10 SUMMARY

Basic overview of pushover analysis, time history and response spectra analysis is discussed in this Chapter. It mainly includes procedure of Time history analysis and Response spectra analysis using ETABS. Lateral load distribution over the height of structure considering site specific time history and response spectrum is studied. Results are obtained inform of capacity, demand, performance point Hinge formation pattern at performance point are presented for building having different no. of story

6. ANALYSIS OF SHEAR WALL BUILDING

6.1 GENERAL

Site Specific Response analysis is carried out for various sites to find out the response of ground when an earthquake occurs. Local soil conditions influence the intensity of shaking and play an important role in earthquake resistant design of buildings. Interaction between ground acceleration and structure system through response spectrum is very important in earthquake engineering. Maximum damage can occur in the building when the resulting seismic wave frequency matches with the resonant frequencies of the structures. The amplification of ground motion is highly depends on local geological, topographical and geotechnical soil condition.

The seismic waves passing through the soil deposits from the bedrock to the surface, the frequency and amplitude are changed based on the soil deposits. Depending upon the type of soil deposits there is variation in certain frequencies and amplitudes of seismic waves. These variations results in increase or decrease of the intensity of seismic waves thus resulting in earthquake damage. The amplification is reduces with increase of epicenter distance from the site.

6.2 GROUND MOTION TIME HISTORY

For engineering purpose the time variation of ground acceleration is the most useful way of defining the shaking of the ground during an earthquake. Time history is required in the development of site specific design ground motion. Time history plots are related to the design response spectra in terms of peak ground acceleration. During occurrence of an earthquake, the base of a structure or soil is subjected to the shaking of the ground thus producing ground motions. These ground motions are measured in terms of acceleration with each increment of time.

The ground motion recorded at ground floor of passport office building during Bhuj earthquake on 26th January 2001 is used to develop the ground motion at the rock or hard soil level which is considered at 15 m below ground level. This artificial developed acceleration time history at 15 m depth at passport office is used as an input motion at other sites for the development of acceleration time history at ground surface. This acceleration time history developed at various site using one dimensional ground response analysis software ProSHAKE [27] are shown in Fig. 6.1 and 6.2. For the development of artificial time history, longitudinal direction is considered because it is critical compared to other directions.

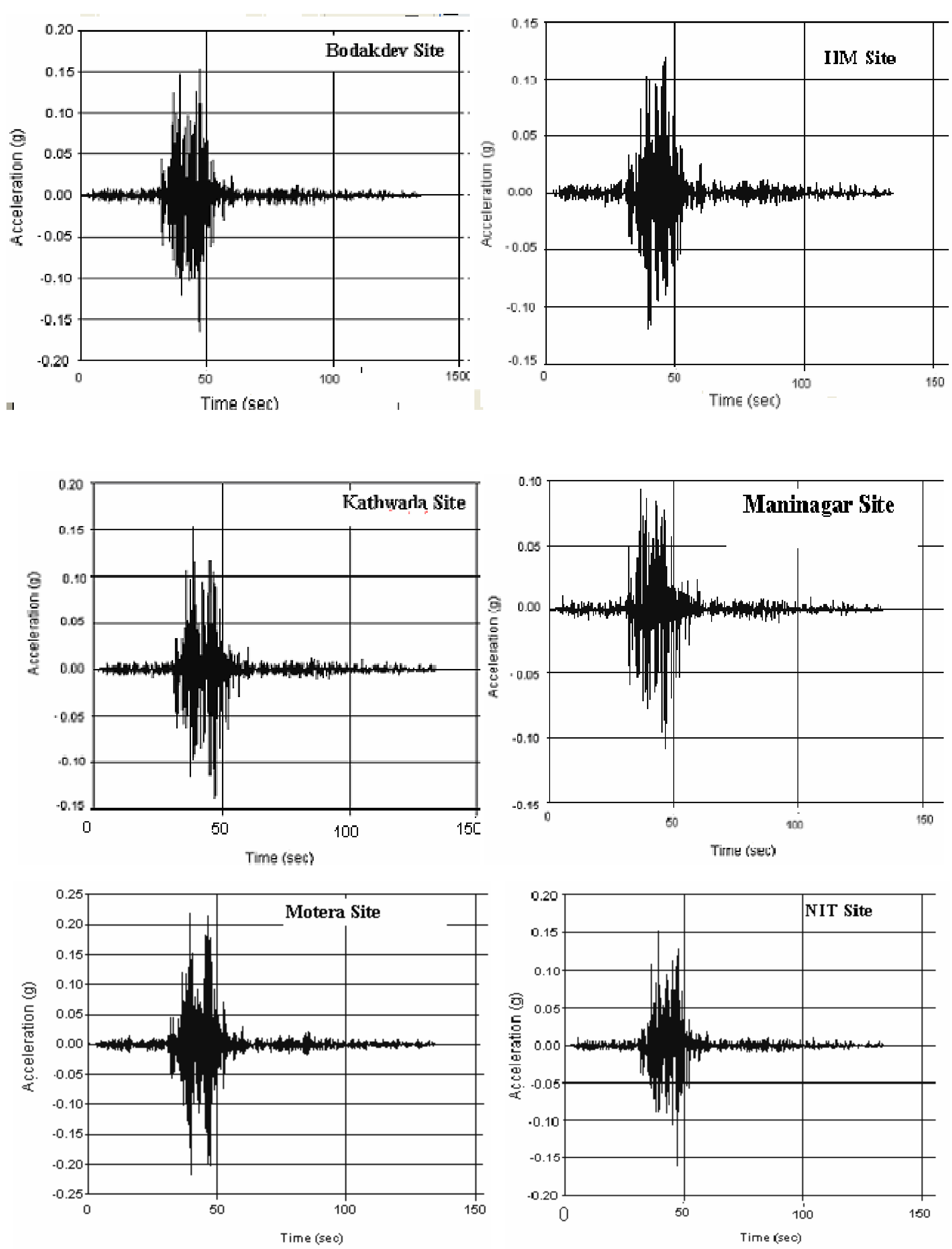

Fig. 6.1 Acceleration Time History plots on ground surface at various sites

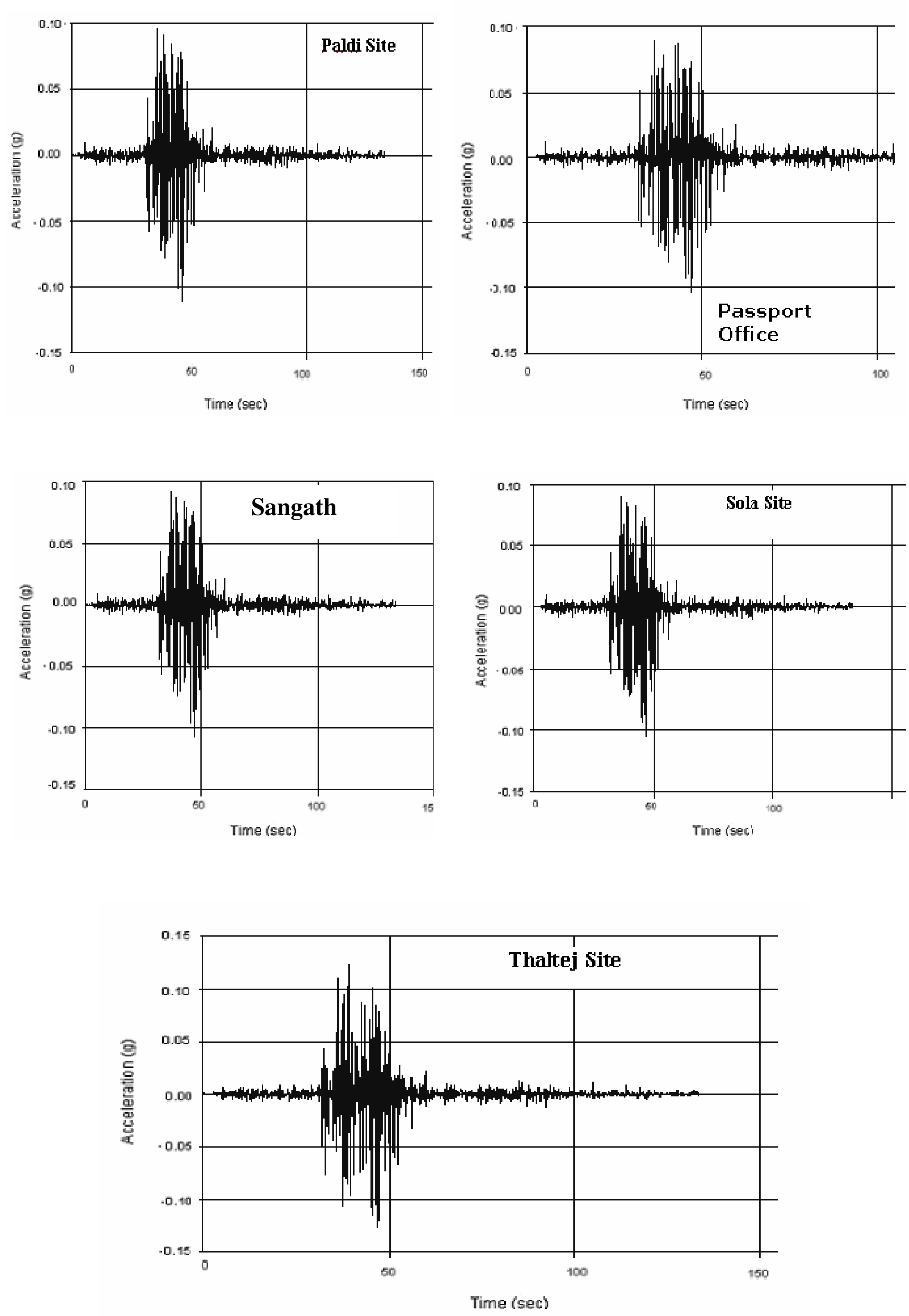

Fig. 6.2 Acceleration Time History plots on ground surface at various sites

6.3 RESPONSE SPECTRUM CURVE

Response spectrum analysis is widely used for seismic design of building. Site specific response spectrum for eleven sites of Ahmedabad city is derived using ProSHAKE software [27]. From the available data of sub-soil strata and input motion of acceleration time history, the response spectrum is obtained by plotting the spectral accelerations against the time periods for 5% damping. The plots of response spectra obtained for various sites are presented in the Fig. 6.3 and 6.4.

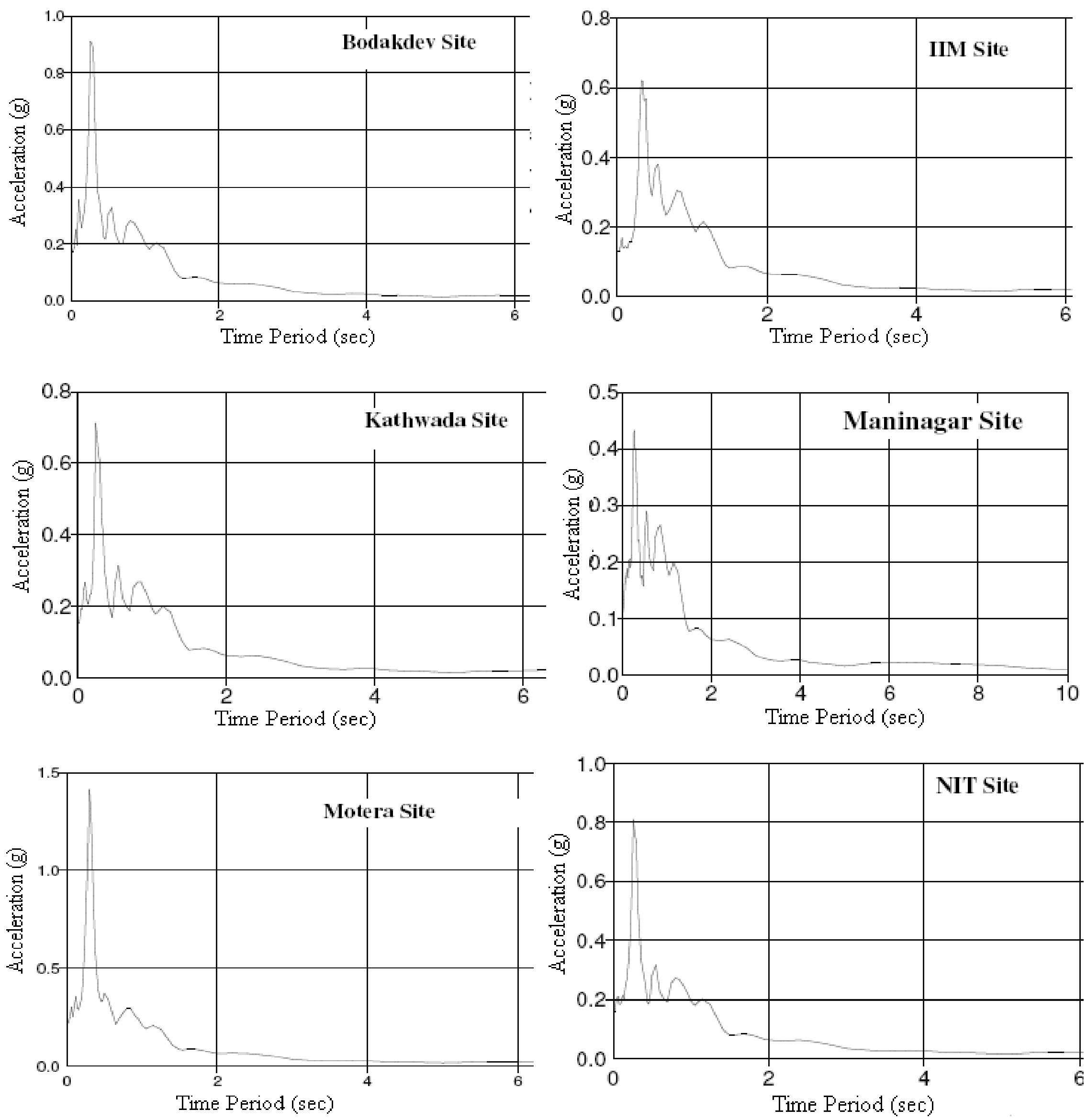

Fig. 6.3 Response spectra plots on ground surface at various sites

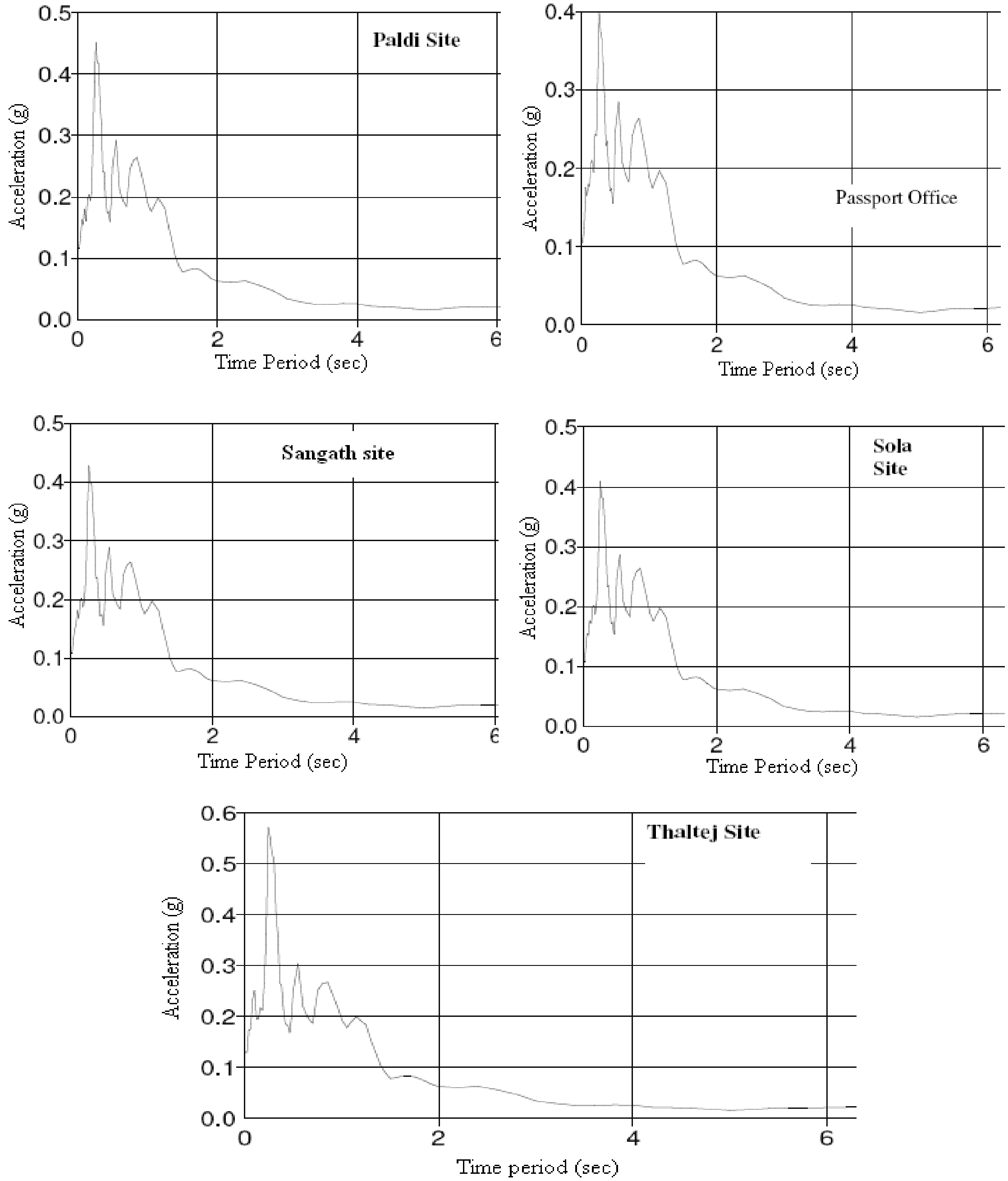

Fig. 6.4 Response spectra plots on ground surface at various sites

6.4 RESULTS AND DISCUSSIONS

10, 15, 20, 25 and 30 story shear walled building as shown in Fig. 1.7 is analyzed considering site specific response spectra and time history. The typical floor plan of shear wall building is shown in Fig 1.7 and the structural data of shear wall building is given in Table 1.1 as mentioned in chapter 1. Analysis of each shear wall building is carried out using ETABS software and result are compared in term of time period, base shear, internal forces in wall, story shear, story moment at ground level.

6.4.1 Fundamental Time period

It is the time period of first mode of vibration. The fundamental time period of structures is its time period of undamped free vibration. The fundamental dynamic time period are derived based on mass and stiffness matrix of structure. The seismic response of structure is depends on fundamental time period of structure.

The fundamental time period of structures is evaluated from the empirical formula given in Clause. 7.6.1 of IS: 1893 (Part1)-2002 as shown in Eq. 6.1.

$$T_n = \frac{0.09h}{\sqrt{d}} \qquad \text{. . . . (6.1)}$$

Where T_n is fundamental time period of structure, h is the height of structure and d is Base dimension of the building at the plinth level along the considered direction of the lateral force.

Alternatively time period can be obtained by dynamic analysis of building using software like ETABS. Comparison of static and dynamic time period of structure is shown in Fig. 6.5. The difference between static and dynamic time period is increases with height of building. Time period increases with increases the height of building.

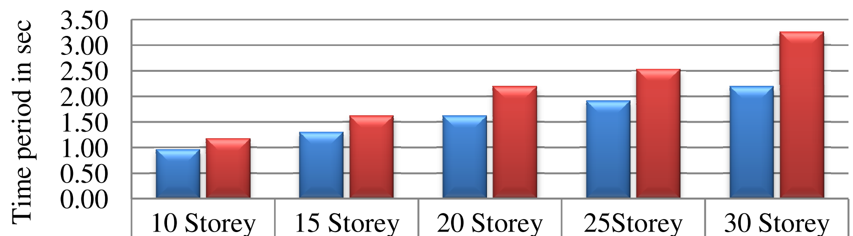

	10 Storey	15 Storey	20 Storey	25Storey	30 Storey
Static Time period (sec)	0.96	1.30	1.62	1.91	2.19
Dynamic Time period (sec)	1.17	1.62	2.19	2.53	3.26

Fig. 6.5 Comparison of time period

6.4.2 Story Force

Static analysis based on IS 1893 gives inverted triangular force distribution along the height of structure and is nearly similar to 1st mode vibration of structure. But it may be different while considering dynamic analysis using site specific response spectra and time history as shown in Fig 6.6 and 6.7.

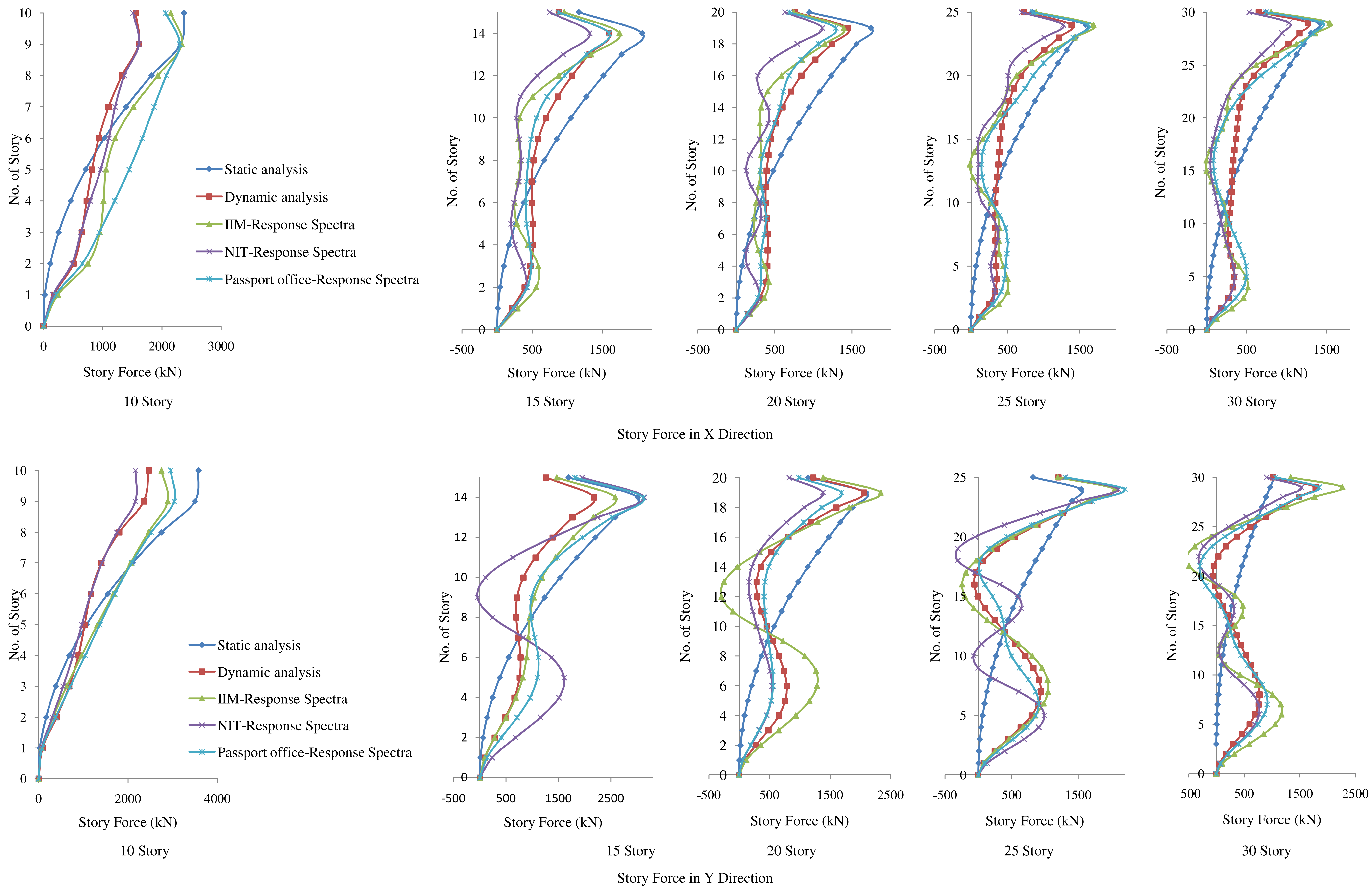

Fig. 6.6 Storey force on shear wall building considering site specific response spectra

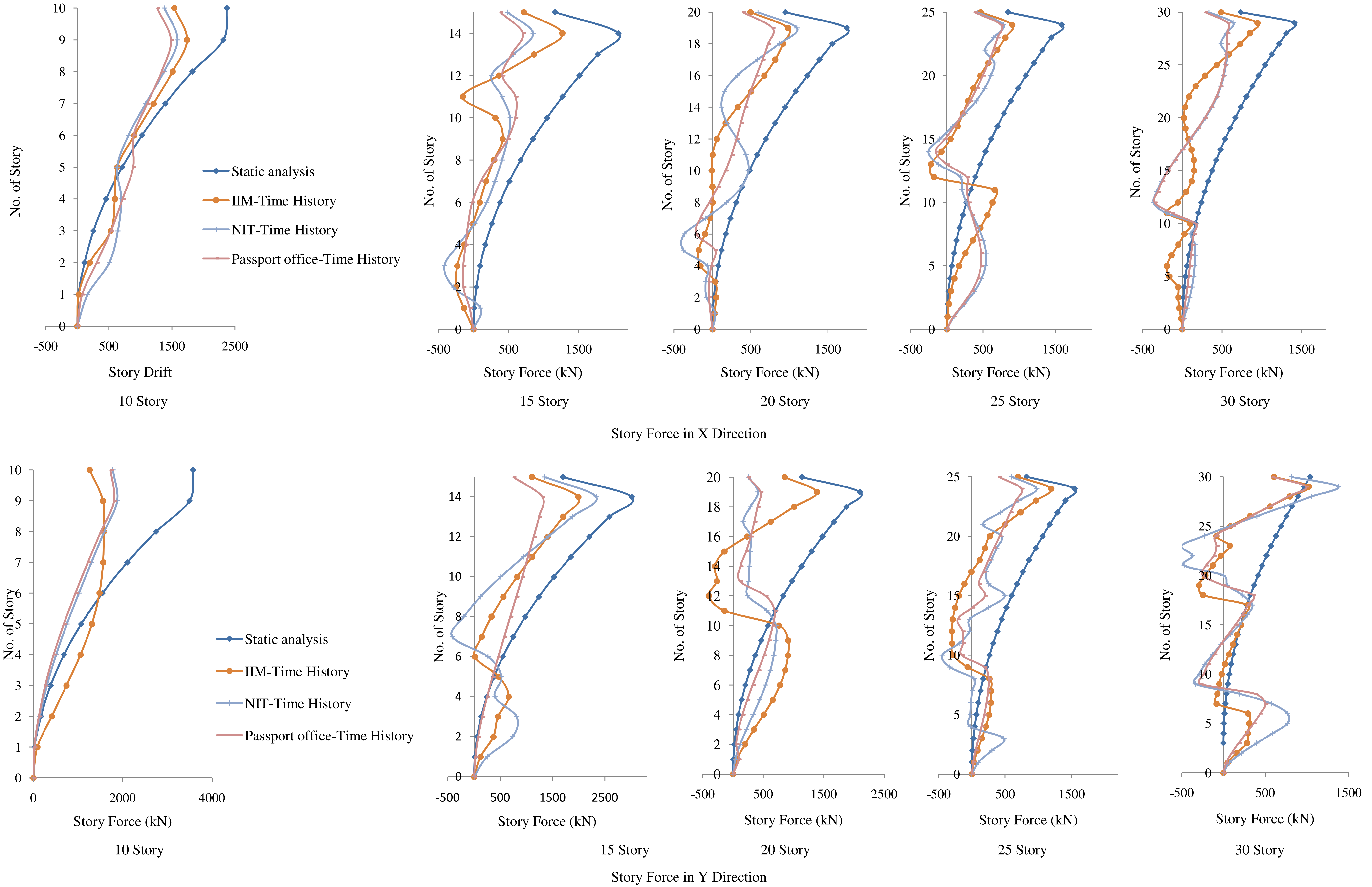

Fig. 6.7 Storey force on shear wall building considering site specific Time history

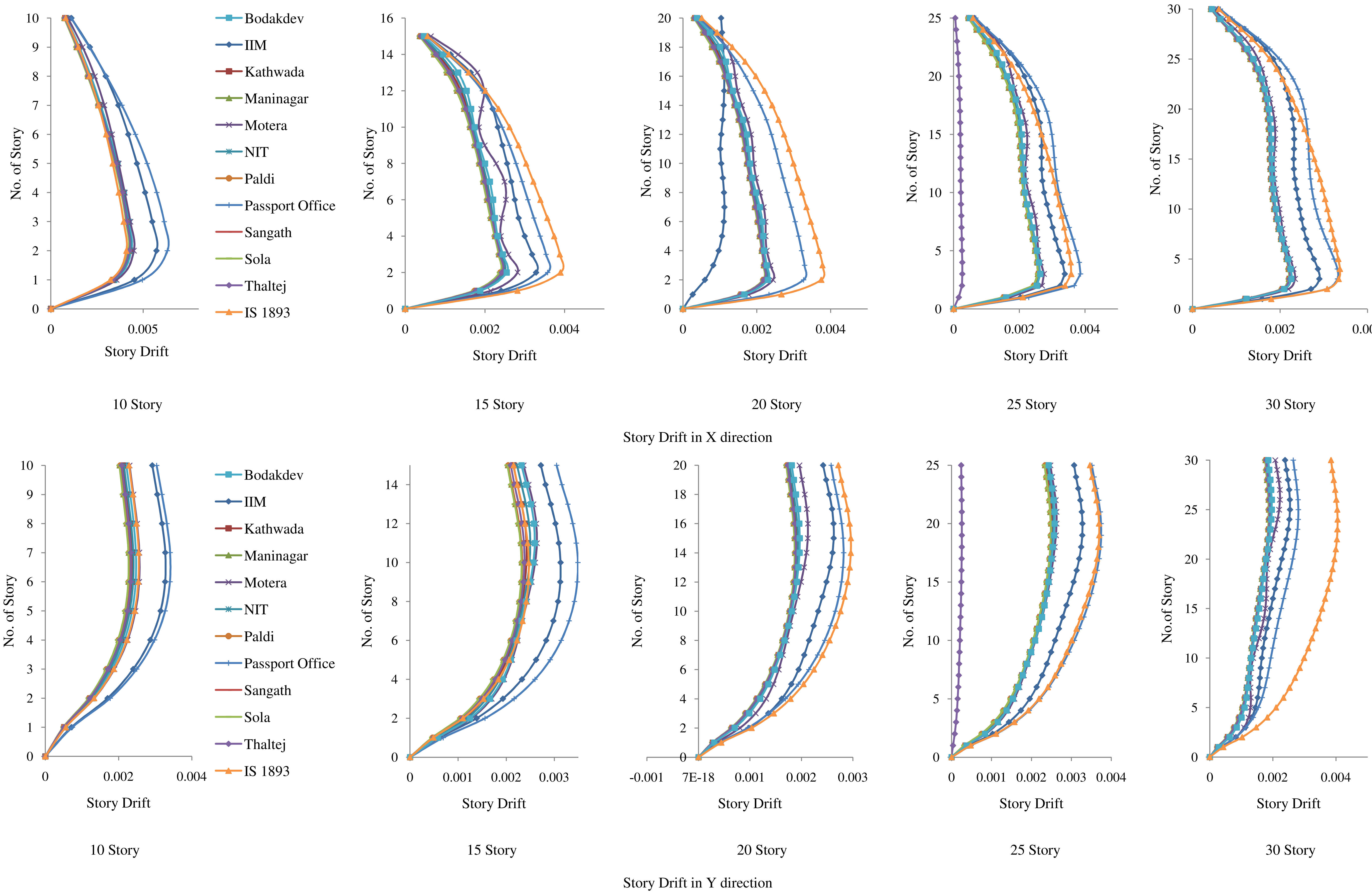

Fig. 6.8 Story drifts comparison using site response spectra

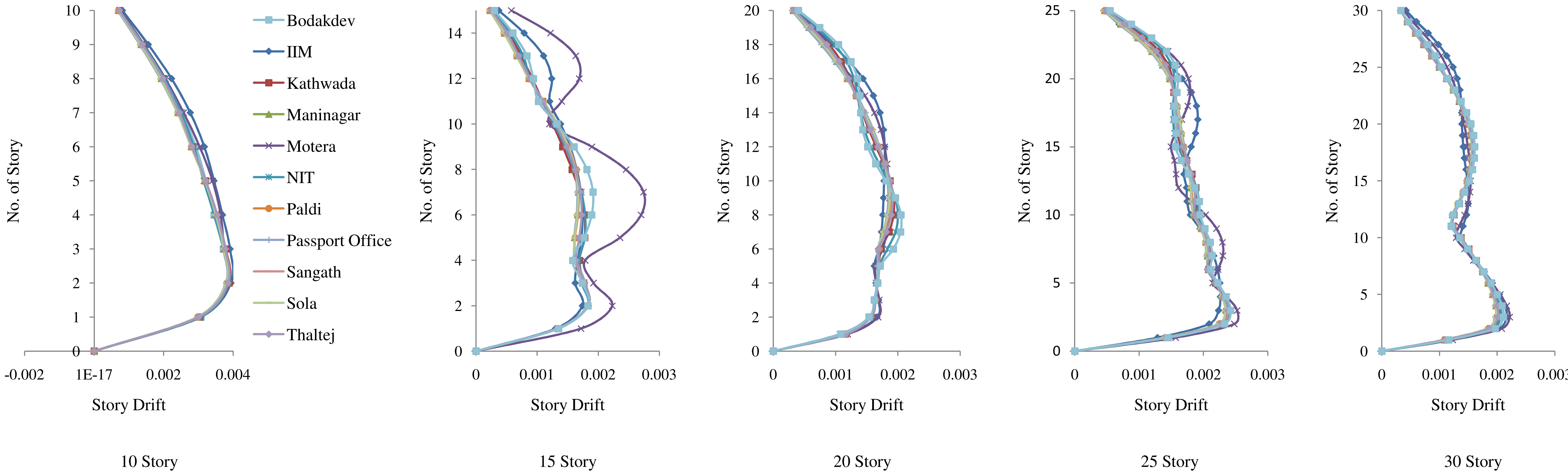

Story Drift in X Direction

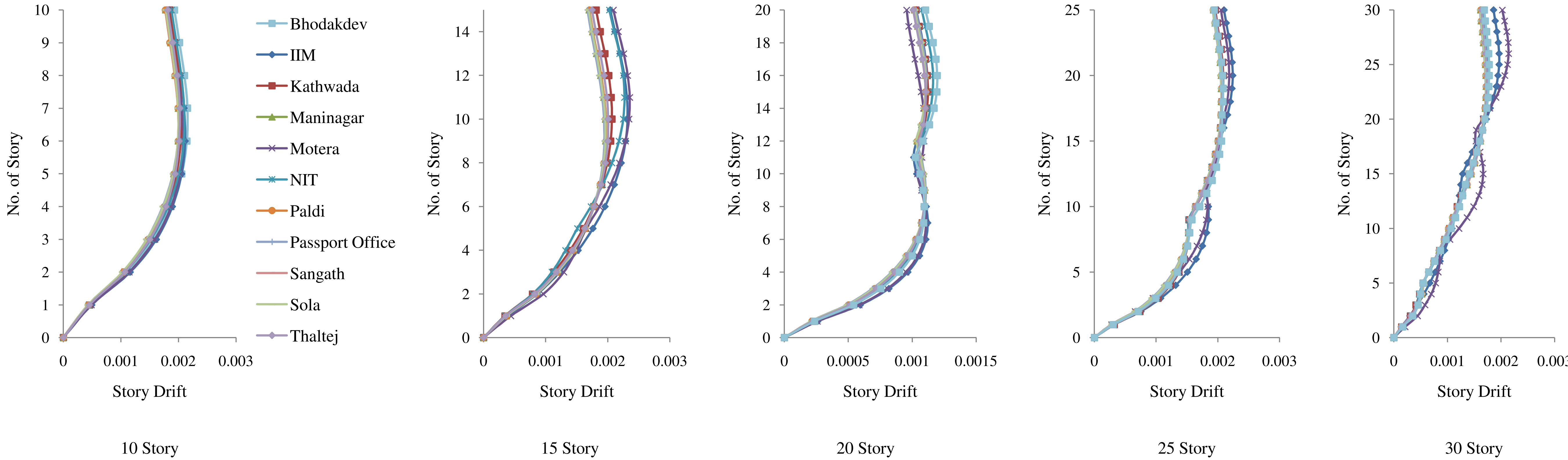

Story Drift in Y Direction

Fig. 6.9 Story drifts comparison using time history

6.4.3 Story Drift

Story drift is defined as a displacement of one floor level with respect to the other floor of building in above or below. In ATC 40, different performance levels are described based on story drift limit (eg. for life safety level and collapse prevention are consider for 0.02H and 0.04H story drift). Story drift for 10, 15, 20, 25 and 30 story is presented in Fig 6.8 and 6.9 for site specific response spectra and time history analysis. Each story height is considered as a 3 m from center to center so maximum story drift for life safety level is 0.02 × 3 = 0.06 m. Results clearly show that the story drift of each building is within permissible limit as consider in life safety level.

6.4.4 Base Shear

The comparison of base shear considering IS: 1893-2002 response spectra and site specific response spectra are shown in Fig. 6.10 & Fig. 6.11. In case of 15 and 20 story building IS: 1893-2002 response spectra are governing, while for 10, 25 and 30 story building site specific response spectra are governing.

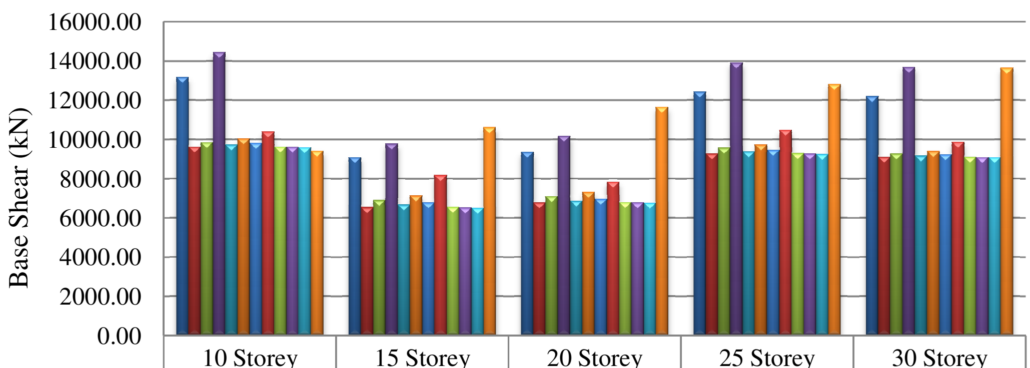

	10 Storey	15 Storey	20 Storey	25 Storey	30 Storey
IIM	13153.26	9074.03	9336.66	12402.00	12168.91
MANINAGAR	9596.29	6504.06	6750.78	9247.10	9075.92
NIT	9827.84	6870.50	7074.91	9534.63	9253.77
PASSPORT	14422.74	9749.26	10147.96	13896.75	13664.25
THALTEJ	9711.47	6647.93	6846.66	9355.21	9148.32
BODAKDEV	10009.07	7111.69	7298.04	9712.39	9376.79
KATHWADA	9785.86	6759.16	6939.60	9438.59	9200.80
MOTERA	10367.94	8146.35	7814.27	10460.30	9851.69
PALDI	9609.28	6525.07	6767.34	9260.25	9083.86
SANGATH	9590.61	6493.46	6747.99	9243.77	9073.56
SOLA	9573.44	6472.36	6738.15	9226.50	9063.26
IS1893	9395.84	10575.63	11626.29	12793.22	13620.89

Fig. 6.10 Base Shear in X direction considering site response spectra

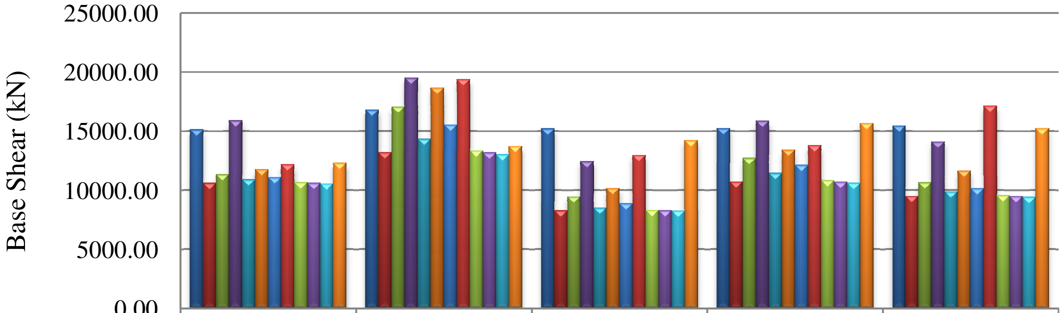

	10 Storey	15 Storey	20 Storey	25 Storey	30 Storey
IIM	15116.56	16804.50	15190.50	15222.57	15452.42
MANINAGAR	10599.97	13186.15	8274.32	10712.91	9486.96
NIT	11329.06	17042.78	9442.13	12701.20	10629.33
PASSPORT	15868.85	19481.55	12427.73	15849.04	14106.39
THALTEJ	10896.59	14326.51	8507.81	11430.02	9881.51
BODAKDEV	11754.94	18658.66	10150.15	13404.38	11622.89
KATHWADA	11075.04	15523.43	8856.70	12123.39	10140.50
MOTERA	12164.57	19361.00	12942.55	13765.00	17121.59
PALDI	10645.73	13341.72	8290.26	10817.29	9541.89
SANGATH	10585.56	13150.04	8265.26	10687.01	9468.81
SOLA	10546.52	13002.26	8241.41	10580.38	9402.79
IS1893	12286.78	13707.07	14205.04	15660.29	15226.79

Fig. 6.11 Base Shear in Y direction considering site response spectra

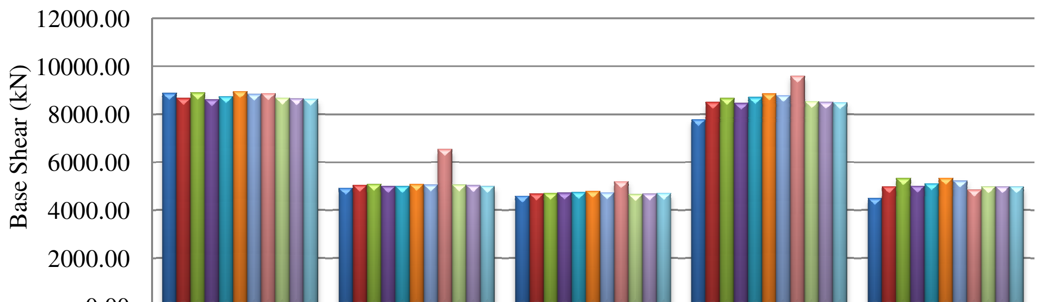

	10 Storey	15 Storey	20 Storey	25 Storey	30 Storey
IIM	8877.01	4927.64	4598.71	7780.11	4494.94
MANINAGAR	8655.52	5041.10	4684.56	8503.70	4984.21
NIT	8884.22	5085.68	4708.30	8662.62	5320.04
PASSPORT	8608.84	4997.96	4722.04	8465.74	5004.45
THALTEJ	8739.11	4993.37	4739.96	8699.70	5106.41
BODAKDEV	8947.18	5084.52	4801.25	8851.46	5340.36
KATHWADA	8835.97	5053.49	4737.00	8790.84	5228.84
MOTERA	8864.95	6538.13	5199.01	9595.65	4851.87
PALDI	8675.94	5053.95	4661.01	8535.58	4984.38
SANGATH	8650.67	5031.31	4681.87	8500.27	4986.33
SOLA	8633.76	5003.09	4709.28	8482.22	4985.15

Fig. 6.12 Base Shear in X direction considering Time History

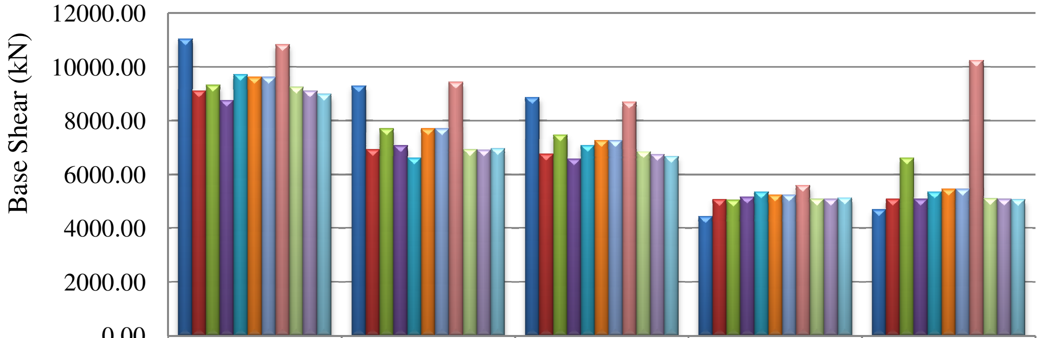

	10 Storey	15 Storey	20 Storey	25 Storey	30 Storey
IIM	11037.74	9293.89	8856.89	4423.72	4681.60
MANINAGAR	9098.06	6914.29	6744.91	5065.10	5075.25
NIT	9305.53	7693.24	7460.11	5036.06	6599.08
PASSPORT	8754.54	7059.07	6568.97	5149.27	5068.95
THALTEJ	9713.56	6603.04	7077.60	5341.64	5341.62
BODAKDEV	9598.31	7684.56	7250.46	5224.51	5441.04
KATHWADA	9598.31	7684.56	7250.46	5224.51	5441.04
MOTERA	10823.93	9424.04	8683.31	5585.13	10236.23
PALDI	9231.20	6916.22	6834.73	5071.97	5100.01
SANGATH	9095.69	6911.65	6736.73	5072.36	5071.92
SOLA	8974.39	6950.88	6663.96	5118.66	5063.30

Fig. 6.13 Base Shear in Y direction considering Time History

The comparison of base shear considering site specific time history is shown in Fig. 6.12 and Fig. 6.13. Motera site time history generates large base shear in Y direction for 30 story building so it indicates the resonance effect on structure.

6.4.5 Comparison of Design Forces in shear wall

The design forces in shear wall of all building are obtained considering site specific response spectra and time history analysis. Results are obtained from all load combinations and show the variation in force in shear wall. The design forces are considered in terms of axial forces, shear forces and bending moments in both direction, at foundation level of building is shown in Table 6.1. 10 story building is governing for passport office site response spectra and 20 story and 30 story building is governing for IS: 1893-2002 specified response spectra.

Table 6.1 Comparisons of Axial force, Shear force and Bending Moment at base level

			Bodak-dev	IIM	Kath-wada	Mani-nagar	Motera	NIT	Paldi	Passport	Sangath	Sola	Thaltej	IS1893
10 story	Site Specified Response Spectra	Axial Force	78929	103648	75366	72709	81754	76634	72977	**108749**	72627	72376	74422	80955
		Shear force in X dir.	10011	13156	9788	9598	10370	9830	9611	**14425**	9592	9575	9713	9398
		Shear force in Y dir.	12161	15564	11455	10965	12567	11718	11012	**16426**	10951	10911	11269	12675
		Moment in X dir.	7888	10325	7495	7207	8180	7638	7236	**10776**	7198	7172	7391	8175
		Moment in Y dir.	17016	22359	16639	16320	17620	16710	16341	**24528**	16310	16281	16514	15972
	Site Specified Time History	Axial Force	65982	**69394**	63892	62330	68426	64339	62456	62034	62286	62054	63419	
		Shear force in X dir.	**8959**	8931	8862	8667	8925	8890	8684	8619	8661	8642	8753	
		Shear force in Y dir.	10017	**11152**	9718	9463	11012	9627	9389	9717	9457	9460	9792	
		Moment in X dir.	6599	7247	6528	6250	**7125**	6442	6312	6307	6247	6187	6548	
		Moment in Y dir.	10813	11541	15030	14726	15073	**15104**	14761	14646	14718	14689	14868	
15 story	Site Specified Response Spectra	Axial Force	102286	121618	95608	90912	104201	98614	91228	**136266**	90821	90514	93367	100854
		Shear force in X dir.	7115	9076	6762	6506	8150	6873	6527	9752	6495	6474	6650	**10577**
		Shear force in Y dir.	20420	18404	17200	14604	21140	18775	14788	**21534**	14560	14382	15909	15442
		Moment in X dir.	9659	9746	8384	7470	9957	8991	7530	**11109**	7455	7398	7918	7836
		Moment in Y dir.	12932	16521	12310	11857	14763	12506	11895	17776	11838	11801	12113	**19293**
	Site Specified Time History	Axial Force	74515	76477	70283	69523	**78344**	71162	69587	69244	69479	69405	69938	
		Shear force in X dir.	5247	4999	5152	5091	**6674**	5219	5106	5042	5080	5051	5076	
		Shear force in Y dir.	**15992**	12224	10867	10480	15215	13424	10491	10379	10471	10430	10575	
		Moment in X dir.	6651	6294	5504	5820	**7306**	5588	5785	5861	5819	5817	5607	
		Moment in Y dir.	9255	8956	9205	9187	**11840**	9254	9208	9114	9169	9120	9103	
20 story	Site Specified Response Spectra	Axial Force	79688	105902	77146	75544	85567	78087	75642	113656	75532	75430	76364	**120989**
		Shear force in X dir.	7299	9338	6940	6751	7816	7076	6768	10149	6749	6739	6847	**11627**
		Shear force in Y dir.	12520	18010	11292	10704	15104	11843	10723	16086	10695	10669	10948	**18057**
		Moment in X dir.	5923	**8533**	5389	5138	7146	5622	5147	7722	5135	5123	5244	8523
		Moment in Y dir.	13327	17074	12689	12355	14253	12929	12385	18575	12351	12333	12525	**21284**

			Bodak-dev	IIM	Kath-wada	Mani-nagar	Motera	NIT	Paldi	Passport	Sangath	Sola	Thaltej	IS1893
20 story	Site Specified Time History	Axial Force	49940	54048	49209	48322	**51577**	49393	48443	48045	48285	48164	48953	
		Shear force in X dir.	4866	5208	5230	5130	**5387**	4882	5167	5057	5123	5088	5252	
		Shear force in Y dir.	9154	**10440**	8813	8474	9663	8880	8482	8457	8454	8414	8665	
		Moment in X dir.	4590	**5127**	4361	4123	5043	4463	4164	4003	4119	4085	4277	
		Moment in Y dir.	8722	9396	9291	9222	**9513**	8580	9282	9105	9210	9151	9367	
25 story	Site Specified Response Spectra	Axial Force	102262	127857	100197	98154	103844	101073	98284	**147580**	98120	97900	101191	144614
		Shear force in X dir.	9714	12404	9440	9248	10462	9536	9261	**13898**	9245	9228	9539	12795
		Shear force in Y dir.	16305	19026	15178	13966	16634	15687	14053	**20803**	13944	13850	14864	20440
		Moment in X dir.	7491	8889	6957	6381	7701	7192	6423	**9496**	6370	6325	6805	9401
		Moment in Y dir.	20862	26653	20296	19905	22403	20495	19932	**29918**	19898	19862	20514	27567
	Site Specified Time History	Axial	74860	**76206**	75563	73693	74675	74760	73818	73355	73648	73548	75211	
		Shear force in X dir.	8889	7861	8851	8549	**9712**	8697	8576	8507	8543	8522	8722	
		Shear force in Y dir.	12811	12471	**13881**	12230	11622	13400	12383	11880	12212	12095	13301	
		Moment in X dir.	5953	6207	**6322**	5580	5228	6231	5649	5415	5572	5525	6131	
		Moment in Y dir.	19042	16805	18906	18307	**20580**	18645	18374	18228	18300	18261	18717	
30 story	Site Specified Response Spectra	Axial Force	83475	106762	81010	79428	94666	81578	79531	119291	79394	79173	80364	**163218**
		Shear force in X dir.	9378	12171	9202	9077	9855	9255	9085	**13666**	9075	9064	9149	13623
		Shear force in Y dir.	13854	18082	12598	12026	18813	12995	12071	17965	12011	11951	12369	**21855**
		Moment in X dir.	6596	8763	5914	5604	9201	6133	5630	8353	5595	5562	5792	**9764**
		Moment in Y dir.	22040	28569	21636	21349	23122	21757	21367	**32144**	21344	21320	21516	32100
	Site Specified Time History	Axial Force	55995	55995	57990	55482	54240	**61714**	55543	53977	54266	54191	54809	
		Shear force in X dir.	9031	9031	4652	8538	8266	**9596**	8749	8195	8262	8240	8432	
		Shear force in Y dir.	8643	8643	7173	7847	7823	**11274**	8150	7843	7811	7780	7886	
		Moment in X dir.	4112	4112	3427	3576	3509	**5277**	3747	3577	3501	3491	3403	
		Moment in Y dir.	20700	20700	10642	19780	19306	**21986**	20149	19159	19298	19253	19584	

6.5 SUMMARY

This chapter is presents the analysis results of site specified response spectra and time history analysis. The parametric study is carried out to understand the behavior of shear wall buildings with the increase of their height. The results of fundamental time period, story drift and base shear has been discussed considering site specified response spectra time history and IS: 1893-2002 specified response spectra with graphical representation.

7. PERFORMANCE BASED DESIGN OF SHEAR WALL BUILDING

7.1 GENERAL

The design objectives considered in current building codes life safety in minor and moderate earthquakes, and collapse prevention in major earthquake. However, the actual design to achieve these objectives is not known. There is a general agreement among researchers and professionals to that future seismic design needs to be based on achieving stated multiple performance objectives. Future seismic design practices will be based on performance criteria that can be quantified considering multiple performance and hazard levels.

Nowadays performance based design (PBD) is widely used for earthquake resistant design. In PBD various performance levels and hazard levels are described. PBD can be carried out using nonlinear static method and nonlinear time history method. Nonlinear time history analysis is one of the most accurate analyses to understand the failure pattern with respect to time but this technique is not used commonly in design purpose because it is a time consuming. So, pushover analysis widely used for performance based design of new and retrofitting of existing building. In present chapter pushover analysis is consider for performance based design of shear wall building using ETABS [19] software.

7.2 PERFORMANCE OBJECTIVE AND CRITERIA

Performance criteria are described in term of performance levels and hazard levels. The target performance objective is divided into Structural Performance Levels and Non-structural Performance Levels as discussed in chapter 1.

The Structural performances are divided in to six levels. The levels are, SP–1: Immediate Occupancy, SP-2: Damage control, SP–3: Life Safety, SP-4: Limited safety SP-5: Structural stability and SP–6: Not considered.

The non-structural performances are divided in to five levels. The levels are NP–A: Operational, NP–B: Immediate Occupancy, NP–C: Life Safety, NP–D: Hazards Reduced, and NP–E: Non – Structural Damage Not Limited.

Combination of structural performance levels in form of number and non-structural performance levels in form of letter are designed for total performance level of building. These combinations to achieve most common performance level such as 1-A: Operational level, 1-B: Immediate Occupancy level, 3-C: Life Safety level, 5-E: Collapse Prevention level and other possible performance level is also described such as 1-C, 2-A, 2-B, 3-B etc.

Table 7.1 Combination of structural and nonstructural level to form building performance level

		Structural Performance Levels					
		SP-1 Immediate Occupancy	SP-2 Damage Control	SP-3 Life Safety	SP-4 Limited Safety	SP-5 Collapse Prevention	SP-6 Not Considered
Non-structural Performance Levels	NP-A Operational	1-A Operational	2-A	NR	NR	NR	NR
	NP-B Immediate Occupancy	1-B Immediate Occupancy	2-B	3-B	NR	NR	NR
	NP-C Life Safety	1-C	2-C	3-C Life Safety	4-C	5-C	6-C
	NP-D Hazards Reduced	NR	NR	3-D	3-D	5-D	6-D
	NP-E Not Considered	NR	NR	NR	NR	5-E Collapse Prevention	Not Applicable

Note: NR- Not Recommended

As per Table 7.1, Standard Performance levels are considered depending on type of damages in the structural and nonstructural element. Most common performance such as negligible impact on building is considered at an operational level. Building is safe to occupancy but possibly not useful until repaired is considered as an immediate occupancy level. Building is safe during event but possibly not afterward is considered as a life safety level and building is very near to collapse is considered as collapse prevention.

The acceptable performance target can be specified by limits of any response parameter such as stresses, strains, displacements, accelerations, etc. It expresses the performance objectives in terms of a specific damage state or probability of failure against a prescribed probability demand level. Table 7.2 presents damage state and deformation limits for various performance levels. Maximum total drift is defined as the interstory drift at the performance point displacement.

Table 7.2 Performance levels corresponding to damage state and deformation limit

Performance Level	**Damages State**	**Interstory Drift limit**
Fully Operational, Immediate occupancy	No Damage	< 0.2%
Operational, Damage control, Moderate	Repairable	< 0.5%
Life safety, Damage state	Irreparable	< 1.5%
Near to collapse, Limited safety, Hazard reduced	severe	< 2.5%
Collapse	-	> 2.5%

Earthquake demands are function of the location of the building with respect to state of building, building type (material/system), ground motion, site-specific geologic characteristics. The most common and significant cause of earthquake damages to buildings is ground shaking so performance objective is also depend on earthquake hazard levels. Earthquake hazards are define in term of the probability that more severe damage will be experience in 50 year. Proposed earthquake hazard levels are shown in Table 7.3.

Table 7.3 Proposed earthquake hazard levels

Earthquake frequency	Return period in years	Probability of exceedance
frequent	43	50% in 30 years
Occasional	72	50% in 50 years
Rare	225	20% in 50 years
Very rare	475	10% in 50 years
Extremely rare	2475	2% in 50 years

The building performance level and Earthquake hazard level are combined to select the design performance level.

		Building Performance Levels			
		Operational	Immediate occupancy	Life safety	Collapse prevention
Earthquake Hazard Levels	50% per 50 Year	a	b	c	d
	20% per 50 Year	e	f	g	h
	10% per 50 Year	i	j	k	l
	2% per 50 Year	m	n	o	p

Fig. 7.1 combination of performance level and hazard level

As mentioned Fig. 1.6 in chapter 1, owner and engineer select any performance level in term of alphabetic letter in between *"a to p"* based on site feasibility for earthquake hazard. Further process is explained step by step in next section.

7.3 PRELIMINARY DESIGN OF BUILDING

Plan of 20 story building as shown in Fig. 1.7 with necessary data as per Table 1.1 is considered. Analysis and design is carried out using ETABS software. For limit state design of reinforced concrete structure, following 26 load combinations are considered:

DL + LL

DL ± EQ

DL ± 0.8(LL+EQ) (EQ in X and Y direction)

1.5DL + 1.5LL

1.2(DL + LL ± EQ) (EQ in X and Y direction)

1.5DL ± 1.5EQ (EQ in X and Y direction)

0.9DL ± 1.5EQ (EQ in X and Y direction)

Modeling procedure is presented in chapter 3.

In first case building is model as a shear wall building and shear wall is considered as a shell element subsequently shear wall is replaced by column element because hinge properties cannot be defined for shell element in ETABS. Variation in time period of building with shear wall as shell element and column element is shown in Table 7.4. Also variation in base shear is presented in Table 7.4.

Table 7.4 Time period and Base shear variation

		Shear wall as shell element	Shear wall as column element
Time Period (sec)	X dir.	2.191	2.234
	Y dir.	1.835	1.866
Base shear (kN)	X dir.	1208.19	1205.42
	Y dir.	1496.60	1436.34

Maximum story drift in X direction is 0.00048 at 5th story level as shown in Fig. 7.2 (a) and in Y direction is 0.00051 at 14th story level as shown in Fig. 7.2 (b). IS: 1893(Part1)-2002 specifies maximum story drift limit as 0.004.

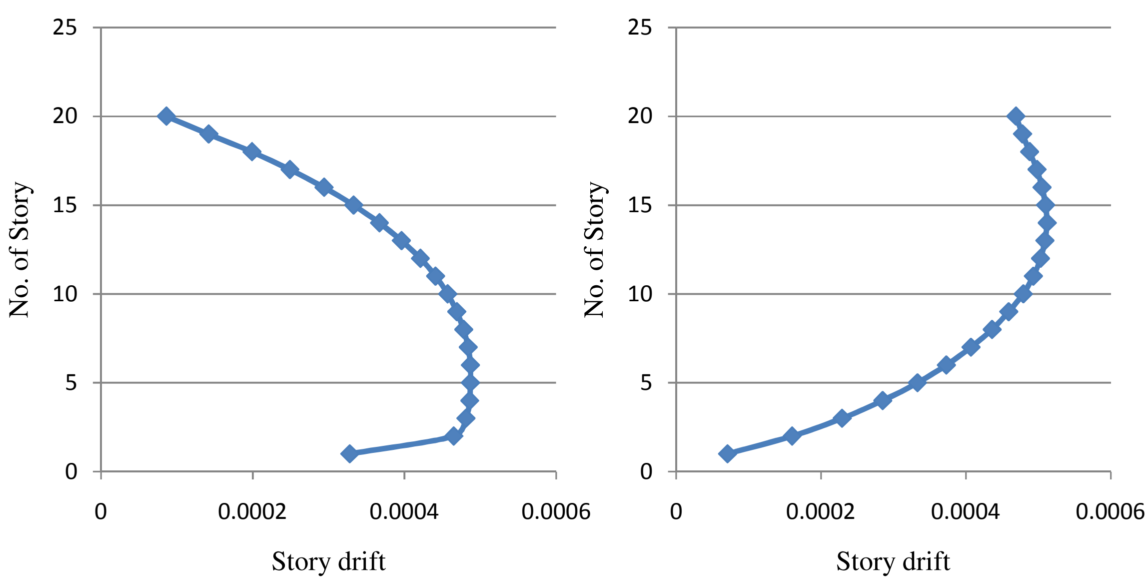

(a) X direction (b) Y direction

Fig 7.2 Interstory drift

So, from drift criteria the building is safe as per linear analysis.

The reinforcement details of various elements are presented in Table 7.5 to 7.8 and reinforcement detailing is shown in Fig 7.9.

Table 7.5 Reinforcement in shear wall

	Shear wall size	SW1, SW6, SW7, SW12	SW2, SW5, SW8, SW11	SW3, SW4, SW9, SW10
Story 8 to Story 20	250×4000	36 no 16ø	22 no 20ø	22 no 20ø
Story 7	250×4000	36 no 16ø	22 no 20ø	22 no 20ø
Story 6	250×4000	36 no 16ø	22 no 20ø	36 no 20ø
Story 5	250×4000	36 no 16ø	28 no 20ø	32 no 20ø
Story 4	250×4000	36 no 16ø	34 no 20ø	38 no 20ø
Story 3	250×4000	36 no 16ø	40 no 20ø	44 no 20ø
Story 2	250×4000	36 no 16ø	44 no 20ø	48 no 20ø
Story 1	250×4000	36 no 16ø	50 no 20ø	56 no 20ø

Table 7.6 Reinforcement in exterior column

	Column size	C1,C5,C6,C10		C2,C4,C7,C9		C3,C8	
		Vertical Steel	Stirrups (mm)	Vertical Steel	Stirrups (mm)	Vertical Steel	Stirrups (mm)
Story 8 to Story 20	300×600	6 no 20ø	8ø-140	6 no 20ø	8ø-140	6 no 20ø	8ø-140
Story 7	300×600	6 no 20ø	8ø-140	6 no 25ø	8ø-140	6 no 25ø	8ø-140
Story 6	300×600	6 no 25ø	8ø-140	6 no 25ø	8ø-150	6 no 25ø	8ø-150
Story 5	300×600	6 no 25ø	8ø-150	8 no 25ø	8ø-150	8 no 25ø	8ø-150
Story 4	300×600	8 no 25ø	8ø-150	10 no 25ø	8ø-150	10 no 25ø	8ø-150
Story 3	300×600	10 no 25ø	8ø-150	12 no 25ø	8ø-150	12 no 25ø	8ø-150
Story 2	300×600	12 no 25ø	8ø-150	12 no 25ø	8ø-150	12 no 25ø	8ø-150
Story 1	300×600	14 no 25ø	8ø-150	14 no 25ø	8ø-150	14 no 25ø	8ø-150

Table 7.7 Reinforcement in internal column

	Column size	C11,C20,C21,C30		C12,C19,C22,C29		C13,C18,C23,C28	
		Vertical Steel	Stirrups (mm)	Vertical Steel	Stirrups (mm)	Vertical Steel	Stirrups (mm)
Story 8 to Story 20	300×600	6 no 20ø	8ø-140	6 no 20ø	8ø-140	6 no 20ø	8ø-140
Story 7	300×600	6 no 20ø	8ø-140	6 no 20ø	8ø-140	6 no 25ø	8ø-150
Story 6	300×600	6 no 20ø	8ø-140	6 no 20ø	8ø-140	6 no 25ø	8ø-150
Story 5	300×600	6 no 20ø	8ø-140	6 no 25ø	8ø-150	8 no 25ø	8ø-150
Story 4	300×600	6 no 25ø	8ø-150	8 no 25ø	8ø-150	8 no 25ø	8ø-150
Story 3	300×600	8 no 25ø	8ø-150	8 no 25ø	8ø-150	10 no 25ø	8ø-150
Story 2	300×600	10 no 25ø	8ø-150	10 no 25ø	8ø-150	12 no 25ø	8ø-150
Story 1	300×600	10 no 25ø	8ø-150	12 no 25ø	8ø-150	12 no 25ø	8ø-150

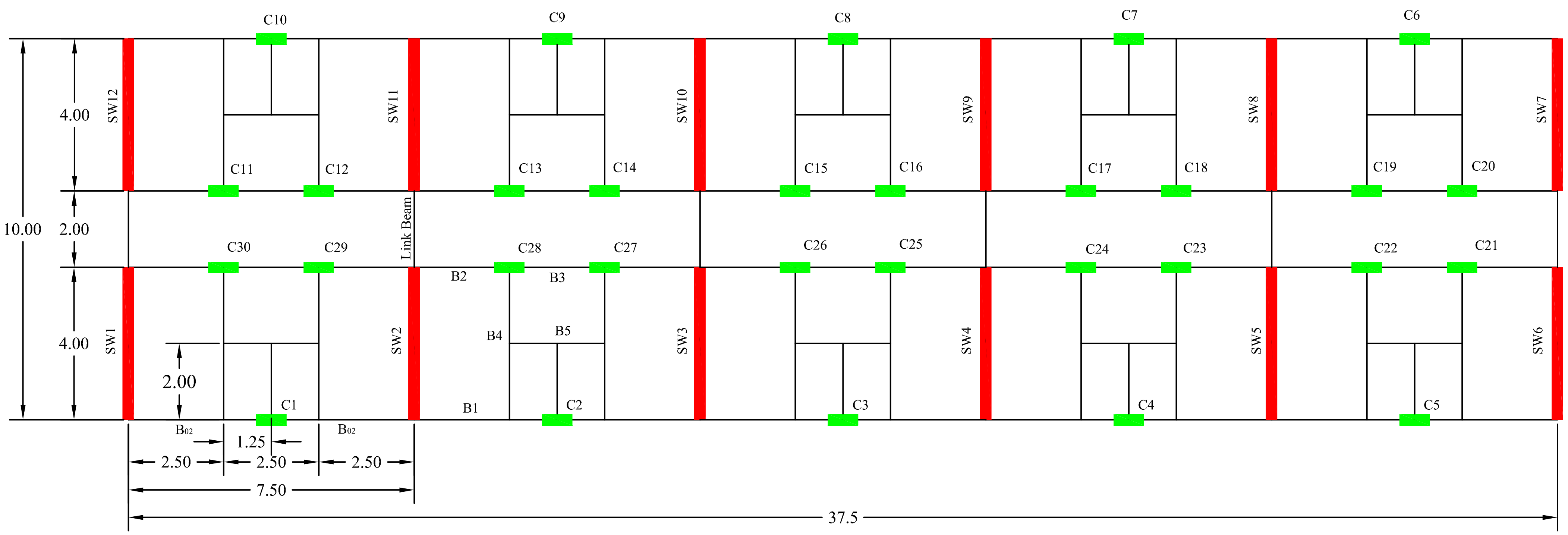

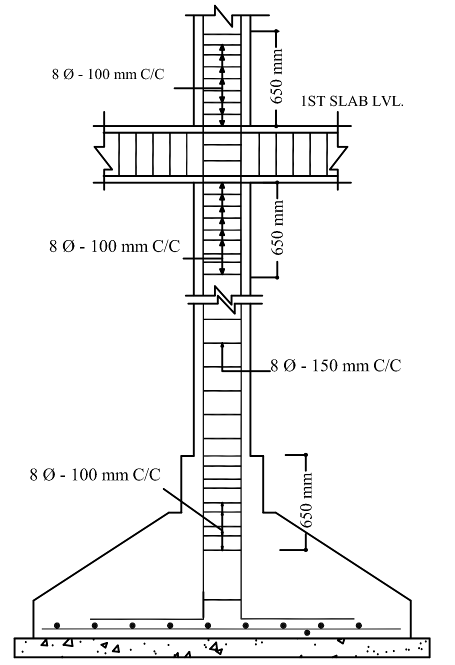

RING POSITION DETAILS FOR TYP. COLUMN

B1 (250×550)

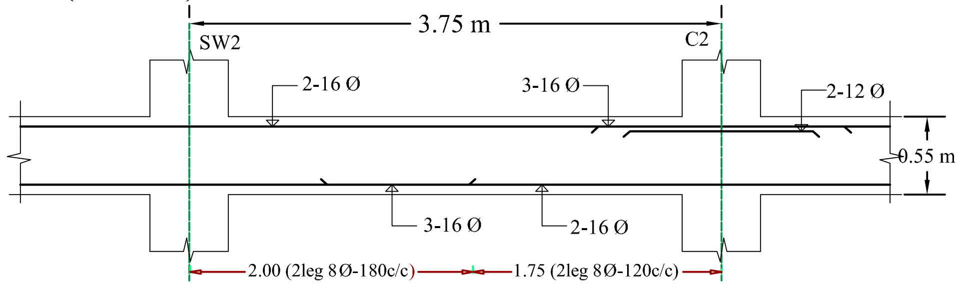

B2 (250×550)

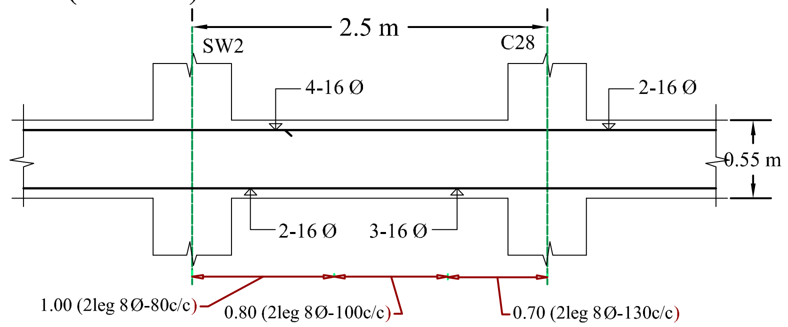

B3 (250×550)

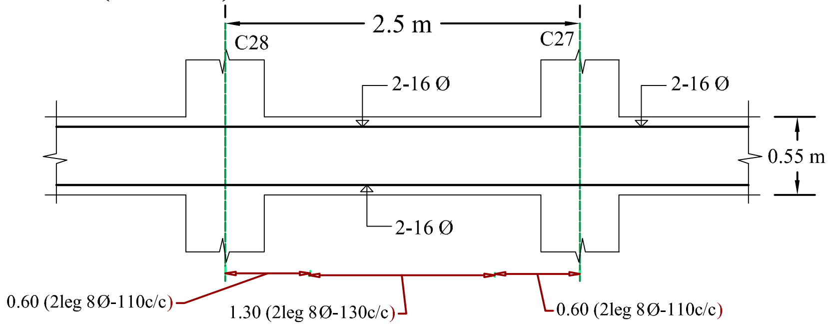

B4 (250×550)

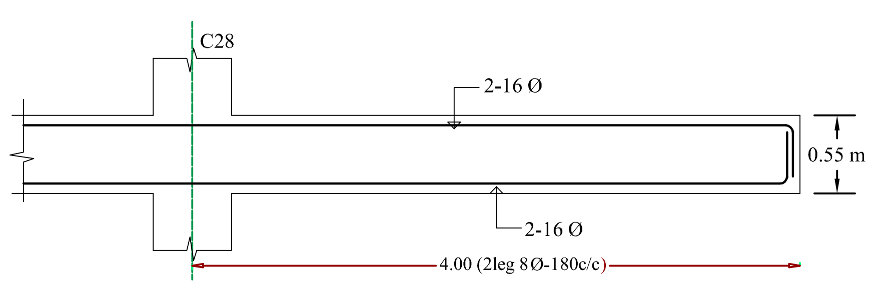

COLUMN SCHEDULE

COLUMN MARK	CONC. MIX	COL. SIZE	UP TO 1st SLAB		ARRANGEMENT
			V.BARS	RINGS	
C1,C2, C3, C4, C5 C6, C7, C8, C9, C10	M 25	300 X 600	14 -25 Ø	8 Ø - 100 mm C/C 8 Ø -150 mm C/C 8 Ø - 100 mm C/C	
C12, C13, C14, C15 C16, C17, C18, C19 C22, C23, C24, C25 C26, C27, C28, C29	M 25	300 X 600	12 -25 Ø	8 Ø - 100 mm C/C 8 Ø -150 mm C/C 8 Ø - 100 mm C/C	
C11, C20, C21, C30	M 25	300 X 600	10 -25 Ø	8 Ø - 100 mm C/C 8 Ø -150 mm C/C 8 Ø - 100 mm C/C	

B5 (250×450)

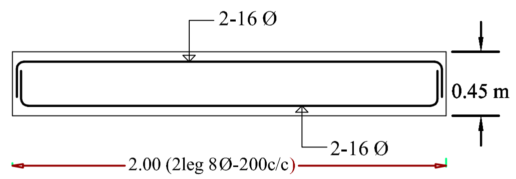

Link Beam (250×600)

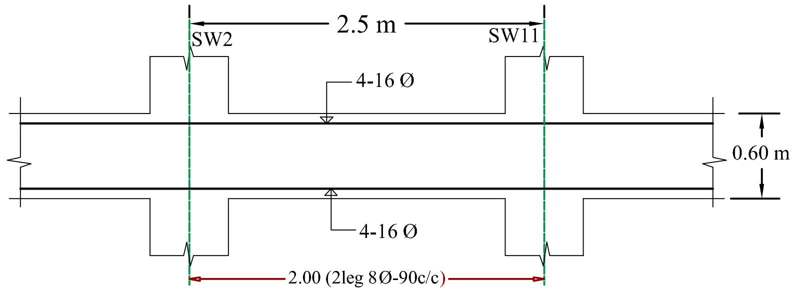

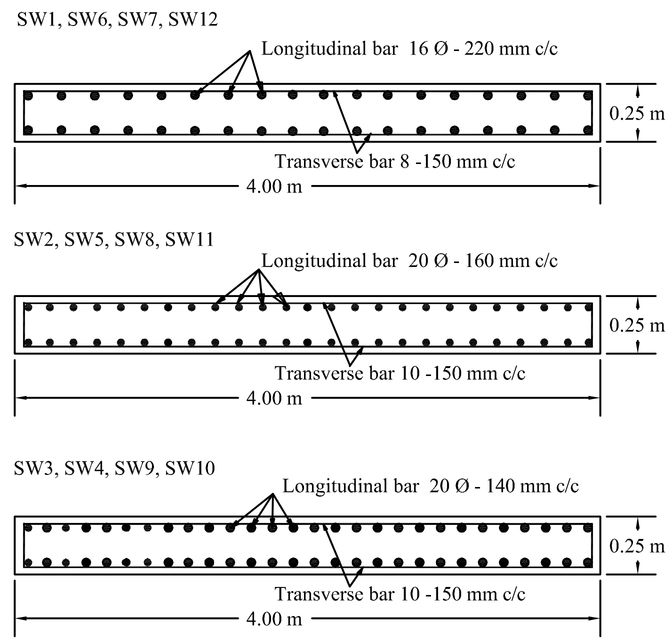

REINFORCEMENT DETAILING IN SHEAR WALL AT GROUND FLOOR LEVEL

Fig. 7.3 Reinforcement detailing

Table 7.7 Reinforcement in internal column

	Column size	C14,C17,C24,C27		C15,C16,C25,C26	
		Vertical Steel	Stirrups (mm)	Vertical Steel	Stirrups (mm)
Story 8 to Story 20	300×600	6 no 20ø	8ø-140	6 no 20ø	8ø-140
Story 7	300×600	6 no 25ø	8ø-140	6 no 25ø	8ø-140
Story 6	300×600	6 no 25ø	8ø-150	6 no 25ø	8ø-140
Story 5	300×600	8 no 25ø	8ø-150	8 no 25ø	8ø-150
Story 4	300×600	8 no 25ø	8ø-150	8 no 25ø	8ø-150
Story 3	300×600	10 no 25ø	8ø-150	10 no 25ø	8ø-150
Story 2	300×600	12 no 25ø	8ø-150	12 no 25ø	8ø-150
Story 1	300×600	12 no 25ø	8ø-150	12 no 25ø	8ø-150

Table 7.8 (a) Reinforment in beam B1 (250×550)

Right to left (Dist.)	0.3	1.25	1.75	3.25	3.75
Top steel	2 no 16ø	2 no 16ø	2 no 16ø	3 no 16ø	3 no 16ø 2 no 12ø
Bottom steel	2 no 16ø	3 no 16ø	2 no 16ø	2 no 16ø	2 no 16ø
Stirrups (mm)	8ø-180	8ø-180	8ø-170	8ø-110	8ø-120

Table 7.8 (b) Reinforment in beam B2 (250×550)

Right to left (Dist.)	0	0.44	1.32	1.76	2.2
Top steel	4 no 16ø	3 no 16ø	2 no 16ø	2 no 16ø	2 no 16ø
Bottom steel	2 no 16ø	2 no 16ø	2 no 16ø	2 no 16ø	3 no 16ø
Stirrups	8ø-80	8ø-80	8ø-100	8ø-130	8ø-160

Table 7.8 (c) Reinforment in beam B3 (250×550)

Right to left (Dist.)	0	0.44	1.32	1.76	2.2
Top steel	2 no 16ø	2 no 16ø	2 no 16ø	2 no 16ø	2 no 16ø
Bottom steel	2 no 16ø	2 no 16ø	2 no 16ø	2 no 16ø	2 no 16ø
Stirrups	8ø-110	8ø-130	8ø-170	8ø-130	8ø-110

Table 7.8 (d) Reinforment in beam B4 (250×550)

Right to left (Dist.)	0.15	1.5	2	2.5	4
Top steel	2 no 16ø	2 no 16ø	2 no 16ø	2 no 16ø	2 no 16ø
Bottom steel	2 no 16ø	2 no 16ø	2 no 16ø	2 no 16ø	2 no 16ø
Stirrups	8ø-180	8ø-180	8ø-180	8ø-180	8ø-180

Table 7.8 (e) Reinforment in beam B5 (250×450)

Right to left (Dist.)	0	0.44	1.32	1.76	2.2
Top steel	3 no 12ø	3 no 12ø	3 no 12ø	3 no 12ø	3 no 12ø
Bottom steel	3 no 12ø	3 no 12ø	3 no 12ø	3 no 12ø	3 no 12ø
Stirrups	8ø-200	8ø-200	8ø-200	8ø-200	8ø-200

Table 7.8 (f) Reinforment in shear link beam (250×600)

Right to left (Dist.)	0	0.5	1	1.5	2
Top steel	4 no 16ø	3 no 16ø	3 no 16ø	3 no 16ø	4 no 16ø
Bottom steel	4 no 16ø	3 no 16ø	3 no 16ø	3 no 16ø	4 no 16ø
Stirrups	8ø-90	8ø-90	8ø-90	8ø-90	8ø-90

7.4 SEISMIC PERFORMANCE ASSESSMENT

If preliminary design is safe for permissible interstory drift limit and percentage of steel is within limit for particular size of element than pushover analysis is carried out for assessing the performance of structure. In pushover analysis default hinges properties are used for column and beam element. For column element P-M-M and V_2 hinge properties are considered and for beam element consider as M_3 and V_2 hinge properties are considered.

Lateral load pattern is important parameter for pushover analysis as discussed in chapter 5. In this example inverted triangular (k=2) load pattern is considered for application of lateral load on the structure. PUSH 1 is considered as gravity load, PUSH 2 is consider as lateral load in X direction and PUSH 3 is consider as lateral load in Y direction. PUSH 2 and PUSH 3 are applied as a lateral displacement controlled during analysis. PUSH 1 is considered as initial load for PUSH 2 and PUSH 3 analysis.

Result of pushover analysis is studied using **Display > Show static pushover curve command**

Maximum lateral load carrying capacity of building in X direction is 4099 kN and in Y direction is 7336 kN is shown in Fig. 7.4. Capacity curve beyond the yielding point in nonlinear range is depending on hinge formation in beam and column element of building. ETABS default hinge properties consider hinge formation pattern in building as per strong column and week assumption.

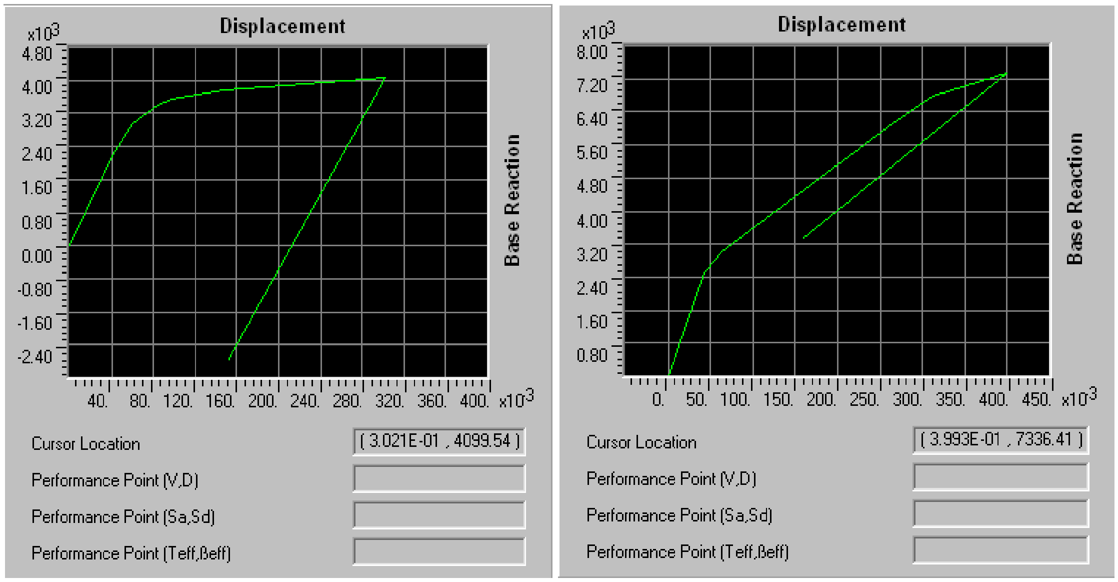

X direction Y direction

Fig. 7.4 Capacity curve

Development of step by step hinge formation in building is shown in Fig. 7.5 and Fig 7.6 for X direction and Y direction respectively.

PUSHOVER CURVE

File

Step	Displacement	Base Force	A-B	B-IO	IO-LS	LS-CP	CP-C	C-D	D-E	>E	TOTAL
0	0.0000	0.0000	5515	5	0	0	0	0	0	0	5520
1	0.0439	2276.1584	5008	512	0	0	0	0	0	0	5520
2	0.0600	2966.2227	4611	909	0	0	0	0	0	0	5520
3	0.0842	3403.1372	4498	1022	0	0	0	0	0	0	5520
4	0.0979	3535.6958	4344	1080	96	0	0	0	0	0	5520
5	0.1484	3751.7017	4033	717	382	388	0	0	0	0	5520
6	0.3024	4066.9160	4033	717	382	388	0	0	0	0	5520
7	0.1513	-2807.5310	5520	0	0	0	0	0	0	0	5520

Fig. 7.5 Pushover curve hinge formation in X direction

PUSHOVER CURVE

File

Step	Displacement	Base Force	A-B	B-IO	IO-LS	LS-CP	CP-C	C-D	D-E	>E	TOTAL
0	-6.132E-05	0.0000	5480	40	0	0	0	0	0	0	5520
1	0.0434	2499.0134	5352	168	0	0	0	0	0	0	5520
2	0.0441	2530.4685	5282	238	0	0	0	0	0	0	5520
3	0.0638	3027.8262	5030	274	56	160	0	0	0	0	5520
4	0.2652	6108.7822	4741	563	36	180	0	0	0	0	5520
5	0.3124	6787.0693	4059	1221	24	212	0	4	0	0	5520
6	0.3993	7352.2148	3951	1329	24	212	0	2	2	0	5520
7	0.1577	3317.2961	5520	0	0	0	0	0	0	0	5520

Fig. 7.6 Pushover curve hinge formation in Y direction

Capacity curve, Demand curve and Performance point are generated in Spectral acceleration versus Spectral displacement co-ordinates as shown in Fig. 7.7 and Fig. 7.8 for X direction and Y direction. C_a and C_v factor are considered as 0.16 and 0.22 based on Indian code as per Appendix C.

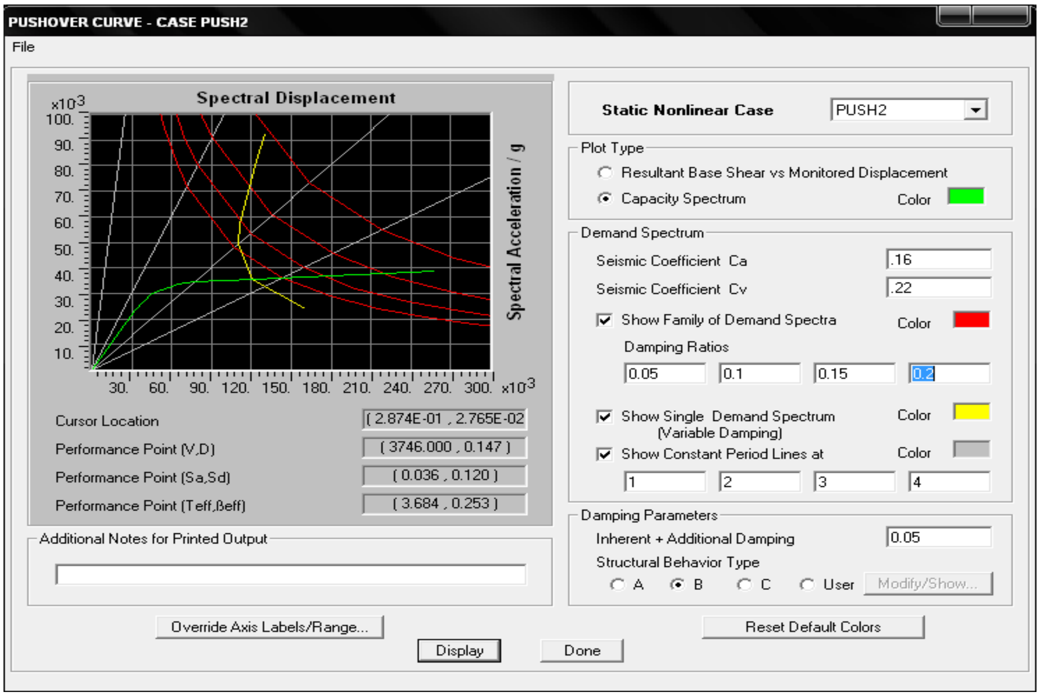

Fig. 7.7 Capacity demand spectrum curve in X direction

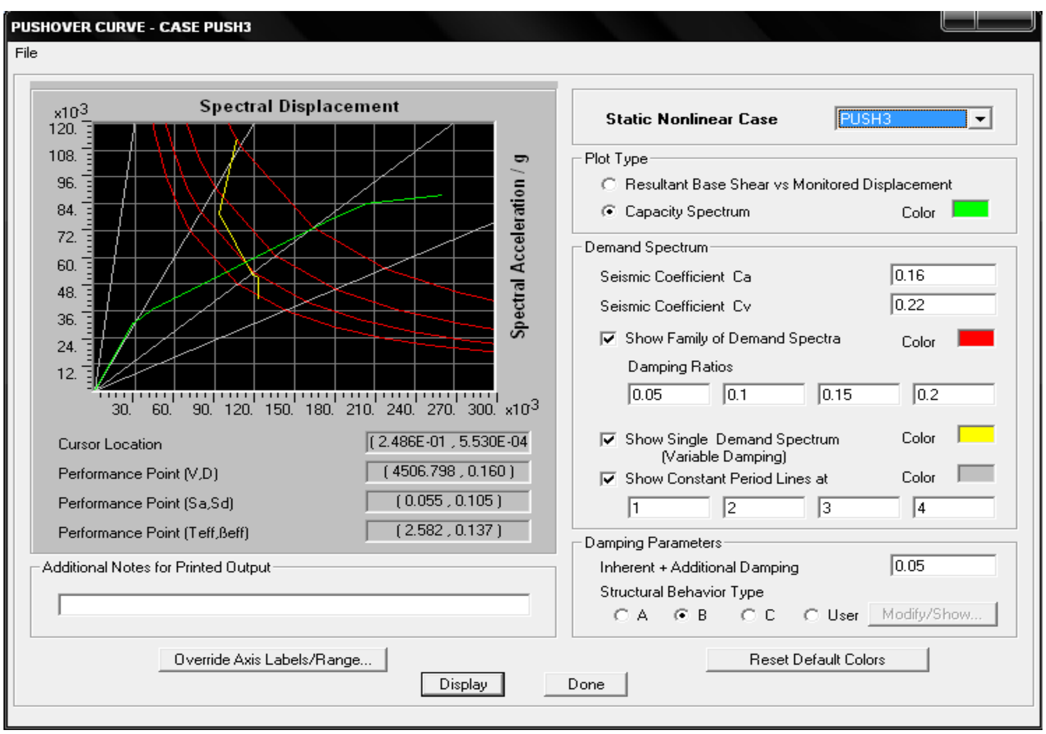

Fig. 7.8 Capacity demand spectrum curve in Y direction

Hinges formation in X direction and Y direction at performance point is shown in Fig. 7.9. Maximum interstory drift is 0.00589 in X direction at 4th floor level and 0.0041 in Y direction at 17th floor level. This indicates the building is in between immediate occupancy to life safety level in X direction and operational to immediate occupancy level in Y direction.

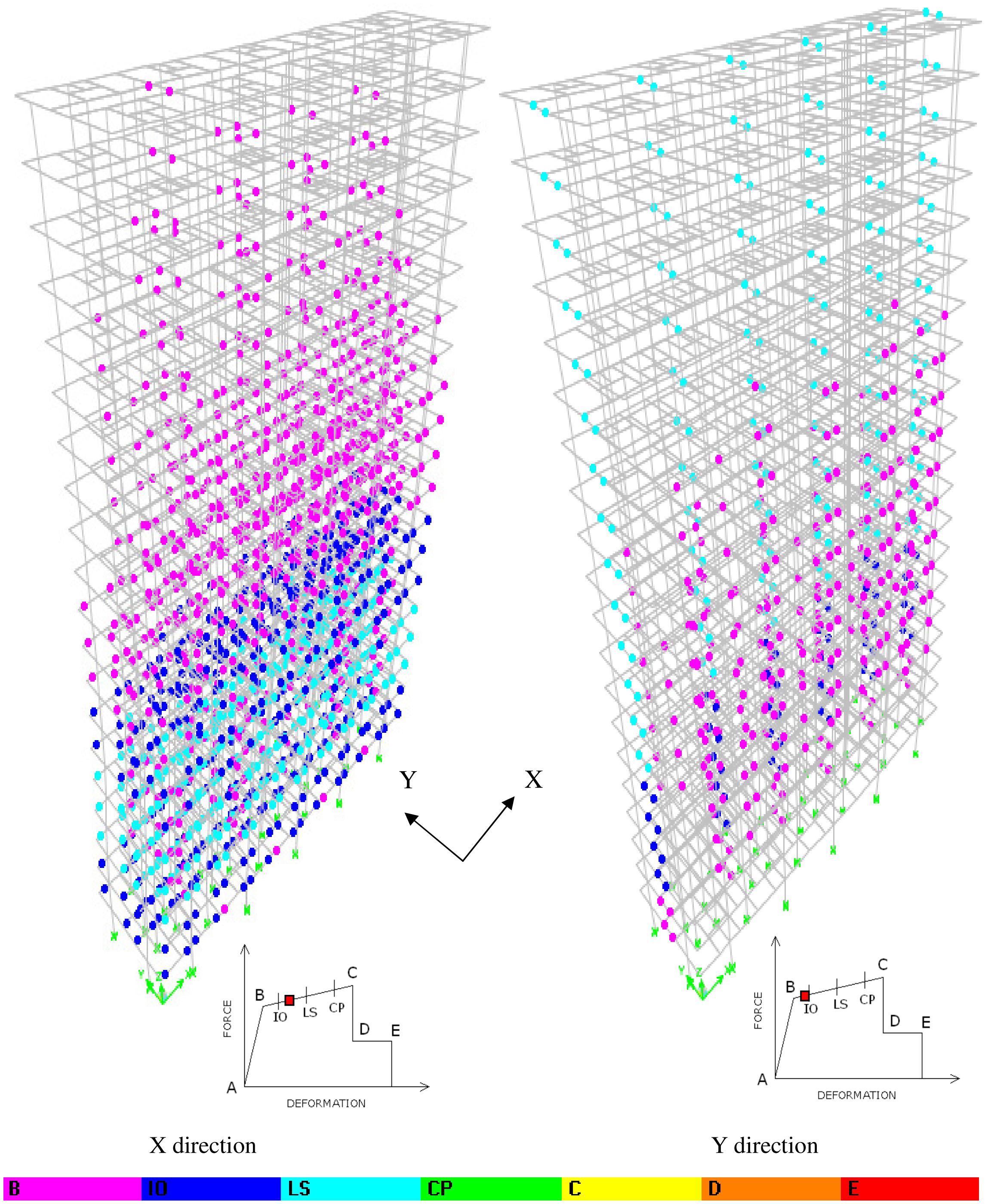

Fig. 7.9 Hinge formation at performance point

Column sizes are considered as 300×1200 mm for 20 story building and another element sizes are same as per Fig. 1.7 for parametric study. Comparison of base shear, top displacement and story drift at performance point are carried out as shown in Table 7.9.

Table 7.9 Comparison of building performance level

<table>
<tr><td></td><td></td><td>Building A
(column sizes 300×600)</td><td>Building B
(column sizes 300×1200)</td></tr>
<tr><td rowspan="2">Time Period</td><td>X Dir.</td><td>2.234 sec</td><td>1.950 sec</td></tr>
<tr><td>Y Dir.</td><td>1.866 sec</td><td>1.785 sec</td></tr>
<tr><td rowspan="2">Base Shear at Performance point</td><td>X Dir.</td><td>3746.11 kN</td><td>4545.26 kN</td></tr>
<tr><td>Y Dir.</td><td>4506.78 kN</td><td>5431.64 kN</td></tr>
<tr><td rowspan="2">Top Displacement at Performance Point</td><td>X Dir.</td><td>0.147 m</td><td>0.134 m</td></tr>
<tr><td>Y Dir.</td><td>0.166 m</td><td>0.162 m</td></tr>
<tr><td rowspan="2">Story Drift at Performance point</td><td>X Dir.</td><td>0.0059 m</td><td>0.0037 m</td></tr>
<tr><td>Y Dir.</td><td>0.0041 m</td><td>0.0035 m</td></tr>
<tr><td rowspan="2">Performance point</td><td>X Dir.</td><td>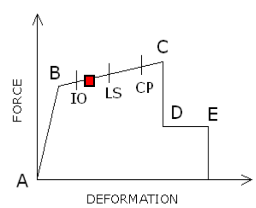
Between Immediate Occupancy to life safety level</td><td>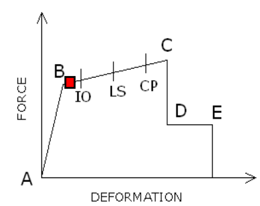
Near to Operational Level</td></tr>
<tr><td>Y Dir.</td><td>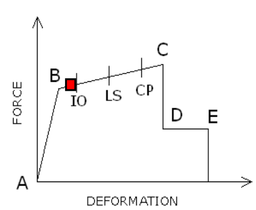
Between Operational to Immediate Occupancy level</td><td>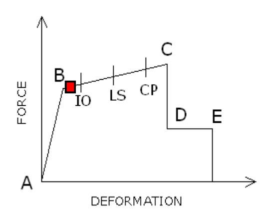
Near to Operational Level</td></tr>
</table>

7.5 SUMMARY

In this chapter the objectives and criteria for performance based design are discussed. Analysis and design of 20 story shear wall building is carried out using shear wall as column element. The time period/base shear of building considering shear wall as column or shell element are nearly same. The design of shear wall building is carried out using ETABS software as per limit state method and result of reinforcement in each element is shown in tabular format. Pushover analysis is used to assess the performance of building. Pushover analysis results are shown in term of capacity, demand, performance point, pattern of hinge formation and hinge formation at performance point.

8. SUMMARY AND CONCLUSIONS

8.1 SUMMARY

The causalities from the earthquakes suffered during the last decade have made it necessary to control and assess buildings that have been constructed without any regard to appropriate seismic design characteristics. The present generation, design codes are based on equivalent elastic force approaches which are ineffective in preventing consequences of destructive earthquakes. Optimization in design can be achieved by using full strength of material beyond their elastic limit. Nonlinear analysis techniques are useful to understand nonlinear behavior of structures. So, during the last decades a trend towards "performance-based design" (PBD) structures, for earthquake resistant is observed.

Understanding of nonlinear analysis is very important for creating modeling in software. Analytical procedure for performance based analysis is necessary to understand the inelastic behavior of building component.

Pushover analysis is widely used for performance based design of new structures and retrofitting of existing structures. The ultimate deformation capacity of component depends on the ultimate curvature and plastic hinge length. In practice, ATC 40 documents are used for default hinge properties due to convenience and simplicity. But the observations clearly show that the user defined hinge model is better than the default hinge modeling in reflecting nonlinear behavior compatible with the element properties. Results of pushover analysis are also affected by distribution of lateral load along the height of building. Seismic demand of structure can be evaluated by considering site specific parameters.

In present study performance based design of shear wall building using ETABS is presented. Theoretical background for generation of hinge properties is discussed. An excel sheet is developed for generation of moment-curvature and moment-rotation relationship. Pushover analysis of 3D frame is carried out considering default hinge properties of ETABS as per ATC 40 and user defined hinge properties developed considering stress-strain in R.C.C. element. Capacity spectrum and demand spectrum obtained considering different hinge properties are compared. An excel sheet is developed to get capacity spectrum and demand spectrum to understand various steps of pushover analysis.

Pushover analysis is based on static nonlinear analysis performed by imposing an assumed distribution of lateral loads over the height of a structure. The lateral loads or lateral displacement are incremented monotonically from zero to the ultimate level corresponding to the incipient collapse of the structure. The accuracy of design is based on applied pattern of loads inducing deformation in the structure which should be similar to that induced by the earthquake ground motion. The result of pushover analysis in term of capacity, demand and performance point are compared considering inverted triangular distribution of lateral load pattern based on codal formula, and lateral load distribution generated from site specific response spectra and time history analysis.

Site Specific Response analysis is carried out for various sites to find out the response of ground when an earthquake occurs. The parametric study is carried out to understand the behavior of shear wall buildings with the increase in height. The analysis results in terms of fundamental time period, story drift and base shear considering site specific response spectra, time history and IS: 1893-2002 specified response spectra are studied.

Analysis and design of 20 story shear wall building is presented. Modeling of shear wall is carried out using shell element and column element. The design of shear wall building is carried out using ETABS software as per limit state method. Subsequently pushover analysis of building is carried out. The results are presented in terms of capacity, demand, performance point, pattern of hinge formation. The results help in identifying damage level of building. The effect of change in design of structural element on performance of building is illustrated.

8.2 CONCLUSIONS

Based on above study following conclusion can be made,

Effects of hinge properties in pushover analysis

1. User defined hinge properties for pushover analysis is easy for simple building but it is difficult and time consuming process for complex structure.

2. The base shear capacity of models with the default hinge properties and the user-defined hinges properties are similar. The variation in the base shear capacity is less within 1%. Thus, the base shear capacity of building does not depend on whether the default or user-defined hinge properties are used.
3. Comparison of sequence of hinge formation indicates that both the models with default hinge and the user-defined hinge properly indicates hinge formation at the yield point. However, there is significant difference in the hinge formation near to collapse.
4. Capacity curve and demand curve nearly match in both the models. So, hinge properties considered based on stress-strain relationship and default hinge properties based on ATC 40 and FEMA 356 indicate identical behavior.
5. Plastic hinge length (L_p) has significant effect on the displacement capacity of the structure. When plastic hinge length is considered more than 0.5 h (h is depth of element) in beam than strong column week beam behavior may not be observed.

Effects of lateral load pattern in pushover analysis

1. Seismic demand can be obtained by IS 1893 specific response spectrum, site specific response spectrum and time history.
2. Static analysis as per IS: 1893-2002 consider only first mode shape vibration of building. But time history analysis and response spectrum analysis consider higher mode of building vibration. So large variation in lateral force over the height of structure is observed in 25 story building while comparing results of time history analysis with IS: 1893-2002 specified Response spectra.
3. Performance point is not obtained in 30 story building when site specific response spectrum is considered. So increase in the size of element or increase in the percentage of reinforcement is required to meet the capacity and demand curve.
4. Difference in base shear at performance point obtained using static analysis and dynamic analysis is quite more compared to base shear difference in time history and site specific response spectra analysis.

5. Higher stage hinge formations are observed in time history analysis which indicates the importance of considering higher mode shape rather than considering only first mode.
6. Higher stage hinge formation in beam element compared to column element indicate strong column week beam behavior under pushover analysis considering default hinge properties.

Site specific response spectra and time history analysis

1. Time history analysis of building considering Motera site generate large base shear in Y direction for 30 story building which indicate the resonance effect on structure.
2. Maximum Story drift is observed at lower story in X direction and upper story in Y direction for shear wall structure considered this study.
3. In most of the cases design forces in shear wall obtained by site specific response spectra is higher than site specific time history.
4. Site specific response spectra give higher story buildings drift for 10 and 15 story while in case of 20, 25 and 30 story building, IS: 1893-2002 specified response spectra give maximum story drift

Performance based design

1. As hinge properties cannot be assigned in shell element, shear wall is considered as an equivalent column element.
2. Time period and base shear are nearly same when shear wall is consider as a column element and shell element. So column element can be used to represent shear wall for pushover analysis.
3. Higher stage hinge formations are observed at bottom story in X direction and top story in Y direction.
4. Performance level of 20 story building is between immediate occupancy to life safety level in X direction and operational to immediate occupancy level in Y direction. So, 20 story building may suffer less damage during earthquake event.

5. By changing design of structural elements performance of building can be improved as per direction of client / architects.

8.3. FUTURE SCOPE OF WORK

The present study can be extended as follows

1. Multi degree of freedom system is not considered in pushover analysis as per ATC 40 document. The multi degree freedom system as per ATC 55 document can be considered.
2. Cost comparison for different performance level of building can be studied.
3. Nonlinear time history analysis can be performed to estimate seismic demand of building.
4. Performance based design can be carried out for other structural system like bundled tube used for tall structures.
5. Computer program for evaluating plastic hinge properties for shear wall can be developed.
6. Performance based design can be carried out for composite structure or steel structure.
7. Comparison of static nonlinear analysis and dynamic nonlinear analysis can be carried out using Drain 2DX or Perform 3D software.

REFERENCES

1. Rui Pinho, "Nonlinear Dynamic Analysis of Structures Subjected to Seismic Action", Book of Advance Earthquake Engineering Analysis by Alain Pecker, pp. 63-89.

2. Farzad Naeim, *The Seismic Design handbook, 2nd Edition*, Kluwer Acadamic Publishers, Boston, London, 2001.

3. Ron Klemencic, J. Andrew Fry, John D. Hooper and Brian G. Morgen, "Performance-based Design of Ductile Concrete Core Wall Building", Wiley Interscience, *Struct. Design Tall Spec. Build. 16,* 2007 pp. 599-614.

4. Ahmed Ghobarah, "Performance-based design in earthquake engineering: state of development*", Engineering Structure*, *23* March 2001 pp. 878-884.

5. S. Chandrasekaran and Varun Gupta, "Performance based Design for RC Framed Buildings", *2nd International Congress on Computational Mechanics and Simulation at IIT Guwahati, India*, December 8-10, 2006.

6. Joe Maffei, S.E. and Noelle Yuen, S.E., "Seismic Performance and Design requirements for High-Rise Concrete Building", *Structure Magazine,* April 2007 pp. 28-31.

7. Benjamin P. Thompson and Lawrence C. Bank, "Risk Perception in Performance-based Building Design and Application to Terrorism-Resistant Design", *Journal of Performance of Constructed Facilities.* Vol.21, No.1, Feb 2007 pp. 61-69.

8. Vipul Prakash, "Whether performance-Based Engineering in India?", *ISET Journal of earthquake Technology*, Paper No. 447, Vol. 41, No.1, March 2004 pp. 201-222.

9. Sigmund A. Freeman, "Review of the Development of the Capacity Spectrum Method", *ISET Journal of earthquake Technology*, Paper No. 438, Vol. 41, No.1, March 2004 pp. 1-13.

10. Ricardo A. Medina, "Story Shear Strength Patterns for the Performance-Based Seismic Design of Regular Frames", *ISET Journal of earthquake Technology*, Paper No. 442, Vol. 41, No.1, March 2004 pp. 101-125.

11. Andreas J. Kappos and Georgios Panagopoulos, "Performance-Based Seismic Design of 3D R/C Buildings Using Inelastic Static and Dynamic Analysis procedures", *ISET Journal of earthquake Technology*, Paper No. 444, Vol. 41, No.1, March 2004 pp. 141-158.
12. Sashi K. Kunnath and Erol kalkan, "Evalution of Seismic Deformation Demands Using Non-linear Procedure in Multistory Steel and Concrete Moment Frames", *ISET Journal of earthquake Technology*, Paper No. 445, Vol. 41, No.1, March 2004 pp. 159-181.
13. Applied Technology Council (ATC)-40, "Seismic Evolution and Retrofit of Concrete Building", Report No.SSC 96-01, Volume I, Applied Technology Council, California, November,1996.
14. Federal Emergency Management Agency (FEMA)-356, "Prestandard and Commentary for the Seismic Rehabilitation of Building", FEMA 356/November 2000, Building Seismic Safety Council, Washington, D.C., 2000.
15. Ashraf Habibullah, S.E., and Stephen Pyle, S.E., "Practical Three Dimensional Nonlinear Static Pushover Analysis", *Structure Magazine*, 1998.
16. Federal Emergency Management Agency (FEMA)-273, "NEHRP Guidelines for the Seismic Rehabilitation of Buildings", Building Seismic Safety Council, Washington, D.C., October 1997.
17. Park R., and Paulay T., Reinforced Concrete structure, *Wiley-Interscience*, 1974.
18. Mehmet Inel, Hayri Baytan Ozmen, "Effects of plastic hinge properties in nonlinear analysis of reinforced concrete buildings", *Journal of Engineering Structures,* 28(2006) pp. 1494-1502.
19. "CSI analysis reference manual", Computer and Structures Inc, 1995 Univercity Avenue. Berkeley, California.
20. Mark A. Aschheim, Tjen Tjhin and Mehmet Inel, "The scaled nonlinear dynamic procedure: A Practical Technique for Overcoming Limitation of Nonlinear Static Procedure", *ISET Journal of earthquake Technology*, Paper No. 447, Vol. 41, No.1, March 2004 pp.127-141.

21. Sigmund A. Freeman, "Performance Based Earthquake Engineering during the last 40 years", *Principal, Wiss, Janney, Elstner Associates, Inc. Emeryville, CA, USA.*

22. Anil K. Chopra, "DYNAMICS OF STRUCTURES-Theory and applications to earthquake engineering" 3rd edition, University of California at Berkeley, 2008.

23. Erol Kalkan and Sashi K. Kunnath, "Method of Modal Combinations for Pushover Analysis of Buildings", *13th World Conference on Earthquake Engineering*, Vancouver, B.C., Canada, August 1-6, 2004, Paper No. 2713.

24. Armagan Korkmaz and Ali Sari, "Evaluation of Lateral Load Pattern In Pushover Analysis", Department of Civil Engineering, University of Texas at Austin, Austin.

25. IS1893: (Part I)-2002, "Criteria for Earthquake Resistant Design of Structures", (Part 1) Bureau of Indian Standards, New Delhi, June 2002.

26. IS: 456-2000, "Plain and Reinforced Concrete-code of Practice" Bureau of Indian Standards, New Delhi, 2000.

27. Dharna Dilip M., "Site Specific Response Analysis of High Rise and Low Rise Buildings", M.TECH Major Project, Nirma University, May, 2007.

APPENDIX – A

A.1 CALCULATION OF SHEAR CAPACITY OF R.C. MEMBER

Calculation of shear hinge properties for beams and columns, the yield shear force for the hinge is calculated considering shear capacities of both concrete and steel. Detailed calculations using excel sheet is given below,

Properties				
		f_{ck} =	25	N/mm²
		f_y =	415	N/mm²
		E_c =	25000	N/mm²
		E_s =	2E+05	N/mm²
Beam or Column size		b =	250	mm
		D =	500	mm
	Cover	d' =	50	mm
		d =	450	mm
Length of member		L =	4	m
Tension Reinforcement				
	Dia. of bar		12	mm
	No. of bar		3	
Area of tension Reinforcement			339.3	mm²
		Pt =	0.271	%
Shear Reinforcement				
	Dia. of bar		8	mm
	Spacing		250	mm
	No. of Legs		2	
Area of Shear Reinforcement			100.5	mm²
Gross Area of concrete			1E+05	mm²
Axial Load		P_u =	0	kN

CALCULATION

As per Clause cl:40.4(a) of IS: 456-2000

$$Vs_y = \frac{0.87 f_y A_{sv} d}{S_v}$$

V_{sy} = 65.33 kN

****** Shear Capacity of Concrete ******

Shear capacity of concrete

$$V_c = \delta \tau_c \, b \, d$$

Where $\delta = 1 + \dfrac{3P_u}{A_g f_{ck}}$ but not exceeding 1.5

As per IS 456 Table 19

$$\tau_c = \frac{0.85\sqrt{0.8 f_{ck}}\,(\sqrt{1+5\beta}-1)}{6\beta}$$

Where $\beta = \dfrac{0.8 f_{ck}}{6.89\, P_t} \leq 1.0$

β = 10.69

τ_c = 0.378

Shear capacity of concrete

$$V_c = \delta \tau_c \, b \, d$$

V_c = 42.52 kN

Total Shear Capacity $V = V_{sy} + V_c$

V = 107.9 kN

But after Yielding, the shear is resisted by the stirrups only.

****** To Calculate Yield Shear Displacement ******

Shear Modulus

G = 10417 N/mm^2

Shear stiffness = $\left(\dfrac{G \times A_g}{L}\right)$

= 324637.26 N/mm

Yield Displacement = F/k

Δ_u = 0.332 mm

Since the shear failure is a brittle type of failure, increase the ultimate deformation by only 50%.

OUT PUT

V_u = 107.9 kN

$0.2\ V_u$ = 21.57 kN

Δ_u = 0.00033 m

Δ_m = 0.00498 m

$\Delta_m = \Delta_y + \Delta_p$

Δ_p = 0.00465 m

Shear Strength	Shear Deformation
21.57	0.004984
21.57	0.000498
113.3	0.000498
107.9	0.000332
0	0.000000
-107.9	-0.000332
-113.3	-0.000498
-21.57	-0.000498
-21.57	-0.004984

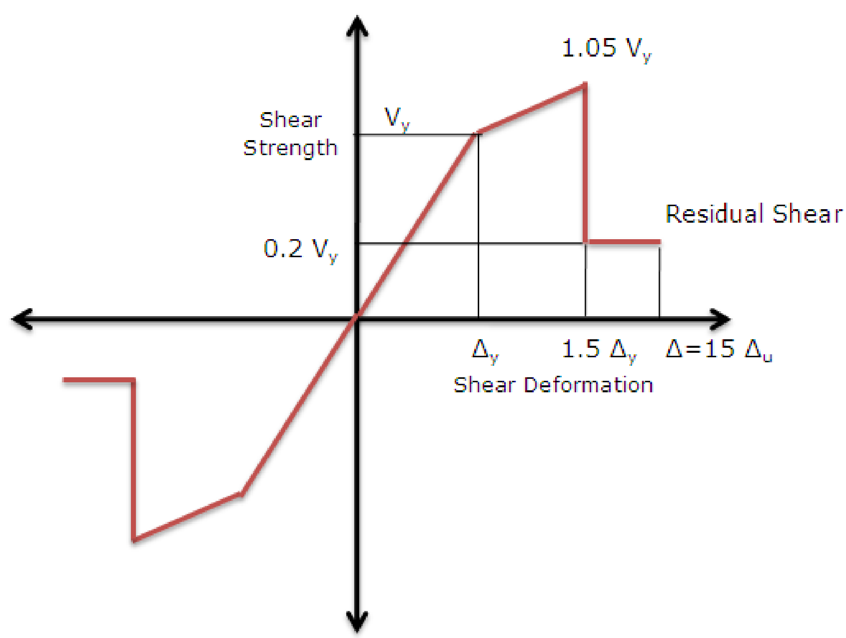

Force versus Displacement curve

A.2 CALCULATION OF MOMENT – CURVATURE (Φ) AND & ROTATION (θ) RELATIONSHIP FOR R.C. MEMBER

Excel sheet developed for calculations of Moment – Rotation relationship for structural member for defining Moment hinge properties. Moment – Curvature – Rotation relationship depends up on sectional properties, material properties, compression and tension reinforcement and length of member.

DATA

	f_{ck}	25	Mpa
Yield strength of steel (f_y)		415	Mpa
Modulus of Elasticity of concrete (E_c)		25000	Mpa
Modulus of Elasticity of steel (E_s)		2.E+05	Mpa
Modulus of rupture		3.5	

length of beam	4000	mm
Width (b)	250	mm
Depth (D)	400	mm
Cover (d')	30	mm
Eff. Depth (d)	370	mm
Area of tension steel (A_s)	481	mm^2
Area of compression steel (A_s')	289	mm^2

Percentage of steel $p_t = \frac{As}{b\,D}$

Tension steel p_t = 0.0052

Compression steel p_t' = 0.0031

Calculate the Moment, Curvature and Rotation

1. At just prior to cracking of concrete
2. At first yield of tension steel
3. When the concrete reaches an extreme fiber compression strain of 0.0032

Construct approximate tri-linear moment-curvature for section

Solution

1, Before cracking

The modulus of ratio = $n = E_s / E_c$ = 8

A = 105390 mm^2

Centroid of transformed section is given by taking moments of the areas about the top edge of the section

$$\bar{y} = \frac{bh \times c.g + A_s \times (n-1) \times c.g + A_s' \times (n-1) \times c.g}{Total\,Area}$$

$\bar{y}$ = 202.168 mm

Hence the moment of inertia is given by

I = 1488609001 mm^4

Cracking will occur when the modulus of rupture = 3.5 reached in bottom fiber.

$$M_{crack} = \frac{f_r I}{y_{bottom}} \quad = \quad 26.3361 \text{ kN-m}$$

and

$$\phi_{crack} = \frac{f_r / E_c}{y_{bottom}} \quad = \quad \begin{matrix} 7.1\text{E-07} & \text{rad/mm} \\ 0.00071 & \text{rad/m} \end{matrix}$$

2, After cracking, at first yield

Assuming the concrete is behaving elastically.

$$k = \left[(p_t + p_t')^2 n^2 + 2\left(p_t + \frac{p_t' d'}{d} \right) n \right]^{1/2} - (p_t + p_t')n$$

k = 0.23621

kd = 87.3961 mm

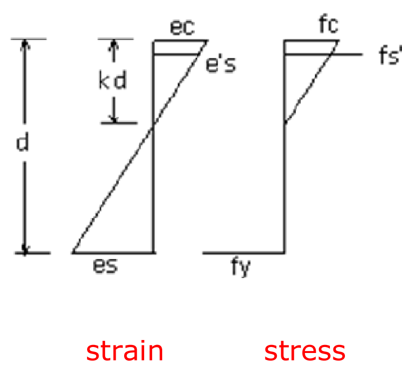

Now $\varepsilon_s = f_y / E_s$

ε_s = 0.0020750

from the strain diagram

ε_c = 0.0006417

f_c = 16.0425

Therefore the triangular stress block is an approximation.

From the strain diagram we find

$\varepsilon_{s'}$ = 0.0004214

f_s' = 84.29 Mpa

$C_c = \frac{1}{2} f_c b\ k\ d$ = 175.26 kN

$C_s = As'\ fs'$ = 24.358 kN

Therefore, total compressive force is 199.6 kN acting @

$\bar{y}$ from top edge,

$\bar{y}$ = 29.238 mm

jd = d - $\bar{y}$ = 340.76 mm

= 68.021 kN-m

= 7.34243E-06 rad/mm
0.00734 rad/m

3, After cracking, at ultimate load

Assume that the compression steel is also yielding;

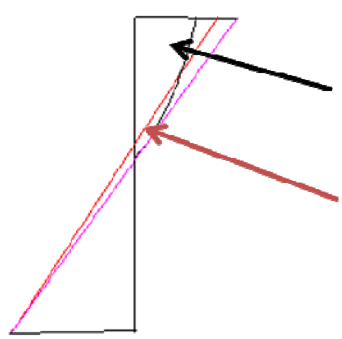

$$a = \frac{A_s f_y - A_s' f_y}{0.85 f_c' b}$$ = 16.6651 mm

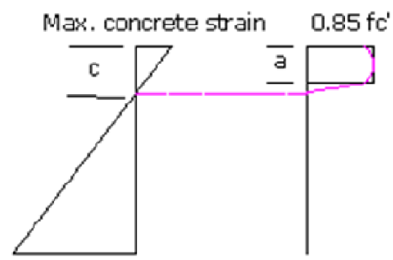

c = 19.606 mm

from strain diagram

ε_s' = -0.0017

f_s' = -339.29 Mpa

actual f_y 415 Mpa

trial and error method

Assume f_s 145 Mpa

a = 32.9851 mm

c = 38.806 mm

ε_s' = 0.00073

f_s' = 145.231 Mpa
Actual f_y 415 Mpa

Which check satisfactorily with the trial value

$$M_u = 0.85 f_c' a b \left(d - \frac{a}{2} \right) + A_s' f_s' (d - d')$$

M_u = 72.2421 kN-m

$$\phi_u = \frac{\varepsilon_c}{c} = \begin{array}{ll} 8.24615E-05 & \text{rad/mm} \\ 0.0824615 & \text{rad/m} \end{array}$$

Moment Curvature Relationship

Moment kN-m	Curvature in term of rad/m(10^{-3})
0.00	0.000
26.34	0.707
68.02	7.342
72.24	82.461

$$\theta_{AB} = \theta_y + \theta_p$$

$$\theta_{AB} = \phi_y \times l + (\phi_u - \phi_p) \times l_p$$

Where $l_p = 0.08L + 0.022 \times f_y \times d_{bl}$

l_p = 394 mm

Rotation at yielding point

$\theta_y = \phi_y \, l_p$ = 0.00278

Plastic Rotation

$$\theta_p = (\phi_u - \phi_y) \times l_p = 0.01878$$

Ultimate Rotation

$$\theta_u = \theta_y + \theta_p = 0.0197$$

Moment Rotation Relationship

Moment	Rotation
0.00	0
26.34	0.0007
68.02	0.0027
72.24	0.0197

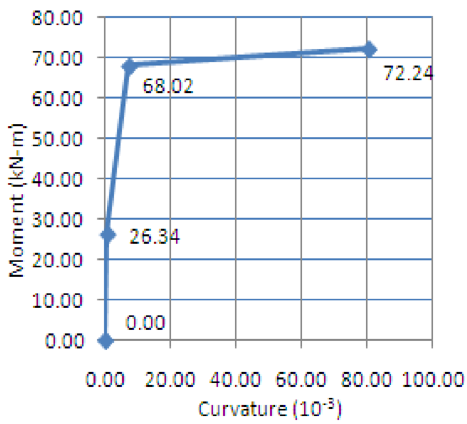

Moment – Curvature

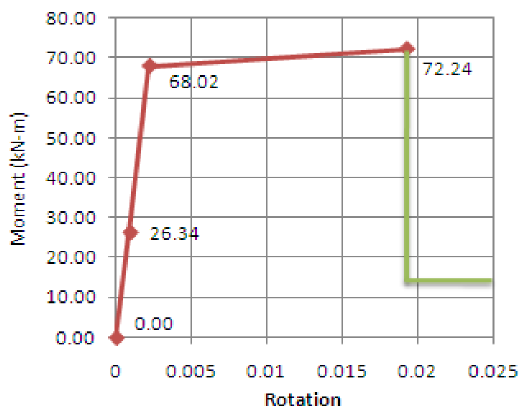

Moment – Rotation

A.3 FINDING PERFORMANCE POINT USING PROCEDURE C (REDUCED DEMAND CURVE)

An Excel sheet is developed to set performance point from Base shear v/s Roof disp. Data. In this Excel sheet, Base Shear versus Roof displacement curve for 7 story building as per example from ATC 40, Performance point is obtained.

Given Data

	0	1	2	3	4
Base Shear (kN)	0.000	9860	11653	12550	13446
Roof Disp. (mm)	0.000	63.75	91.44	129.5	276.86
PF (from above Eq.)	0.000	1.310	1.280	1.350	1.390
α (from above Eq.)	0.000	0.828	0.800	0.770	0.750

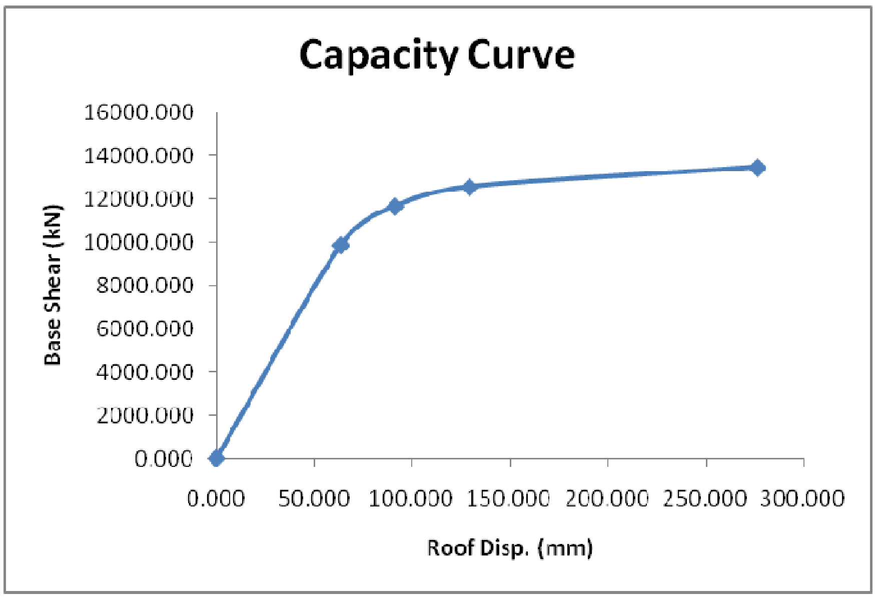

PF and α change Because the mode shape is changing as Yielding occurs

$$S_a = \frac{V_i / W}{\alpha_i}$$

$$S_d = \frac{\delta}{PF_{roof}}$$

$$T = \sqrt{\frac{S_d}{S_a \times 9810}}$$

Conversion of V & δ to Sa & Sd

point	V (kN)	δ_R (mm)	V/W	PF @ Roof	α	Sa (g)	Sd (mm)	T (sec)
1	9860	63.75	0.210	1.31	0.828	0.254	48.67	0.878
2	11653	91.44	0.249	1.28	0.800	0.3107	71.44	0.962
3	12550	129.54	0.268	1.35	0.770	0.3476	95.96	1.054
4	13446	276.86	0.287	1.39	0.750	0.3824	199.2	1.448

CAPACITY SPECTRUM CURVE

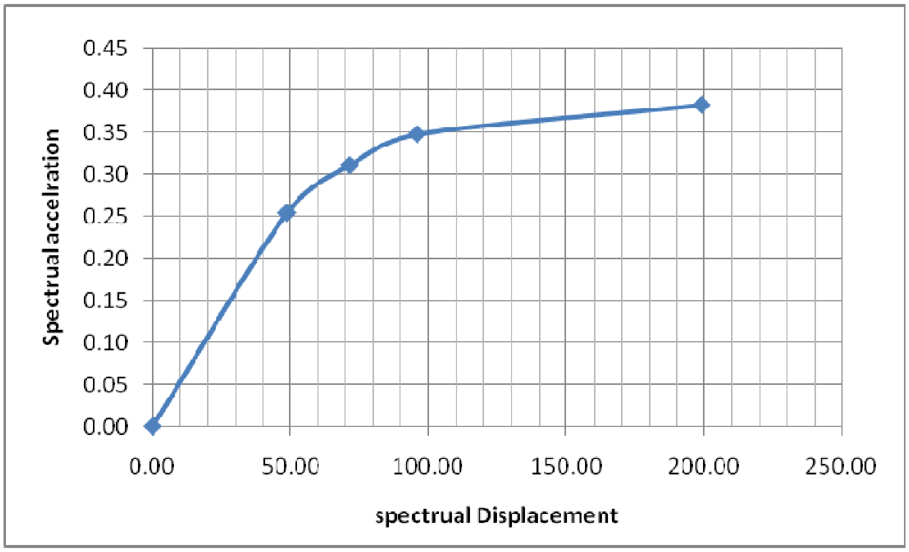

	0	1	2	3	4
Sa (g)	0.00	0.254	0.311	0.348	0.3824
Sd (mm)	0.00	48.67	71.44	95.96	199.18

The demand for the building for the performance level desired is determine to be soil type S with

C_A	0.44
C_V	0.64

The Demand spectrum converted in to ADRS format using EQ.

a_{p1} =	0.36	g	d_{p1} =	132.7	mm
a_y =	0.31	g	d_y =	71.16	mm

$$B_{eff} = \lambda B_o + 0.05$$

$$B_{eff} = \frac{63.7\,\lambda\,(a_y d_{pi} - d_y a_{pi})}{a_{pi} \times d_{pi}} \quad + \quad 5$$

Value for damping Modification factor λ = 0.33
(which is depend on type of Structure)
ATC 40 --- Table 8.1 page (8-17)

B_{eff} = 6.829 + 5
= 11.83 %

Reduction Factor

$$SR_A = \frac{3.21 - 0.68\ \ln(B_{eff})}{2.12}$$

SR_A = 0.722

$$SR_V = \frac{2.31 - 0.41 \ln(B_{eff})}{1.65}$$

SR_V = 0.786

Calculate Value to Plot the Demand Curve

Sa = 2.5 SR_A C_A
= 0.794 g

Ts = SR_v C_v / (2.5 SR_A C_A)
= 0.634 sec

Sd = Sa $(Ts/2\pi)^2$

= 79.23 mm

Calculate Performance Point

		0	1	2	3	4	
Sa (g)		0	0.254	0.311	0.348	0.3824	
Sd (mm)		0	48.67	71.44	95.96	199.18	
0.794	0.794	1.01	0.50	0.34	0.25	0.20	0.17
0	79.23	62.51	125.02	187.53	250.04	312.55	375.06

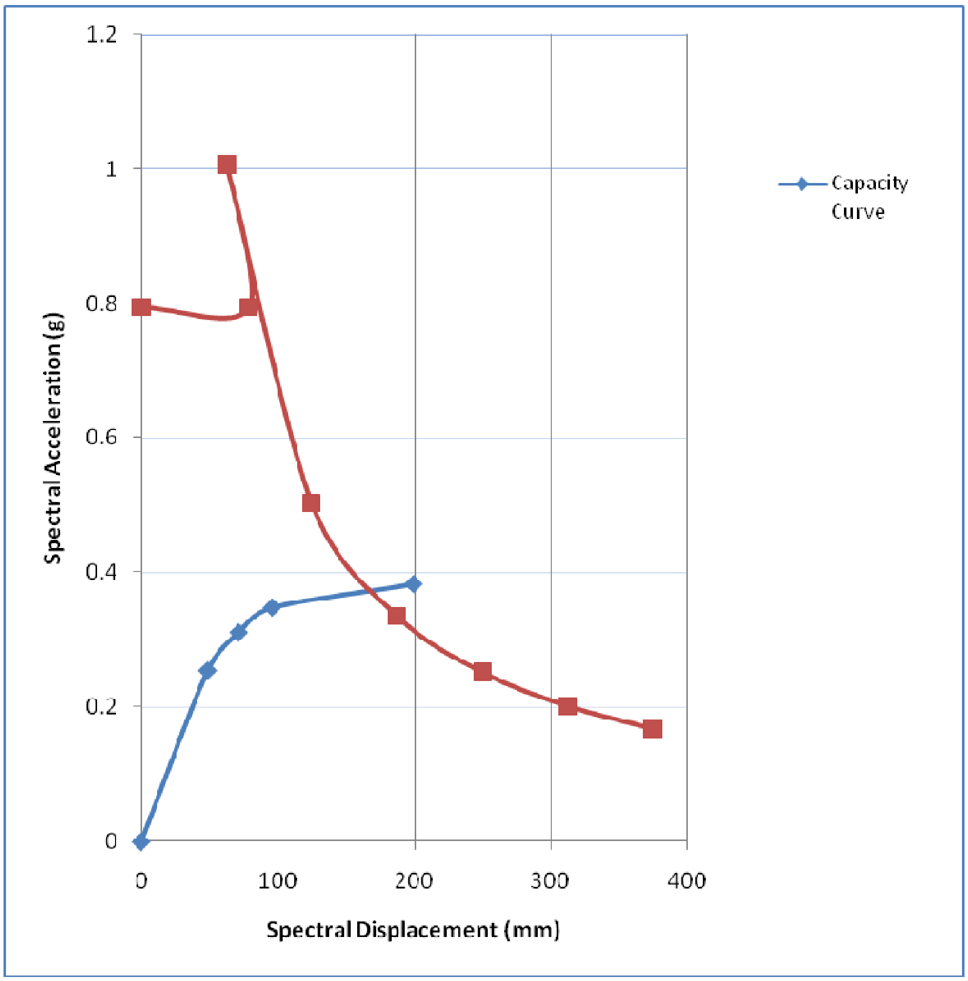

Performance point curve

APPENDIX – B

CALCULATION OF COEFFICIENT C_a AND C_v

The seismic coefficient C_a represented the effective peak acceleration of the ground. A factor 2.5 times C_a represent the average value of peak response for 5% damped.

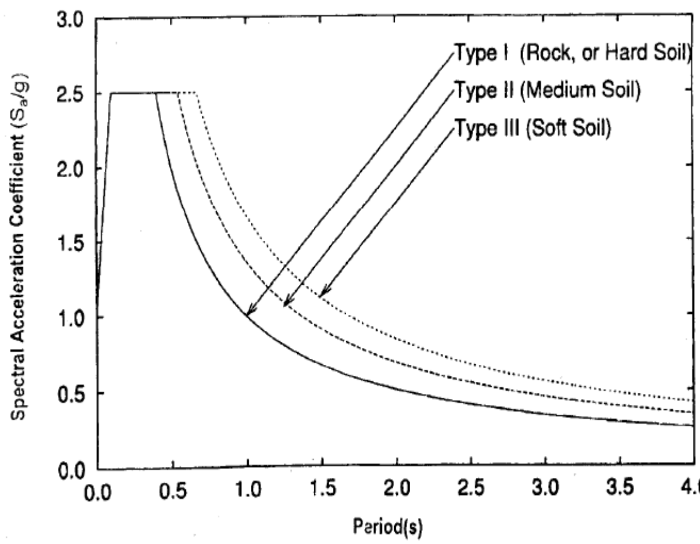

Fig.1 Response Spectra for Rock and Soil sites for 5% damping (IS 1893-2002)

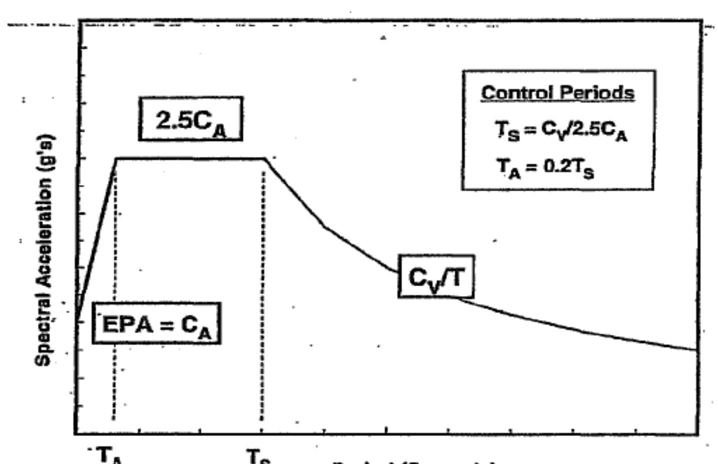

Fig. 2 Construction of 5% damped Elastic Response Spectra (ATC 40)

Coefficient of acceleration (C_a) = Z

Coefficient of velocity (C_v) = $2.5 \times C_a \times T_s$

For Zone IV (IS 1893-2002)

$C_a = 0.24$

$T_s = 0.40$ (Type I - Rocky or Hard soil sites)

$T_s = 0.55$ (Type II - Medium soil sites)

$T_s = 0.67$ (Type III - Soft soil sites)

$C_v = 2.5 \times C_a \times T_s$

$= 2.5 \times 0.24 \times 0.40 = 0.24$ (Rocky or Hard soil sites)

$= 2.5 \times 0.24 \times 0.55 = 0.33$ (Medium soil sites)

$= 2.5 \times 0.24 \times 0.67 = 0.40$ (Soft soil sites)

The value of C_a and C_v is calculated for all the zones for considering soil conditions. Table B Shown the values of C_a and C_v.

Table-B Coefficient of Acceleration and Coefficient of Velocity

Seismic Coefficient C_a				
Soil	Zone II	Zone III	Zone IV	Zone V
Type I	0.1	0.16	0.24	0.36
Type II	0.1	0.16	0.24	0.36
Type III	0.1	0.16	0.24	0.36
Seismic Coefficient C_v				
Type I	0.100	0.160	0.240	0.360
Type II	0.138	0.220	0.330	0.495
Type III	0.168	0.268	0.402	0.603

APPENDIX – C

LIST OF USEFUL WEBSITES

- www.csiberkly.com
- www.asce.com
- www.sciencedirect.com
- www.nicee.org
- www.iitk.ac.in
- www.gigapedia.com

APPENDIX – D

LIST OF PAPER PUBLISHED

1. Prakash K. Siyani and Paresh V. Patel, "Effects of plastic hinge properties in performance based design", *National Conference on Advances and Innovations in Civil Engineering (AICE'09)*, Tamilnadu, 25th March, 2009.

LIST OF PAPER COMMUNICATED

1. Prakash K. Siyani and Paresh V. Patel, "Effect of plastic hinge properties in non-linear analysis", *National Level Technical Festival (SAMANNVAY'09)*, Ahmedabad, 18-20 February, 2009. (Paper Presented)

2. Prakash K. Siyani and Paresh V. Patel, "Comparison of Pushover Analysis considering Site Response Spectra and Time History", *International Conference on Advance in Concrete, Structure and Geotechnical Engineering*, Bits Pilani, 25-27 October, 2009. (Abstract accepted)